2009

Electrochemical Detection o f Chemical Warfare Agent Mimics

Yizhi Xiao

Electrochemical Detection of Chemical Warfare Agent Mimics

(Spine title: Electrochemical Detection of Chemical Warfare Agent Mimics)

(Thesis Format: Monograph)

By

Yizhi Xiao

Graduate Program in Chemistry

Submitted in partial fulfillment
of the requirements for the degree of
Master of Science

The School of Graduate and Postdoctoral Studies
University of Western Ontario
London, Ontario, Canada

ABSTRACT

Rising concern over the use of chemical warfare agents (CWAs) in criminal terrorist attacks has attracted a great deal of interest in having rapid, reliable and affordable methods for the detection of CWAs and their related degradation products.

Four ferrocene-amino acid / peptide conjugates, Fc-CO-Lys(Boc), Fc-CO-Leu-Lys(Boc), Fc-CO-Lys(Boc)-Leu, and (Boc)Arg(NO_2)-NH(CH_2)$_4$NH-CO-Fc were synthesized and used to modify acid-treated multi-walled carbon nanotubes (MWCNTs) chemically.

Fc-conjugate-modified-MWCNTs were deposited on ITO surfaces as the key component for electrochemical detection sensors for chemical warfare agent (CWA) mimics and their decomposed products in water. The electrical properties of the MWCNTs and Fc group were affected significantly upon the adding of CWA mimics to the system. In some cases, new peaks were observed at the presence of CWA mimics. Presumably, electrochemical changes are caused by the intermolecular interaction of the CWA with the peptide component of the sensors. This kind of electrochemical sensors were found stable and allowed trace-level detection of CWA mimics in aqueous solutions.

Key Words: electrochemistry, chemical warfare agent, carbon nanotube, ferrocene, peptide, ITO

ACKNOWLEDGEMENTS

I would like to thank my supervisor, Dr. Heinz-Bernhard Kraatz for his help and support throughout my study here. His dedication and encouragement made this experience invaluable.

I would also like to thank all of the members of the Kraatz group. It has been an honor working with all of you, and I could not have made it without your support and friendship. Special thanks go to Mark Milne, Haifeng Song, and Chantelle Davidson for help with synthesis experiments and Kagan Kerman, Xiaomin Bin, Piotr Diakowski for technical support. Also, I would like to thank Drs Gillies and Ragogna for use of their instruments.

At last, a very special thank you to my family and friends for their never-ending support and love.

CONTENTS

LIST OF SCHEMES

LIST OF EQUATIONS

LIST OF TABLES

LIST OF FIGURES

LIST OF ABBREVIATIONS

AchE	acetylcholinesterase
AD	anno domini
Arg	arginine
ATP	adenosine-5'-triphosphate
BC	before Christ
Boc	*t*-butoxy carbonyl
CE	capillary electrophoresis
2-CLEES	2-cloroethyl ethyl sulfide
CNT	carbon nanotube
CV	cyclic voltammetry
CWA	chemical warfare agent
DCM	dichloromethane
DECP	diethyl cyanophosphonate
DESH	diisopropylethyl mercaptoamine
DNA	deoxyribonucleic acid
DPV	differential pulse voltammetry
EA 2192	*S*-(2-diisopropylaminoethyl) ethylphosphonothioate
EtOAc	ethyl acetate
EMP	ethyl methylphophonate
Fc	ferrocene
FT-IR	Fourier transform infrared
GA	Tabun
GB	Sarin
GC	gas chromatography
GD	Soman
GF	Cyclosarin
HBTU	O-benzotriazole-*N,N,N',N'*-tetramethyl-uronium-hexafluoro-phosphate
HD	sulfur mustard
HN	nitrogen mustard

HOBt	*N*-hydroxybenzotriazole
IMS	ion mobility spectrometry
ITO	indium-tin oxide
LC	liquid chromatography
Leu	leucine
Lys	lysine
MPA	methyl phosphoric acid
MS	mass spectrometry
MWCNT	multi-walled carbon nanotube
NMR	nuclear magnetic resonance
OPAA	oranophosphorus acid anhydrolase
OPH	organophosphate hydrolase
OV_{25}	phenyl methyl polysiloxane
PECH	poly(epichlorohydrin)
PET	photo-induced electron transfer
PMP	pinacolyl methylphosphonate
PTFE	polytetrafluoroethylene
QCM	quartz crystal microbalance
SAW	surface acoustic wave
SEM	scanning electron microscope
SWCNT	single-walled carbon nanotube
SXFA	hexafluoro-2-propanol-substituted polysiloxane
TEA	triethylamine
TFA	trifluoroacetic acid
WWI	World War I
WWII	World War II

Chapter 1 INTRODUCTION

1.1 Chemical Warfare Agents

Chemical warfare agents (CWAs) are poisonous chemicals that are mainly used in war to disable enemies. However, the abuse of CWAs in terrorist attacks started to be seen in twentieth century and this emergence of chemical terrorism seems to be a significant threat in twenty-first century though there have been many attempts to ban CWAs. It is thought to be necessary to understand the potential of current and future threats that help further precautions for protection of both military persons and civilians.

1.1.1 History

The use of CWAs dates from the late Stone Age (10,000 BC) when hunters in southern Africa used poison arrows, in which the poisons were from scorpion and snake venoms as well as poisonous plants.[1] During the BC period, toxic fumes, smokes, flames, and liquids were used in wars occurred in India, China, and Greece.[2] Greek fire was invented in seventh century AD, which probably contained saltpeter, quicklime, sulfur, rosin, naphtha and pitch.[2, 3] It was a flaming weapon that could continuously burning on water so that it was used in naval battles to great effect.[4] Later, shells filled with toxic smoke, liquid or powder were used in war.[2, 5] They were more portable and ready for a long distance attack as well as a more powerful effect on vast destruction.

Modern CWAs were born in the early twentieth century. The CWAs first used in World War I (WWI) were eighteenth- and nineteenth-century discoveries, including chlorine (Cl_2) in 1774, hydrogen cyanide (HCN) in 1782, cyanogen chloride (CNCl) in 1820, and phosgene ($COCl_2$) in 1812. Mustard agent (dichloroethyl sulfide, 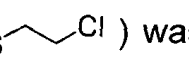) was synthesized in 1822 and chloropicrin (CCl_3NO_2) in 1848.[2] The use of tear agents was brought up in Germany in 1887. The first large-scale use of chemicals during WWI was initiated by Germany against British in 1914.[6] The shortage of artillery shells led to the concept of creating a toxic gas cloud directly from its storage cylinder. With the help of wind, an attack from Germany to Allied troops in 1915 caused devastating effect that resulted in probably between 800 and 5000 deaths.[7, 8]

Mustard agent was first used by the Germans against French in 1917.[9] It poisoned the air, ground as well as equipments because its relative non-volatility and persistence. It was also effective in low doses and affected lungs, eyes and skin.[10] Until the mid 1930s, phosgene and mustard agents were considered the most dangerous chemical weapons.

The discovery of nerve agents (Fig. 1.1) changed this situation. Tabun was discovered accidentally in 1936, which had withering effects on the nervous system and caused death within 20 min of exposure.[11] In 1938, Sarin was invented, a nerve agent which is 10 times more effective than Tabun.[11]

During WWII, research continued to find new CWAs. Soman was developed by the Germans in 1944. It combines features of both Sarin and Tabun and was more toxic than both of them. The Germans also researched two other nerve agents, ethyl Sarin and Cyclosarin, which were not known by the

Allies until 1945.[12] More blistering and stable distilled mustard was produced by the United States in 1944 and meanwhile, nitrogen mustard agents were being developed as well.[13]

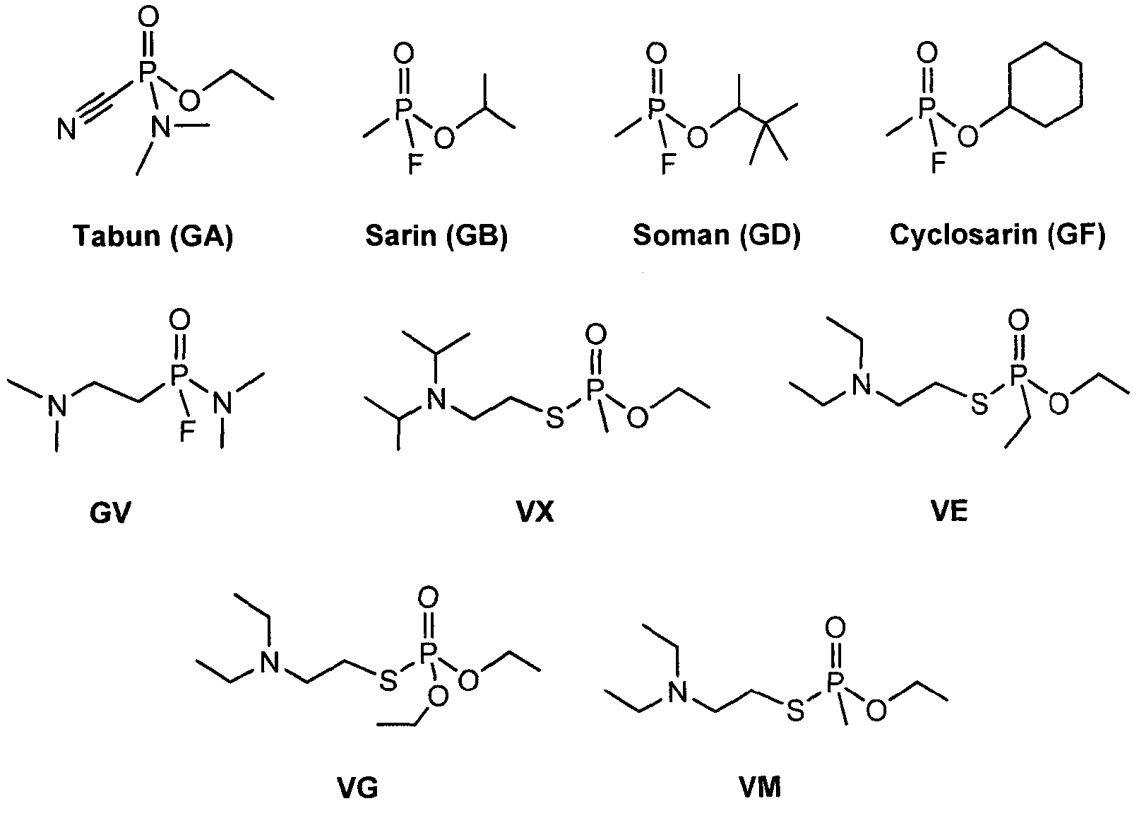

Fig. 1.1 Chemical structure of nerve agents.

The end of WWII did not stop the development of chemical weapons. VX, a new nerve agent was discovered by the British in 1952.[14] It is a colorless and odorless liquid which was immediately toxic to mammals as well as insects. So far nerve agents are the most toxic of the known CWAs, which can cause death within minutes after exposure.

Production and research of CWAs continued after WWII, particularly in the United States and previous Soviet Union. During the 1980s, Russians had

developed a highly toxic binary nerve agent series designated Novichuk, which is publicly unknown and uncovered by existing detection and warning devices, as well as current protective equipments.[15]

Terrorism, which was thought to be far off our life, began to draw serious concerns in the 1980s. The first large-scale chemical terrorism incident occurred in the United States in 1982, in which seven young people died by taking Tylenol capsules that had been tampered with cyanide.[16] Sodium cyanide was reported to have been in the bomb that ruined the first World Trade Center in 1993, but had burned in the heat of the explosion. It was speculated that if it had vaporized, the cyanide would have been dispersed into the North Tower and killed all of the people inside.[17] Perhaps the most publicized chemical terrorism incident is the Tokyo subway incident in Japan in 1995. Sarin was used in a crowded Tokyo subway, causing 22 victims' death and over 5000 injured.[18] This is an example that tells us what a significant threat it could be to the civilian population if terrorists use CWAs in terrorism attacks. Therefore, modern precautions to protect and help people are necessary.

1.1.2 *Classification*

There are several different schemes to classify CWAs systematically. The most common one is by their target organism in the human body and physiological effects (Table 1.1).[1, 19] The best known lethal agents include nerve, blister, choking, and blood agents.

Table 1.1 General class of CWAs[1, 19]

Class of agent	Common agents	Mode of action	Persistency
Nerve	Tabun (GA) Sarin (GB) Soman (GD) Cyclosarin (GF) VX	Inactivate enzyme cholinesterase, causing an increase in neurotransmitter acetylcholine throughout the body.	VX is persistent and a contact hazard; others are non-persistent and present mostly inhalation hazards.
Blister	sulfur mustard (HD) nitrogen mustard (HN-1, HN-2, HN-3) Lewisite (L) phosgene oxime (CX)	Damage skin and respiratory system, resulting in burns and respiratory problems.	Persistent and an contact hazard.
Choking	phosgene (CG) diphosgene (DP)	Damage respiratory system, causing excess body fluid and resulting in suffocation.	Non-persistent and an inhalation hazard.
Blood	hydrogen cyanide (AC) cyanogens chloride (CK) arsine (SA)	Prevent the normal use of oxygen by the blood cells, causing damage to tissues.	Non-persistent and an inhalation hazard.
Incapacitating	Agent 15 (BZ)	Produce physiological or mental effects	Extremely persistent in soil and water and on most surfaces; contact hazard.
Lachrymatory	chloroacetophenone (CN) chloroacepophenone in chloroform (CNC) bromobenzylcyanide (CA)	Cause weeping and skin irritation.	
Vomiting	diphenylchlorarsine (DA) adamsite (DM) diphenylcyanoarsine (DC)	Cause great discomfort	

1.1.2.1 Nerve Agents

Nerve agents form the most deadly group among the CWAs. They are organophosphates including fluorine- or cyanide-containing G-type and sulfur-containing V-type agents. V-agents are less volatile than G-agents and present a severe contact risk as they are readily absorbed through the skin[20, 21] The toxicity of VX when absorbed through the skin is about 1000 times greater than that of Sarin.[22]

Nerve agents attack the nervous system of human body. The primary target is the enzyme acetylcholinesterase (AchE). The enzyme catalyzes the hydrolysis of the neurotransmitter acetylcholine to choline and acetic acid, which is a reaction necessary to allow a cholinergic neuron to return to its resting state after activation (Scheme 1.1a).[23] If acetylcholine is not removed by AchE, the signal remains triggered and the nerve system will be jammed so that it cannot transmit further signals. Nerve agents inhibit AchE by phosphorylating an essential serine residue in the AchE active site (Scheme 1.1b), resulting in the completely loss of AchE enzymatic activity against acetylcholine.

The organophosphorus compounds that can inhibit AchE have some essential structural features: (1) oxygen or sulfur directly bonded to the phosphorus atom to form a phosphoryl- or thiophosphoryl- group; (2) R_1 and R_2 being either an alkoxy, alkyl, N-alkylamino or N,N-dialkylamino; (3) leaving group typically being a halogen or pseudohalogen, aryloxy-, thioxy- or phosphate-group.[24] The chemical structure of common nerve agents is shown in Fig. 1.1.

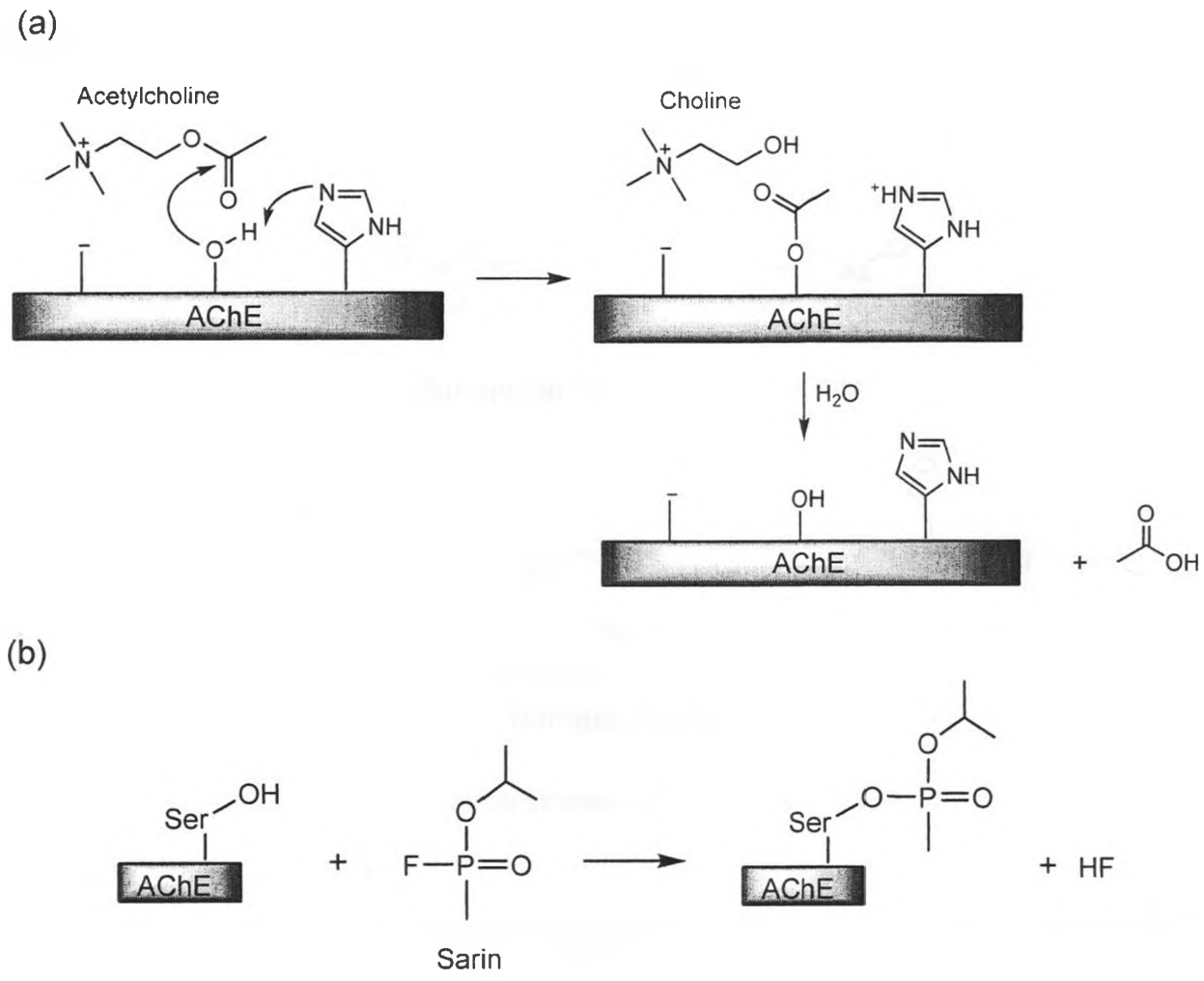

Scheme 1.1 AchE catalyzes the hydrolysis of acetylcholine (a), and loses enzymatic activity by being phosphorylated by nerve agent Sarin (b). (Modified from reference 23)

1.1.2.2 Blister Agents

Blister agents include mustards and arsenicals which blister the skin and produce chemical burns to any exposed part of the body. They are less toxic than nerve agents.

Mustards generally contain the Z-(CH_2)-L fragment in which the heteroatom Z is separated from a leaving group L by two atoms (Fig. 1.2).

Replacing sulfur by nitrogen or oxygen results in nitrogen mustard or oxygen mustard.

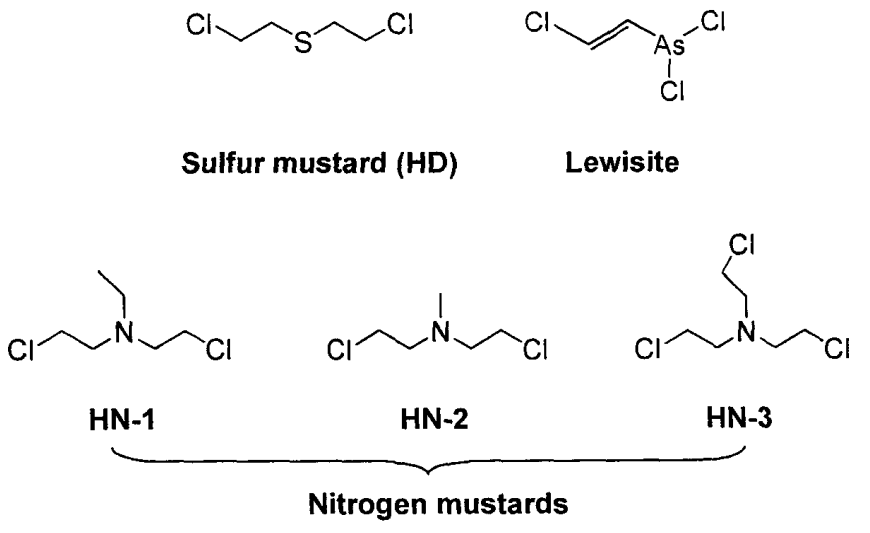

Fig. 1.2 Chemical structure of selected blister agents.

The effects of mustards are mostly due to their forming of alkylating intermediates which can further react with nucleophilic substances, including such biologically important moieties as phosphate, amino, hydroxyl, and carbonyl groups. Sulfur mustard remains a severe risk in today's conflicts and terrorism activities because it is relatively easy to manufacture and highly effective against unprotected civilian population.

Composed of small, oily droplets, sulfur mustard is heavier than air and persists for days in the environment.[24] Sulfur mustard damages DNA mainly by alkylating and cross-linking the purine bases (Scheme 1.2).[25, 26]

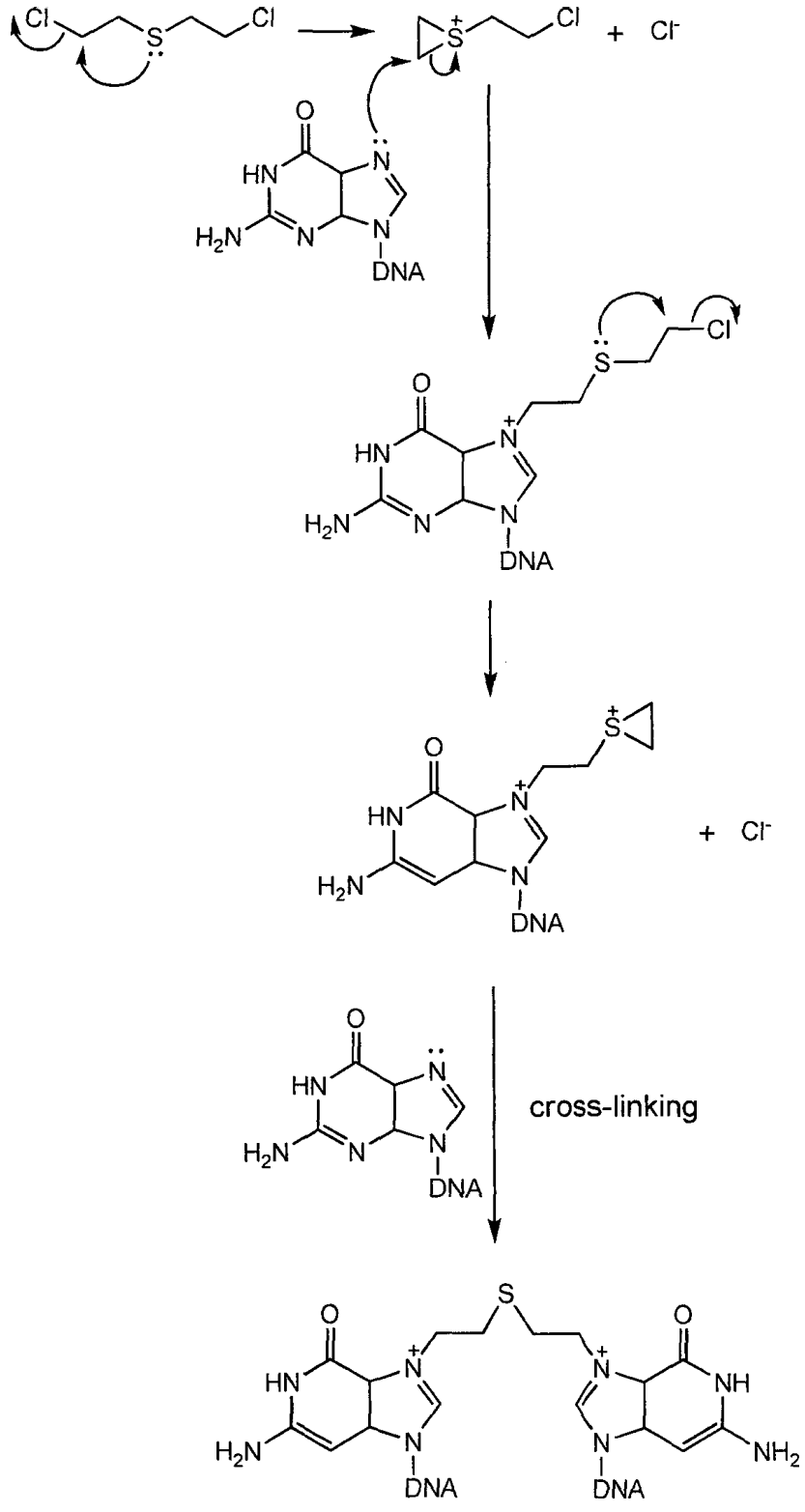

Scheme 1.2 Alkylation and cross-linking of sulfur mustard with guanine in DNA. Ethylene sulfonium ion is formed through cyclization and subsequently binds to guanine. A second cyclization of guanine-ethylene-sulfonium and subsequent binding to another guanine molecule leads to cross-linking product. (Modified from reference 25, 26)

1.1.2.3 Blood Agents

Blood agents enter the body primarily through the respiratory tract and prevent the normal utilization of oxygen by blood cells. Included are hydrogen cyanide (HCN), cyanogen chloride (ClCN), and arsine (AsH_3).

This group of agents is less important for military actions because its use in open terrain requires high concentration, but the dispersal and dilution by wind and air currents will reduce the concentration. On the other hand, inhalation is the main way of entry into the body and modern protective masks are effective enough to protect against these agents.[27]

1.1.2.4 Choking Agents

Choking agents decompose into hydrochloric acid and oxygen free radicals after entering the airway, which irritates the respiratory tract, and causes membrane swelling. These agents include chlorine, chloropicrin, phosgene, and diphosgene (Fig. 1.3).[2, 19]

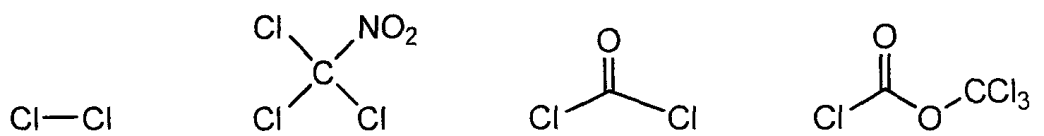

Chlorine **Chloropicrine** **Phosgene** **Diphosgene**

Fig. 1.3 Chemical structure of selected choking agents.

Toxication with phosgene and diphosgene is via inhalation. The effect is often delayed, sometimes for several hours. Secondary infections are mostly fatal, even after already recovery from the main toxication.[2]

Choking agents are of little importance in modern military scenarios since they are less effective and can be prevented by modern protective equipment and apparels.

1.1.3 Degradation of CWAs

CWAs may degrade in environment via processes of hydrolysis, biodegradation, oxidation, and photolysis.[28, 29] Different conditions are involved in these processes, therefore there are potentially different breakdown products related to a given CWA.

1.1.3.1 Degradation of Nerve Agents

The common nerve agents (Fig. 1.1) of both categories (G-type and V-type) are susceptible to hydrolysis. They have different water solubility and hydrolysis rates. VX and GD are less soluble and VX hydrolyzes the most slowly. Nerve agents may also undergo biodegradation such as *O*-dealkylation and *C*-dealkylation in soil.[28]

GA (Tabun) is subject to hydrolysis to *O*-ethyl *N,N*-dimethylamido phosphonate and hydrogen cyanide under neutral condition (Scheme 1.3). The initial reaction is fairly rapid but the further hydrolysis of *O*-ethyl *N,N*-dimethylamido phosphonate to dimethylphosphoramidate and then phosphoric acid is much slower.[30] Hydrolysis is faster in acidic or basic conditions, as well as at elevated temperature.[31, 32]

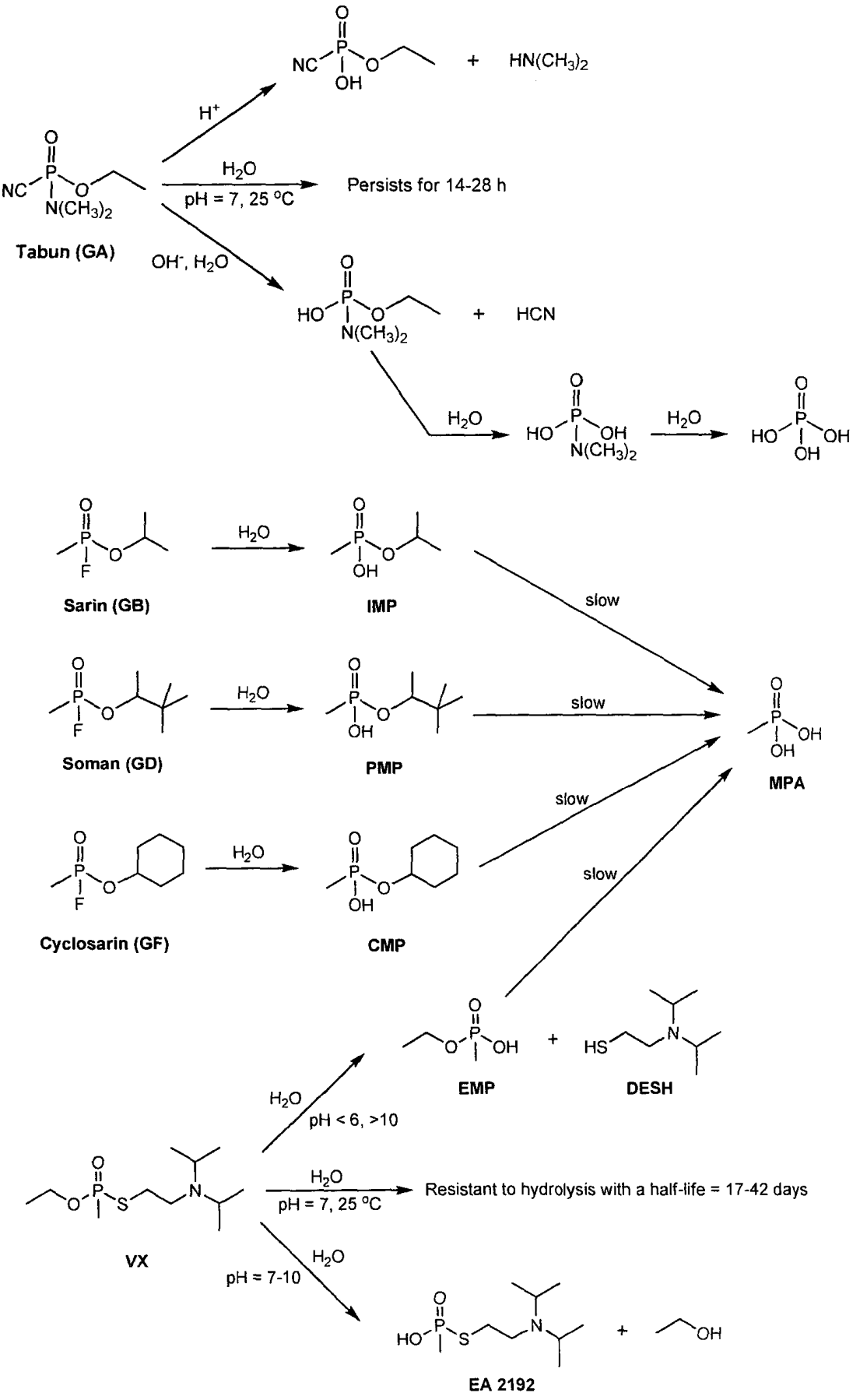

Scheme 1.3 The main hydrolysis pathways of nerve agents[32-36].

Other G-agents are rapidly hydrolyzed by water, particularly under alkaline conditions. Hydrolysis firstly takes place through the loss of fluoride (Scheme 1.3) that gives alkyl methylphosphonates. The further hydrolysis of the phosphonates to methyl phosphoric acid (MPA) occurs at much slower rates.[32-35]

VX is relatively resistant to hydrolysis with a half-life in water at 25°C and pH 7 raging from 17 to 42 days.[32, 36] The hydrolysis proceeds via several pathways, producing various degradation products (Scheme 1.3).[37, 38] EA 2192, a hydrolysis product of VX under basic condition, is relatively stable in water with no further degradation products observed after 1,000 h in distilled water or within 12 days in alkaline conditions.[39] While EMP, a hydrolysis product of VX under acidic condition, was reported being further hydrolyzed to MPA with a half-life of 8 days.[40]

MPA, the final hydrolysis product of nerve agents, is stable in the environment since it is resistant to hydrolysis, photolysis, and thermal decomposition.[41] It might undergo biodegradation, but the C-P bond is resistant to cleavage.[37, 41]

1.1.3.2 Degradation of Blister Agents

Sulfur mustard (HD) is rapidly hydrolyzed in distilled water, but its rate is limited by the slow rate of dissolution.[42] Furthermore, the intermediate hydrolysis products could wrap the droplets of HD, which may retard further hydrolysis. Hydrolysis occurs by two routes according to the availability of water.[43] Both routes lead to formation of thiodiglycol and hydrochloric acid (Scheme 1.4).[28, 43]

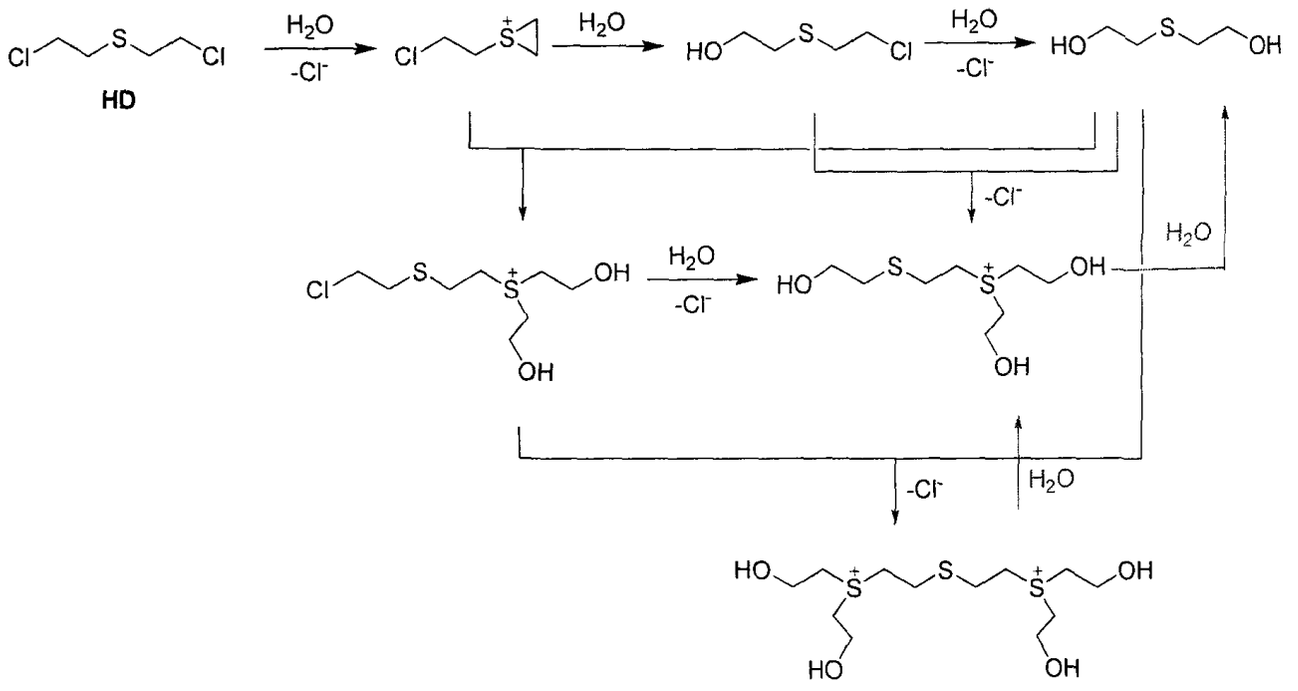

Scheme 1.4 Main hydrolysis pathways of sulfur mustard. In a dilute aqueous solution, HD is quickly hydrolyzed to a sulfonium ion and then to hemimustard and finally thiodiglycol. In a solution without enough water to dissolve all HD, sulfonium ion aggregates (thiodiglycol-mustard aggregates) are formed. (Modified from reference 28, 43)

Lewisite ($Cl\text{-}CH{=}CH\text{-}AsCl_2$) is only slightly soluble in water, but hydrolyzed rapidly, resulting in the formation of soluble dihydroxy arsine. Lewisite oxide and polymerized Lewisite oxide might be formed if dehydration reaction occurs (Scheme 1.5)[28].

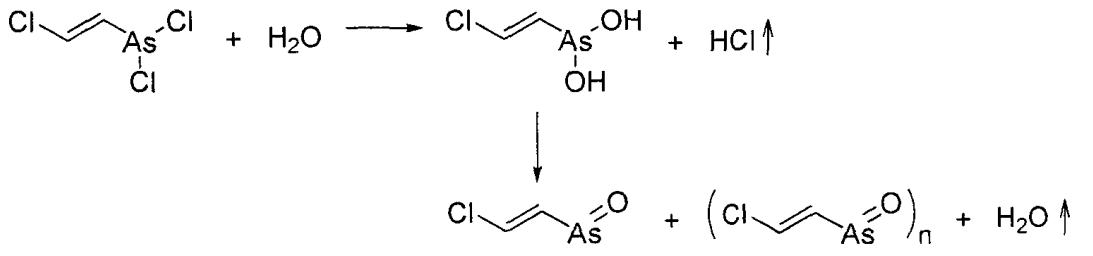

Scheme 1.5 Hydrolysis of Lewisite and formation of (polymerized) Lewisite oxide. (Modified from reference 28)

1.2 CWA Detection

The rise in the concern over the use of CWAs in criminal terrorist attacks has caused the growing interest in the detection of CWAs.[44-47] CWAs have been developed throughout the world and most of them are easily produced and have extreme toxicity. This makes it necessary to have rapid, reliable and affordable methods for the determination of CWAs and their related degradation products. Ideally, such a detection system will possess a high sensitivity and reproducibility, have a high selectivity to specific agents, will require little or no sample preparation, and will be suitable for field operations in terms of rugged design, thermal stability, insensitivity to common contaminants, modest power requirements, and low reliance upon consumables.

A lot of methods, techniques, and instruments have been developed for the detection of CWAs and their degradation products.[48-54] Especially after the Tokyo subway incident aggressive efforts have focused on obtaining better detectors for diverse scenarios.[55-58]

Conventional analytical techniques for CWAs fall into two main categories: one-dimensional sensors, which depend on the selective detection of analytes; and multi-dimensional sensors, in which analyte separation is coupled with their selective detection by single or combined analytical techniques.[48]

1.2.1 One-Dimensional Sensors

The most direct approach for chemical detection is to detect the targeted compound of interest selectively in the presence of other compounds and interferences. One-dimensional sensors are such selective detectors that measure the change in mass (quartz crystal microbalance), frequency or phase (surface acoustic wave devices), potential, current, or resistance (electrochemical sensors), and color or spectrometric information (fiber-optic sensors, colorimetric, fluorescence, phosphorescence, luminescence devices) upon the interaction of the analytes with the sensing probes.[59-61] Major analytical techniques applied in detection of CWAs and their degradation products are summarized in Table 1.2. Interactions between the analytes and the detecting probes depend on the properties of the sensing elements attached to the probe surfaces. They can be physical, chemical, or biological interactions. Nowadays sensors have been being developed to perform combination of these three interactions in order to enhance both sensitivity and selectivity.

1.2.1.1 Chemosensors

Polymer coatings are generally used in QCM and SAW sensors as chemical interfaces to detect organic vapors due to their high sensitivity, fast

Table 1.2 Analytical techniques for the detection of CWAs[19, 59, 60, 62]

Techniques	Detection mechanism	Selectivity	Sensitivity	Response time	Pros and Cons
Quartz Crystal Microbalance (QCM)	Changes of acoustic wave frequency from piezoelectric crystal caused by the mass change on the functionalized crystal surface due to the addition/removal of molecules onto the surface.	All absorbed chemicals affect the detection	1 ng/cm^2		Miniaturized, relatively low cost, good sensitivity, rapid response; Affected by surrounding temperature, false positive, relatively long time for an analysis cycle
Surface acoustic wave (SAW)	Changes of acoustic wave propagation path property on piezoelectric crystal caused by the sorption/desorption of chemicals on the substrate surface of the crystal.	All absorbed chemicals affect the detection	ppb (vapor)	Within seconds	
Electro-chemistry	Changes of potential or current generated by the oxidation or reduction reactions occurring on sensor surface; or the resistance upon absorbing targeted chemicals	Chemicals with similar redox reaction affect the detection	ppm (vapor) ppb (liquid)	Fast	Long-term monitoring, real-time measurement, process control, miniaturized, little power required; Low selectivity, sensitivity affected by environmental conditions and usage time
Colorimetry	Color changes resulted from the reaction between targeted chemicals and reagents.	High selectivity due to carefully selected reagents	Depends on human eyes	Depends on reaction time	Easy to use, small & simple, low-cost, visual detection, no electric power required, low false alarm rate; Many sensors needed for various kinds of targeted analytes
Optical spectrometry	Changes in absorption or emission bands of substances in the presence of targeted analytes.	High selectivity in luminescence spectroscopy		Within a minute	Reasonably high sensitivity; remote detection Energy generating source needed, affected by environmental conditions

vapor diffusion, reversible response and good ability to work at room temperature.[63, 64] In the selection of polymer materials, solubility interactions and linear solvation energy relationships that include such parameters as acidity, basicity, and polarizability have been considered.[65] For example, in the case of classifying nerve and mustard gases simulates, hexafluoro-2-propanol-substituted polysiloxane (SXFA), poly(epichlorohydrin) (PECH) and phenyl methyl polysiloxane (OV_{25}) were selected that approximately cover the full range

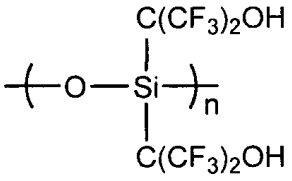

SXFA

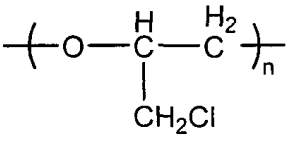

PECH

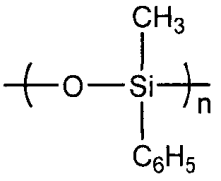

OV_{25}

of solubility parameters. SXFA, which is a highly acidic viscous liquid, could be selective for basic gases of organophosphorus compounds; while PECH with ether backbone and chloromethyl pendant groups that make it moderately dipolar and weakly hydrogen bonding could have preference for chlorinated hydrocarbons and moderately dipolar oxygenated vapors.[66] This type of polymer sensing systems was able to recognize the components in the mixture of warfare agent simulants.[66, 67] It was also reported that the thickness of the polymer film affected the sensitivity.[68] Although the response time of QCM and SAW sensors is within seconds, a complete analysis cycle including sampling time, desorption time from the preconcentrator, analysis time by the sensors, and recovery time to

clear the absorbed chemicals from the polymer takes some time,[69] which is still a challenge for the sensor development.

While both physical and chemical interactions are involved in above-mentioned sensors, chemical reaction is the essential element for optical detectors. Usually sensing reagents are selected to react only with a specific class of chemical compounds that produce the proper color change or optical signal for detection. Reactions range from simple pH-induced color changes to complex reactions such as phosphorylation, cyclization, and metal ion complex coordination.[62, 79, 80]

Phosphorylation and cyclization are major reactions in the detection of nerve agents by PET-based (photo-induced electron transfer) fluorescent chemosensors.[62] Several fluorescent indicator molecules were designed for the detection of nerve agents (Fig. 1.4).[70-72] Amine-containing fluorophore or hybrid materials were also produced for the detection using this reaction.[73, 74]

If the reactive moieties are connected to an azo dye, the phosphorylation and further intramolecular cyclization will affect the charge transfer band of the recognition molecule, resulting in a visible detection of the targeted analytes.[75]

In order to overcome the problem caused by the slow rates of phosphorylation reactions, highly nucleophilic oximate-containing sensors have been synthesized for colorimetric and fluorescent detection of CWAs (Fig. 1.5).[76-78]

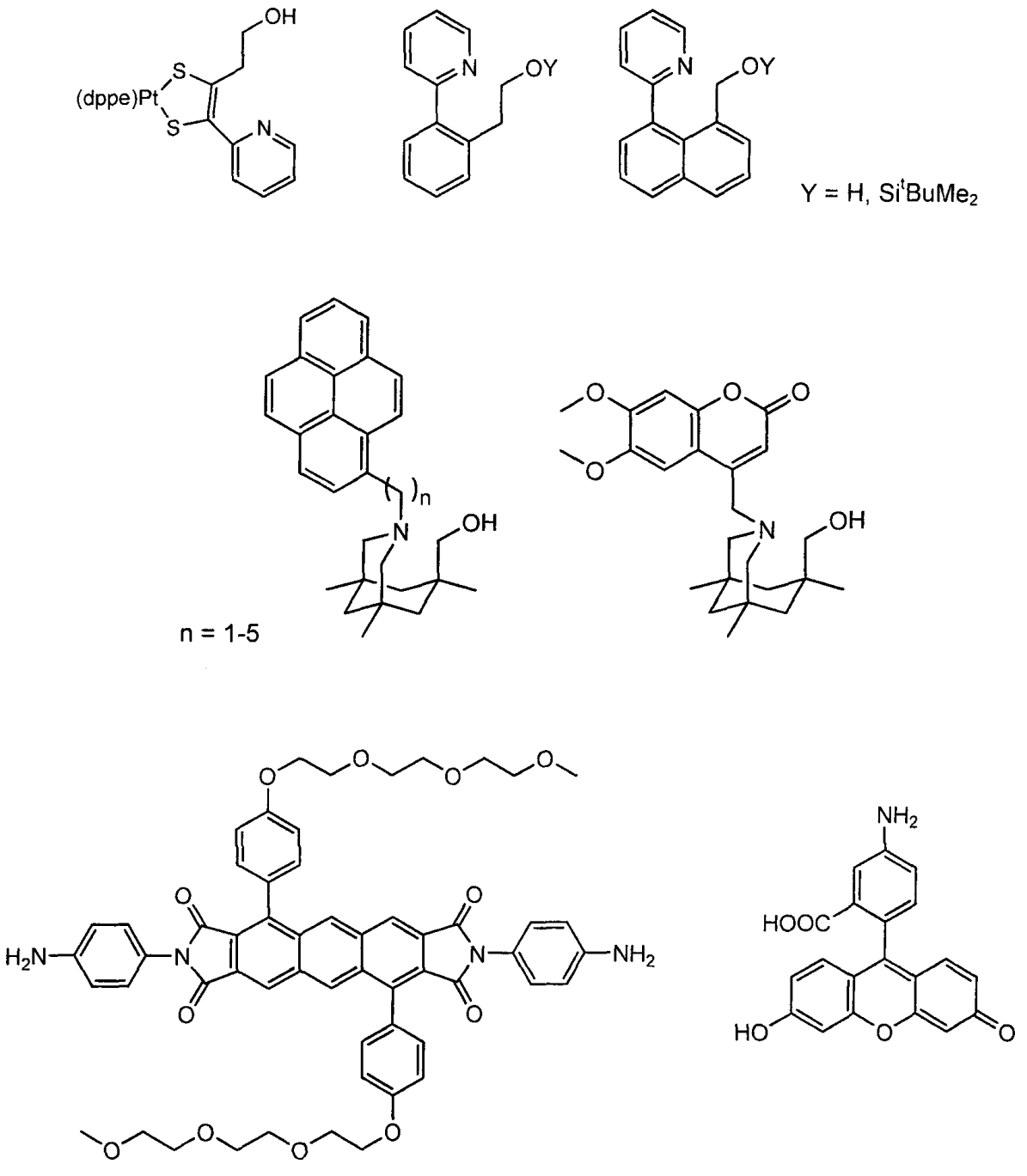

Fig. 1.4 PET-based fluorescent indicating molecules designed for detection of nerve agents.[71-73]

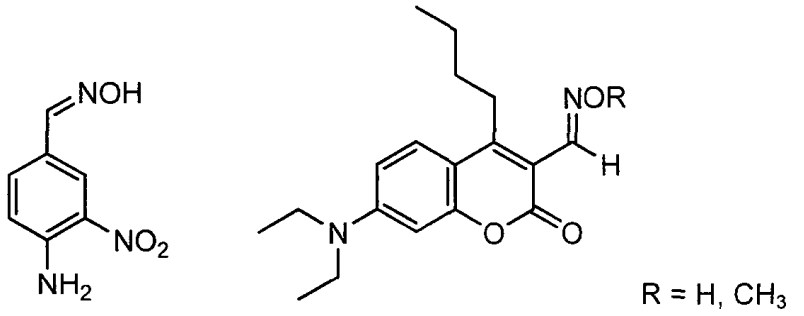

Fig. 1.5 Oximate-containing indicating molecules for detection of nerve agents. [76-78]

In general, chemosensors that are mainly based on a chemical interaction with analytes exhibit high sensitivity and selectivity to certain class of chemicals owing to the carefully selected or designed reagents. However, accurate detection for an analyte remains a challenge. Response time for the detection depends on the time needed for the specific chemical reactions which may be too long for a real-time continuous monitoring. And irreversible reactions will lead to disposable sensors only.

1.2.1.2 Biosensors

In biosensors, the sensing element is a molecule that has biological activity, such as an enzyme, antibody, DNA, or microorganism, which interacts with analytes mainly via biological or biochemical processes.[81] They are highly selective and able to be applied in many analytical techniques as transducers.

Cholinesterase molecules are the most common selected enzyme in the design of biosensors for detection of nerve agents.[74] However, this approach has several limitations. For example, the cholinesterase receptors are sensitive to less toxic organophosphate pesticides or even non-related compounds like heavy

metal and pH variation. Also, this kind of sensor needs a length incubation time and is unable to be reused because of the loss of enzyme activity due to the irreversible enzyme-ligand interactions, which is inefficient and time-consuming in many cases.

A "kinetic" approach for direct detection of nerve agents has been reported by Wild and co-workers,[82] in which agents were hydrolyzed by the enzyme organophosphate hydrolase (OPH). They also developed multi-enzyme strategy for discrimination among different classes of neurotoxins.[83] An OPH which is capable of cleaving P-O, P-F, and P-CN bonds via a S_N2 mechanism was used,[84, 85] resulting in unique classes of hydrolysis products and pH change of the solution. Thus direct detection is possible via measuring the pH change related to the enzyme activity.[82] In other research, organophosphorus acid anhydrolase (OPAA) has also been used for direct detection, which preferentially hydrolyzes P-F bond rather than P-O or P-S bonds.[86] This high specificity for a single substrate makes it the best for discriminative detection of fluorine containing organophosphates such as Sarin and Soman. Therefore, combined use of OPH and OPAA enables the discrimination among various organophosphate compounds.[87]

Despite the ease of handling such relatively simple one-dimensional sensors, they are nonseparation-based analytical methods that often experience interferences due to the complicated nature of the agents, resulting in false positive or negative responses.

1.2.2 Multi-Dimensional Sensors

In contrast, multi-dimensional methods often use instruments with separation steps prior to the measurement. The most common separation methods include gas and liquid chromatography (GC and LC), capillary electrophoresis (CE), ion mobility spectrometry (IMS), and mass spectrometry (MS).[88] The above techniques, either individual or in combination use exhibit increased sensitivity and reliability for CWA detection over most one-dimensional sensors.[89-91]

For example, single-particle aerosol MS allowed real-time, on-line detection of liquid CWAs at the ppb level.[92] Using GC with a pulsed-flame photometric detector, it was possible to detect of 20 ng/m^3 of organophosphorus compounds and 200 ng/m^3 for organosulfur within 30 s.[55] Combined use of GC and ICP-MS can separate and detect seven of both V-type and G-type nerve agents.[90] However, mistakes can be made with respect to identification of unknown analytes. Thus, for absolute identification, data obtained using complicated combination of three to four separation and analytical methods are normally recommended.[93, 94]

Though they have more accurate identification to the analytes, particularly to a mixture, such multi-dimensional sensors usually require a process of sample preparation and trained professionals to operate the equipments. Instruments with higher accuracy often cost higher in purchase and maintenance. Generally, such systems are not very portable. Performing on-site and real-time field operation remains a serious challenge for multi-dimensional detection systems.

1.2.3 Material Development for CWA Detection

Addition to the development in the analytical techniques for CWA detection the recent emergence of new materials including nanomaterials has offer excellent prospects for interfacing recognition in sensing area.[95-97] Due to their distinguishing structural, physical, or mechanical properties, nanomaterials have attracted widely interest in their synthesis and application. Carbon nanotubes (CNTs) are one of such materials.

1.2.3.1 Characteristics of CNTs

CNTs are hollow cylindrical tubes with diameters ranging between 1 and 100 nm. It can be envisioned as a rolled up graphite sheet into a seamless cylinder with fullerene caps for single wall carbon nanotubes (SWCNTs) or multiple sheets as multi-walled carbon nanotubes (MWCNTs) (Fig. 1.6).[98]

CNTs are well known for their combination of high electrical conductivity, high chemical stability and high mechanical strength in a unique way. Their tensile strength is 100 times of steel and thermal conductivity better than all but the purest diamond, as well as electrically conductivity similar to copper but with the ability to carry much higher currents.

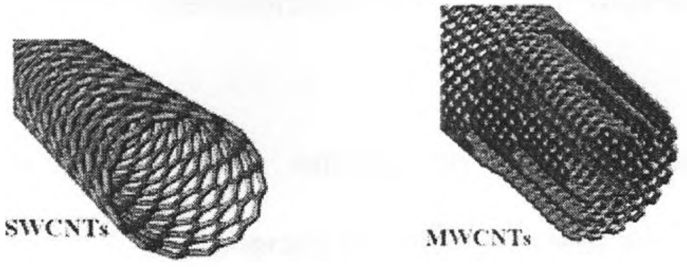

Fig. 1.6 Single-walled carbon nanotubes (SWCNTs) and multi-walled carbon nanotubes (MWCNTs).

The CNT could be metallic, semimetallic, or semiconducting according to the way in which the graphite sheet is rolled up.[99, 100] Their small size often accounts for their unique properties and gives important advantages for electroanalysis such as their large surface area (typically 200-300 m^2 per gram) and the ability to construct arrays of "nanoelectrodes". It is believed that the ends of the nanotubes are responsible for much of the chemical and electrochemical activity of the CNTs.[101, 102]

1.2.3.2 Modification of CNTs

The electronic, chemical and mechanical properties of CNTs can be tailored by physical or chemical modification. For example, boron or nitrogen doping generates *p* or *n* type conductors;[103, 104] metal-filled (i.e. Fe, Ni, Co, and Mo) CNTs have excellent protection of metals against oxidation that leads to a new kind of long-term stable ferromagnetic materials.[103]

As being used in sensing area, modification of CNTs, particularly on the surfaces, is necessary in many cases. CNTs can be modified by following strategies: (1) physical adsorption (physisorption) of the modifier to the CNT surfaces; (2) covalent bonding of the modifier to the CNT side walls or ends; (3) non-covalent interaction (chemisorption) of modifier with (functionalized) CNT surfaces.

There have been many reports on chemical and electrochemical modification of CNTs.[105, 106] Generally the the open end sites and defects are the most reactive spots for the modification reaction. Oxidation of the ends is often performed prior to modification to introduce reactive groups.[105, 106] For example,

concentrated sulfuric acid and/or nitric acid are often used to pretreat CNTs, resulting in shorter tubes and carboxyl groups on the side walls and at the ends of the tubes, which are for further modification and better solubility of CNTs.[107, 108]

Side wall functionalization can be achieved by carbene chemistry, nitrene addition, hydrogenation via the Birch reduction, fluorination, alkylation, arylation and 1,3-dipolar cycloadditon.[106] This direct covalent addition of reactive molecules to the nanotube sidewalls leads to partial destruction of the conjugated sp^2 lattice by the formation of sp^3 carbon atoms in the sidewalls. This can strongly influence the electronic properties of CNTs. The band-gap transition in the semiconducting tubes could be completely disrupted at a functionaliztion level of 2% of the SWNT carbon atoms.[109]

1.2.3.3 CNT Sensors for CWA Detection

CNTs are an ideal candidate material for a new class of molecular sensors due to their unique properties such as their high aspect ratio and simple adsorption of molecules causing significant changes in their electrical properties.[110, 111] Recently CNT-based chemical and electrochemical sensors for the detection of CWA and their simulants have been reported.[112]

Novak and his coworkers used SWCNTs random networks to detect the gas of nerve agent simulate at sub-ppb concentration levels by observation of the big changes in CNT resistance.[113] The mechanism of this simple fabricated SWCNT-based chemosensor depends on the adsorption of the basic nerve agent on SWCNTs, resulting in an effecting transfer of negative charge that manifests itself as a shift of the transistor threshold voltage. The molecular adsorption can

be fully reversible by applying a small positive gate bias that releases the mimics from the nanotube surface.

Wang, Gu, and Swager[114] used spin-casting to fabricate a conductive polymer/SWCNTs chemiresistor sensor which provided increased sensitivity and selectivity in detecting nerve agent simulant gas. The sensory mechanism involves the charge transfer, introduction of scattering sites, and an increased physical separation of the SWCNTs caused by the interaction of the polymer and the analytes.

An Fc-amino acid conjugate physically modified MWCNT electrochemical sensor was developed by Khan and his coworkers.[115] The interaction between the CWA mimics and the transducer surface caused significant changes in electrochemical signals, which allowed a detection to sub-ppb level.

CNT-based amperometric enzyme electrodes,[116-118] disposable thick film strip electrodes,[119-121] and flexible biosensors[122] for V-type nerve agent detection were also reported. It is suggested that a large surface and catalytic activity of CNTs play vital roles in these sensors which provided a high sensitivity, large linear range and low detection limit for analysis of CWAs.

1.3 Research Motivation and Approach

My thesis research focused on the detection of mimics of nerve agents and sulfur mustard and their decomposition products in solution by electrochemical techniques. Electrochemical sensors with specially functionalized surfaces to enhance selectivity are potentially very sensitive and

applicable to long-term monitoring with the development of receptors.[123] Previous research in our group has shown the use of thin films prepared from a number of ferrocene (Fc) conjugates for the detection of CWA mimics.[124] More recently our group reported on the non-covalent modification of multi-walled carbon nanotubes (MWCNTs) with Fc-peptides on indium-tin oxide (ITO) surfaces for the detection of CWA mimics, which were found to exhibit a high sensitivity for G-type nerve agents.[115] However, the mechanical stability of the sensor system is insufficient, presumably due to the weak physisorption of Fc-conjugates on the MWCNTs.

In my research, the focus was on using covalently linked Fc-peptide-CNT conjugates as recognition layers. Fc-peptide derivatives were obtained by Fc-COOH reacting with amino acid or peptide, such as lysine or leucin-lysine. Next, MWCNTs modified with these Fc derivatives were carried out by covalent attachment in order to improve the mechanical stability. The properties of prepared Fc-peptide derivatives and modified MWCNTs were evaluated with spectroscopic and electrochemical methods. Basically cyclic voltammetry (CV) and differential pulse voltammetry (DPV) are used in this research. In particular, the detection studies were focus on a mimic of Tabun and hydrolysis products of nerve agents, as well as a simulant of sulfur mustard (Fig. 1.7).

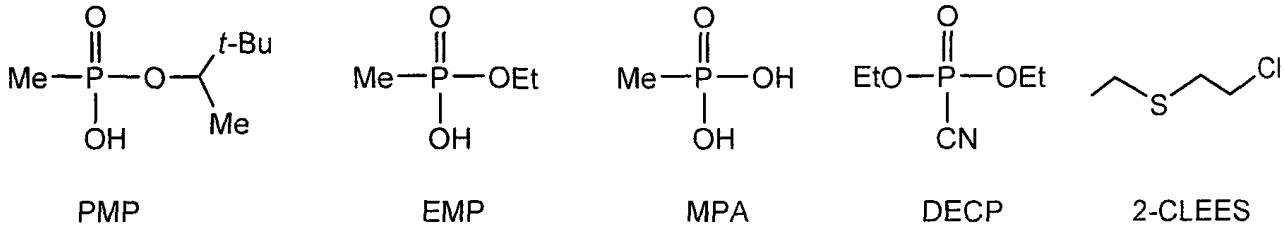

Fig. 1.7 Chemical drawings of the chemical warfare agent mimics: pinacolyl methylphosphonate (PMP), ethyl methylphosphonate (EMP), methylphosphonic acid (MPA), diethyl cyanophosphonate (DECP), and 2-chloroethyl ethyl sulfide (2-CLEES).

Chapter 2 EXPERIMENTAL

2.1 General Remarks

CH_2Cl_2 (Caledon laboratoryes Ltd, Ontario, Canada, 99.5%) was dried over CaH_2 and distilled under nitrogen prior to use. Other reagents were used without subsequent purification. H-Lys(Boc)-Ome·HCl, H-Leu-Ome·HCl, and Arg(NO_2)(Boc)-OH were purchased from EMD Chemicals Inc., Gibbstown, New Jersey. Pinacolyl methylphosphonate (PMP), ethyl methylphosphonate (EMP), methylphosphonic acid (MPA), diethyl cyanophosphonate (DECP), and 2-chloroethyl ethyl sulfide (2-CLEES) were purchased from Sigma-Aldrich Corp. St. Louis, Missouri. MWCNTs with 3–8 μm in length and 8–15 nm in diameter were purchased from NanoNB Corp., Fredericton, New Brunswick. ITO substrates were purchased from SPI Supplies, West Chester, Pennsylvania, U.S. Polytetrafluoroethylene (PTFE) membranes were purchased from Sartorius AG, Goettingen, Germany. Fc-COOH was obtained from Mark Milne. Fc-CO-$NH(CH_2)_4NH$(Boc) was obtained from Chantelle Davidson. NMR spectra were recorded on a Varian MERCURY 400 MHz spectrometer operating at 400.1 MHz (^1H) and 100 MHz ($^{13}C\{H\}$). Peak positions in both ^1H and ^{13}C spectra are reported in ppm relative to TMS and coupling constants J in Hz. The ^1H NMR spectra are referenced to residual solvent proton. $^{13}C\{^1H\}$ NMR spectra are referenced to the $CDCl_3$ signal at δ 77.23. Mass spectrometry was carried out on a Finnigan MAT 8200 instrument by Doug Hairsine. SEM was performed on a Leo 1540 FIB/SEM CrossBeam microscopy by Todd Simpson. IR experiments

were carried out on Bruker FT-IR spectrometer as KBr disc. Raman spectra were recorded on a Renishaw system 2000 Raman spectrometer equipped with a LN_2 cooled CCD detector by Shuntai Xie.

2.2 Synthesis of Ferrocene-amino acid / peptide Conjugates

Fc-CO-Lys(Boc)-OMe (1). Fc-COOH (0.240 g, or 1.00 mmol) was dissolved in 100 mL DCM with HOBt (1.1 eq) and HBTU (1.1 eq) with TEA. This stirred for 30 min on ice followed by the addition of Lys(Boc)-OMe (1.2 eq) and was then stirring overnight. The solution was subsequently washed with saturated $NaHCO_3$, 10% citric acid, and finally distilled H_2O. The crude product was then purified by column chromatography on SiO_2 using a mobile phase of EtOAc (R_F = 0.5), giving the desired orange-red products. 60% yield (0.280 g). ESI-MS (m/z) calc. for $C_{23}H_{32}FeN_2O_5$: 472.17, found 472.54. ^{1}H NMR (400 MHz, $CDCl_3$, 293 K): 6.19 (s, 1 H, CONH) ; 4.73 (s, 2 H, Fc-H) ; 4.67 (s, 1 H, α-H) ; 4.58 (m, 1 H, Boc-NH) ; 4.35 (s, 2 H, Fc-H) ; 4.21 (s, 5 H, Fc-H) ; 3.77 (s, 3 H, $COOCH_3$) ; 3.11 (s, 2 H, CH_2) ; 1.92 (s, 1 H, CH_2) ; 1.75 (s, 1 H, CH_2) ; 1.52 (s, 2 H, CH_2) ; 1.41 (m, 2 H, CH_2) ; 1.41 (s, 9 H, Boc). ^{13}C NMR ($CDCl_3$, 293 K): 173, 170, 156, 70.86, 70.76, 70.00, 68.70, 68.27, 52.67, 51.97, 40.39, 32.57, 29.77, 28.63, 22.86.

Fc-CO-Leu-Lys(Boc)-OMe (2). Fc-CO-Leu-OMe (0.070 g, or 0.20 mmol) was prepared according to the procedure described above for the synthesis of Fc-CO-Lys(Boc)-OMe. Fc-CO-Leu-OMe was hydrolyzed under basic conditions to give Fc-CO-Leu-OH which was then dissolved in 100 mL DCM with HOBt

(1.1 eq) and HBTU (1.1 eq) with TEA. This was stirring for 30 min on ice followed by the addition of Lys(Boc)-OMe (1.2 eq) and stirring overnight. The solution was next washed with saturated $NaHCO_3$, 10% citric acid, and finally distilled H_2O. The crude product was purified by column chromatography on SiO_2 using a mobile phase of EtOAc (R_F = 0.5), giving the desired orange-red products. 70% yield (0.080 g). ESI-MS (m/z) calc. for $C_{29}H_{43}FeN_3O_6$: 585.25, found 583.83. ^1H NMR (400 MHz, $CDCl_3$, 293 K): 6.93 (m, 1 H, CONH) ; 6.22 (m, 1 H, CONH) ; 4.95 (s, 1 H, Boc-NH) ; 4.7 (m, 2 H, Fc-H) ; 4.58 (m, 2 H, α-H) ; 4.36 (s, 2 H, Fc-H) ; 4.22 (m, 5 H, Fc-H) ; 3.74, 3.69 (s, 3 H, $COOCH_3$) ; 3.09 (m, 2 H, Boc-NH-$C\underline{H_2}$) ; 1.86 (m, 2 H, β-H) ; 1.73 (m, 2 H, β-H) ; 1.67 (m, 2 H, β-H) ; 1.45 (m, 1 H, Leu-CH) ; 1.42 (m, 9 H, Boc-H) ; 1.25 (m, 2 H, Lys-CH_2) ; 0.99 (m, 6 H, Leu-CH_3). ^{13}C NMR ($CDCl_3$, 293K): 197, 183, 173, 71.01, 70.06, 68.59, 52.63, 52.33, 51.89, 28.70, 25.61, 25.20, 25.08, 25.08, 23.22, 22.34.

Fc-CO-Lys(Boc)-Leu-OMe (3). Compound **1** (0.112 g, or 0.200 mmol) was hydrolyzed to give Fc-CO-Lys(Boc)-OH which was then dissolved in 100 mL DCM with HOBt (1.1 eq) and HBTU (1.1 eq) with TEA. This was stirred for 30 min on ice followed by the addition of Leu-OMe (1.2 eq) and stirring overnight. The solution was then washed with saturated $NaHCO_3$, 10% citric acid, and finally distilled H_2O. The crude product was purified by column chromatography on SiO_2 using a mobile phase of EtOAc (R_F = 0.5), giving the desired orange-red products. 65% yield (0.090 g). ESI-MS (m/z) calc. for $C_{29}H_{43}FeN_3O_6$: 585.25, found: 583.75. ^1H NMR (400 MHz, $CDCl_3$ 293 K): 6.56 (m, 1 H, CONH) ; 6.36 (m, 1 H, CONH) ; 4.74 (m, 1 H, Boc-NH) ; 4.71 (s, 2 H, Fc-H) ; 4.60 (m, 2 H, α-H) ; 4.36 (s, 2 H, Fc-H) ; 4.22 (m, 5 H, Fc-H) ; 4.20 (3 H, s) ; 3.75, 3.70 (s, 3 H,

$COOCH_3$) ; 3.10 (m, 2 H, Boc-NH-C$\underline{H}_2$) ; 1.95 (m, 2 H, β-H) ; 1.67 (m, 2 H, β-H) ; 1.57 (m, 2 H, β-H) ; 1.46 (m, 1 H, Leu-CH) ; 1.42 (m, 9 H, Boc-H), 0.95, 0.93 (m, 6 H, Leu-CH_3). ^{13}C NMR ($CDCl_3$, 293K): 197, 183, 173, 71.01, 70.06, 68.59, 52.63, 52.33, 51.89, 28.70, 25.61, 25.20, 25.08, 25.08, 23.22, 22.34.

(Boc)Arg(NO_2)-NH(CH_2)$_4$NH-CO-Fc (4). Fc-CO-NH(CH_2)$_4$NH(Boc) (0.440 g or 1.10 mmol) was dissolved in 50 mL DCM with trifluoroacetic acid (TFA, 1.5 eq). This stirred for 30 min in ice bath followed by rotoevaporation of solvent and excess TFA. This Boc-removed Fc-CO-NH(CH_2)$_4$$NH_2$ was washed by DCM and then dissolved in 10 mL DCM with TEA.

(Boc)Arg(NO_2) –OH (0.320 g or 1 mmol) was dissolved in 10 mL DCM with TEA (0.5 mL) and stirring until solution turned clear. HOBt (1.1 eq) and HBTU (1.1 eq) were added and the mixture was stirred for 30 min on ice followed by the addition of above solution of Fc-CO-NH(CH_2)$_4$$NH_2$ and was then stirred overnight. The solution was subsequently washed with saturated $NaHCO_3$, 10% citric acid, and finally distilled H_2O. The crude product was then purified by column chromatography on SiO_2 using a mobile phase of EtOAc : MeOH 4:1 (R_F = 0.5), giving the desired orange-red products. 60% yield (0.360 g) ESI-MS (m/z) calc. for $C_{23}H_{32}FeN_2O_5$: 601.48, found 601.10. ^1H NMR (400 MHz, CD_3OD, 293 K): 6.88 (m, 1 H, CONH) ; 6.78 (m, 1 H, CONH) ; 5.64 (m, 1 H, Boc-NH) ; 4.71 (s, 2 H, Fc-H) ; 4.36 (s, 2 H, Fc-H) ; 4.20 (m, 5 H, Fc-H) ; 3.98 (m, 1 H, Boc-NH-C$\underline{H}_2$) ; 3.27 (m, 6 H, α-H) ; 1.74 (m, 2 H, β-H) ; 1.57 (m, 6 H, β-H) ; 1.42 (m, 9 H, Boc-H).

2.3 Modification of MWCNTs with Ferrocene-amino acid / peptide Conjugates

Pretreatment of MWCNTs. MWCNTs were shortened according to the standard literature procedure[107, 125] and our previous publication[115]. Briefly, 10 mg of MWCNTs were put into 10 mL of the mixture of concentrated 3:1 H_2SO_4 and HNO_3. The mixture was sonicated at 70°C for ~12 h. The cutting reaction was quenched by diluting the MWCNT suspension with approximately five times the amount of MilliQ water and the mixture were cooled to room temperature in an ice bath, followed by precipitation of all MWCNTs with centrifugation (Eppendorf Centrifuge 5415C, 12000 rpm for 20 min) and thoroughly washed with MilliQ water to remove acids and filtration with PTFE membranes, and finally dried under vacuum at 60°C for 1 h.

Deprotection of Fc-amino acid / peptide conjugates. Boc protected Fc-amino acid / peptide conjugates (0.02 mmol) were dissolved in 5 mL DCM with trifluoroacetic acid (TFA, 1.5 eq). This mixture was stirred for 30 min in ice bath followed by rotoevaporation of solvent and excess TFA. These Boc-removed Fc-conjugates were washed by DCM and then dissolved in DMF with TEA.

Coupling reaction. Pretreated MWCNTs in DMF was ultrasonicated for 1 h and another 10 min with the addition of HBTU and TEA. To the suspension was added above Boc-removed Fc-conjugates solution. The reaction mixture was stirred overnight, followed by precipitation of all CNTs and thoroughly washed with methanol to remove any unreacted Fc-compounds by centrifugation (Eppendorf Centrifuge 5415C, 12000 rpm for 20 min) and filtration with PTFE

membranes, and finally dried under vacuum at 40°C for 1 h. The prepared Fc-conjugates modified MWCNTs were listed in Table 2.1.

Table 2.1 Fc-conjugates modified MWCNTs

Abbr. names	Modified MWCNTs
1-sMWCNT	Fc-CO-Lys(MWCNT)-OMe
2-sMWCNT	Fc-CO-Leu-Lys(MWCNT)-OMe
3-sMWCNT	Fc-CO-Lys(MWCNT)-Leu-OMe
4-sMWCNT	(MWCNT)Arg(NO_2)-NH(CH_2)$_4$NH-CO-Fc

2.4 Modification of ITO with Modified MWCNTs

Cleaning of ITO substrates. ITO substrates were first rubbed with a soft cotton cloth saturated with soapy water and thoroughly rinsed with MilliQ water; then were cleaned in an ultrasonic bath (30 min each cycle) in MilliQ water/Triton X-100, MilliQ water and finally pure ethanol. Samples then were dried in a stream of nitrogen prior to use.

Deposition of MWCNTs on ITO surface. The suspension of modified MWCNTs in DMF was ultrasonicated for 1 h. An aliquot (5 μL) of the suspension was put on the cleaned ITO surface. The substrates were dried at room temperature in the air in a Hamilton SafeAire fume hood.

For the MWCNT films prepared for SEM measurements, the suspension of MWCNTs / modified MWCNTs was diluted with 10 times of solvent. A small drop

(3 μL) of the suspension was put on a silicon wafer, followed by a quick dry on a hotplate.

2.5 Electrochemical Measurements

The electrochemical experiments were carried out at room temperature using a potentiostat from CHI 660B Instruments. For the measurements with prepared Fc-compounds in solution, a glassy carbon electrode was used as working electrode with Pt wire as counter electrode and Ag/AgCl as reference electrode. 1 mM solution of the compounds in MeCN was prepared and 0.1 M $LiClO_4$ was used as supporting electrolyte.

In the study of Fc-conjugates-MWCNTs modified ITO sensors, a modified ITO substrate was placed into the homemade electrochemical cell (Fig. 2.1)[115], to which 5 mL of supporting electrolyte (2.0 M $NaClO_4$) was added. Pt wire was used as counter electrode and Ag/AgCl as reference electrode. According to the plan of the homemade electrochemical cell, the surface area of the ITO electrode is 2.01 cm^2.

For the measurements with CWA mimics, a desired concentration of the CWA mimic solution was added into the electrolyte and the resultant mixture incubated for 15 min before measurements were taken. Serial dilutions of CWA mimic solution were prepared with MilliQ water (18.2 mΩ).

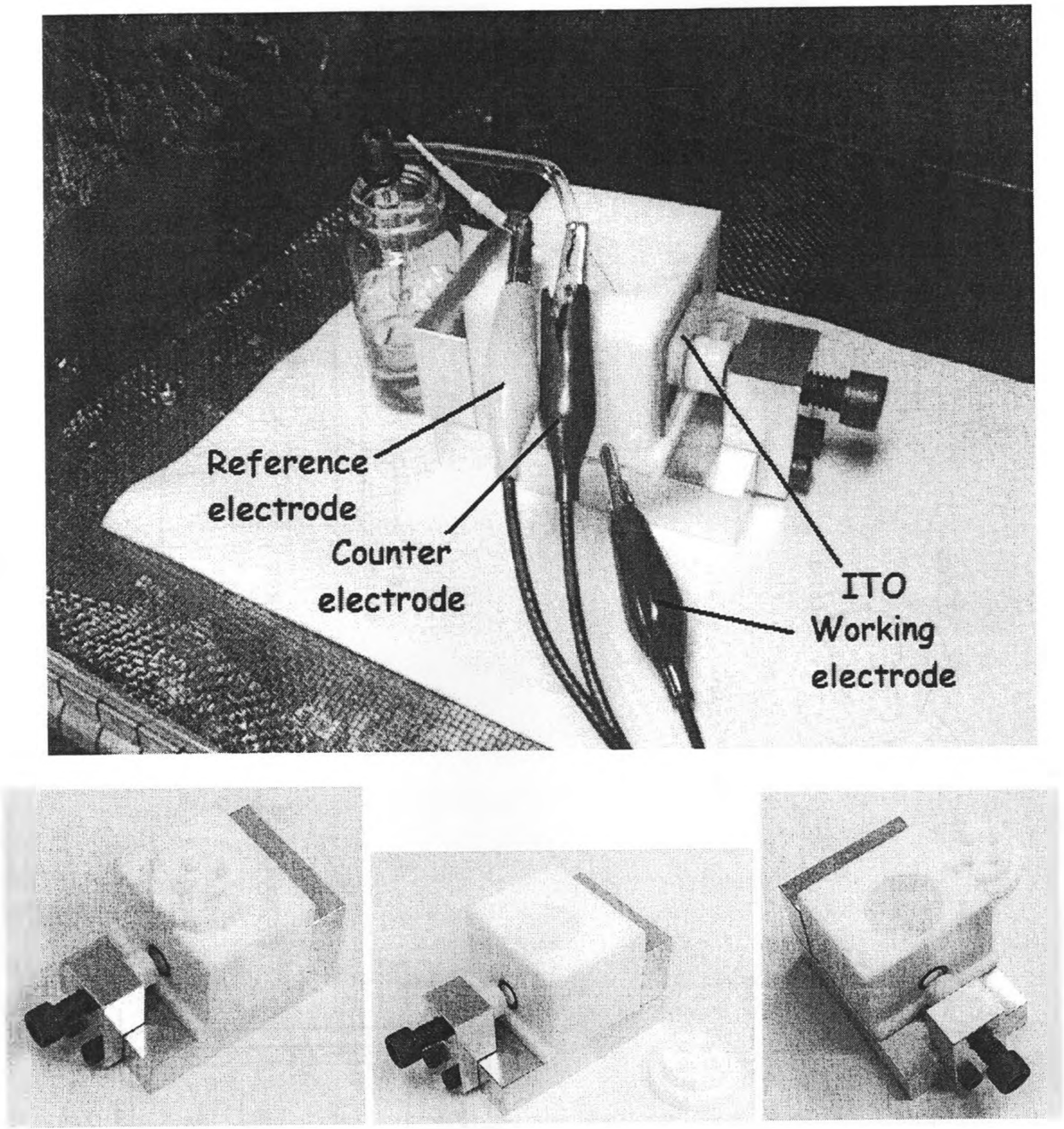

Fig. 2.1 The homemade electrochemical cell for the MWCNT modified ITO electrodes.

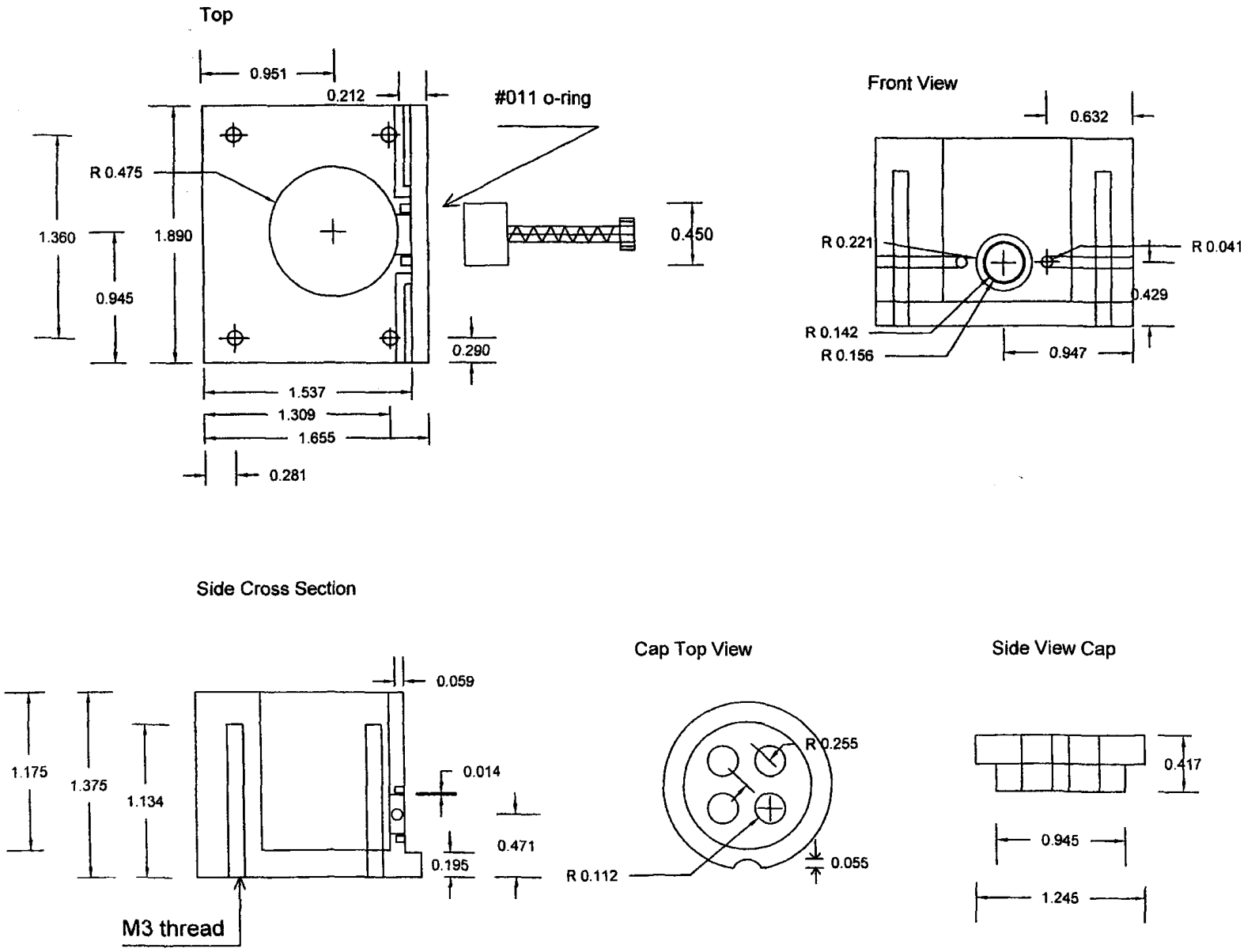

Scheme 2.1 The plan for the homemade electrochemical cell.

Chapter 3 RESULTS AND DISCUSSION

3.1 Synthesis of Ferrocene-amino acid / peptide Conjugates

The Fc-amino acid / peptide conjugates were synthesized according to the HBTU/HOBt protocol[126] using ferrocene carboxylic acid reacting with Boc-protected lysine, leucin ester, or diamine as briefly shown in Scheme 3.1. For the synthesis of compound **2**, Fc-CO-Leu-Lys(Boc)-OMe, the intermediate product, Fc-CO-Leu-OMe, was hydrolyzed under basic conditions to produce Fc-CO-Leu-OH for further coupling reaction with Boc-protected lysine ester to form compound **2**. Similar hydrolysis procedure was applied to Fc-CO-Lys(Boc)-OMe prior to the coupling reaction with Leu-OMe to generate compound **3**, Fc-CO-Lys(Boc)-Leu-OMe. For the synthesis of compound **4**, Fc-CO-NH$(CH_2)_4$NH(Boc) was removed Boc by TFA before coupling with Boc protected arginine to form compound **4**. These Fc-conjugates were purified by column chromatography, giving orange-yellow solids. The NMR and mass spectra of the prepared compounds are compatible with their composition.

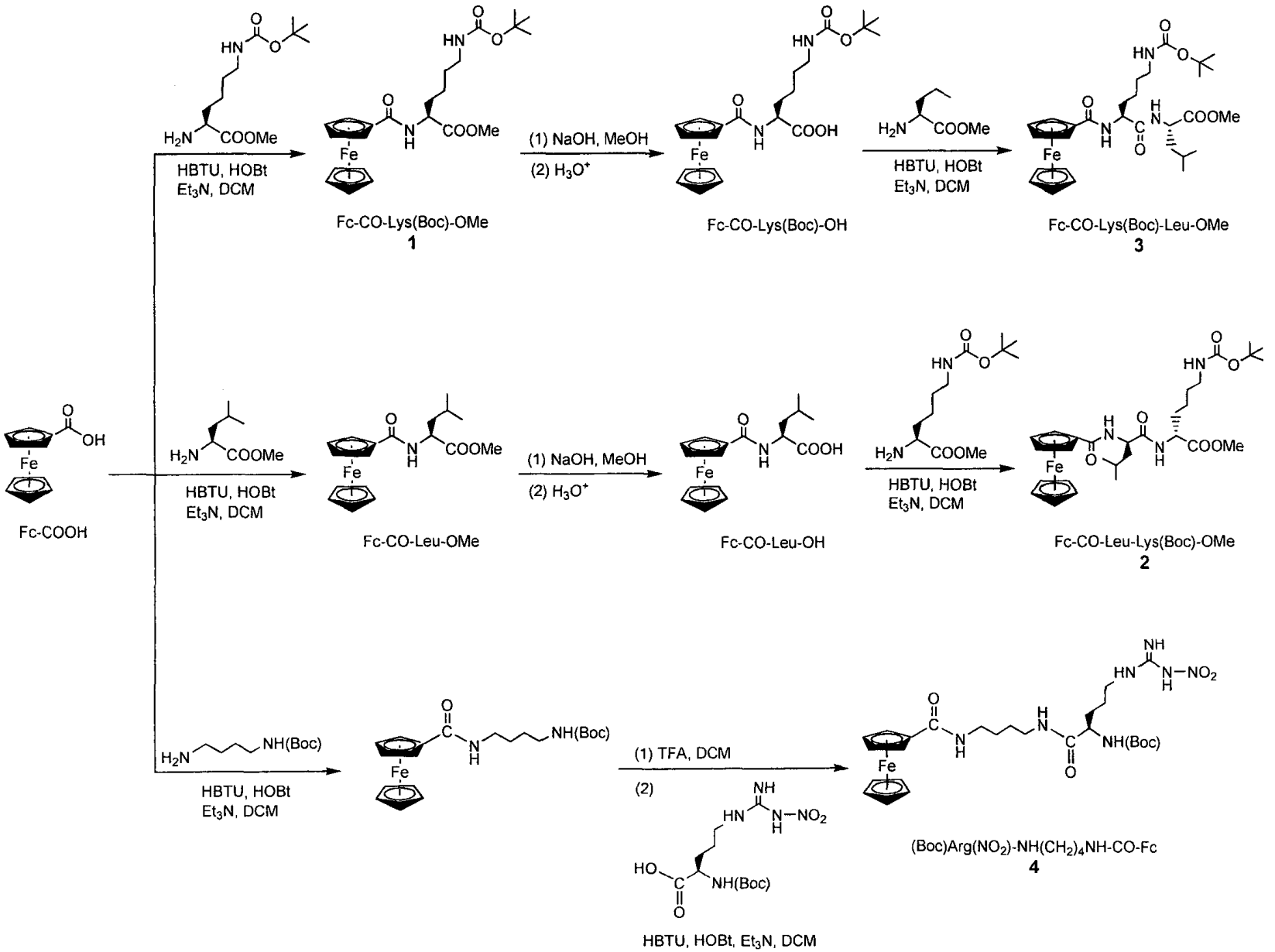

Scheme 3.1 Synthesis of Fc-amino acid / peptide conjugates

Electrochemical study of the synthesized Fc-compounds was carried out using cyclic voltammetry (CV). CVs for the four prepared compounds are shown in Fig. 3.1 and a summary of results is presented in Table 3.1. All compounds exhibited a quasi-reversible one-electron oxidation with peak current ratios close to unity. The halfwave potentials ($E_{1/2}$) for the three compounds were observed in the range of 520–550 mV versus Ag/AgCl with anodic to cathodic peak separation values (ΔE) of around 70 mV. It is likely that the electronic environment around Fc group in these compounds is similar since the alkyl chains close to the ferrocene ring have similar structural and electronic properties.

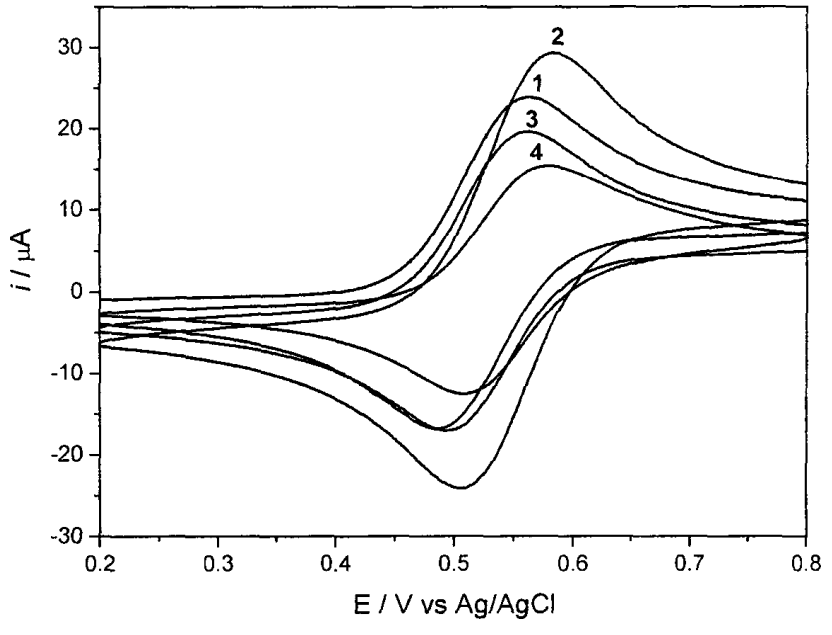

Fig. 3.1 CV responses of solution of 1 mM compounds **1** (Fc-CO-Lys(Boc)-OMe), **2** (Fc-CO-Leu-Lys(Boc)-OMe), **3** (Fc-CO-Lys(Boc)-Leu-OMe), and **4** ((Boc)Arg(NO_2)-NH(CH_2)$_6$NH-CO-Fc) in MeCN, respectively. Measurements were taken in solution of 0.1 M $LiClO_4$ in MeCN with glassy carbon as working electrode at a scan rate of 100 mV s^{-1}.

Table 3.1 CV parameters for compounds **1**, **2**, **3**, and **4**

Compound	$E_{1/2}$ / mV	ΔE / mV	i_{pa} / i_{pc}
1	526 (±1)	77 (±3)	1.04 (±0.01)
2	529 (±1)	68 (±1)	1.04 (±0.01)
3	546 (±2)	76 (±3)	1.03 (±0.01)
4	543 (±1)	65 (±2)	0.93 (±0.01)

Experimental conditions were as described in **Fig. 3.1**.

It may be noted that there is relatively big difference in the current intensity of these four compounds. According to Randles-Sevick equation (eq 3.1) and Stokes-Einstein relationship (eq 3.2), peak current intensity is proportional to square root of diffusion coefficient which depends on the temperature, viscosity of the fluid and the size of the particles. The CV measurements of these four compounds were taken under the same conditions using the same working electrode. Their peak current should be inversely proportional to their particle size. Since compound **4** is a big molecule with higher molecular weight than the other three compounds, it displayed decreased peak current intensity in the measurement.

$$i_p = (2.69 \times 105) n^{3/2} A D^{1/2} v^{1/2} C$$

Equation 3.1 Randles-Sevick equation. n is the number of electrons, A is the electrode area (in cm^2), C is the concentration (in mol cm^{-3}), D is the diffusion coefficient (in $cm^2\ s^{-1}$), and v is the scan rate (in $V\ s^{-1}$).

$$D = \frac{k_B T}{6\pi\eta R}$$

Equation 3.2 Stokes-Einstein relationship. K_B is the Boltzmann constant, T is the temperature (in K), η is the viscosity (in Pa s), R is the radius of a particle (in m).

3.2 Modification of MWCNTs with Ferrocene-Conjugates

MWCNTs were shortened by heating and ultrasonication in strong acids (concentrated H_2SO_4 and HNO_3) according to the literature procedure[107, 125] (Scheme 3.2). The strong acids help a smooth cut and enable nanotubes to be shortened at a rate of roughly 130 nm/h.[107, 108] Therefore, this oxidation procedure created short MWCNTs (sMWCNTs) with carboxylic functions on the ends and side walls, which can be easily suspended, sorted and modified with other molecules. For example, the sMWCNTs could be dispersed in polar solvents, such as DMF, ethanol and water more easily than the crude ones. The suspension of sMWCNTs in DMF was stable without aggregation for more than two months.

Chemical modification of the MWCNTs was carried out by the reaction of sMWCNTs with Fc-conjugates **1**, **2**, **3**, and **4**, in the present of HBTU in organic solvent under basic conditions (Scheme 3.2).[127] The reaction product was collected by precipitation via centrifugation and washed thoroughly with methanol then dried in vacuum. The modified sMWCNTs showed a lesser degree of dispersion in ethanol or water than did the unmodified sMWCNTs. This is due to the reduced hydrophilic carboxylic groups on the sMWCNTs surface and the introduction of alkyl chains from the Fc-amino acid conjugates.

The sMWCNTs before and after modification of Fc-conjugates were investigated by FT-IR spectroscopy. The IR spectra of sMWCNTs exhibit the typical C=O band at 1721 cm^{-1} (trace (a) in Fig. 3.2), which indicates the presence of carboxylic acid group. This absorption feature is absent in the original CNTs. After modification of the sMWCNTs, a C=O amide stretching band characteristic of a Fc-conjugates' functional group appeared at 1637–1657 cm^{-1}. The presence of C–H stretching band in the range of 2850–2950 cm^{-1} region (Table 3.2) suggests the formation of amide bonds during the coupling reaction of MWCNTs with Boc deprotected Fc-conjugates.[126]

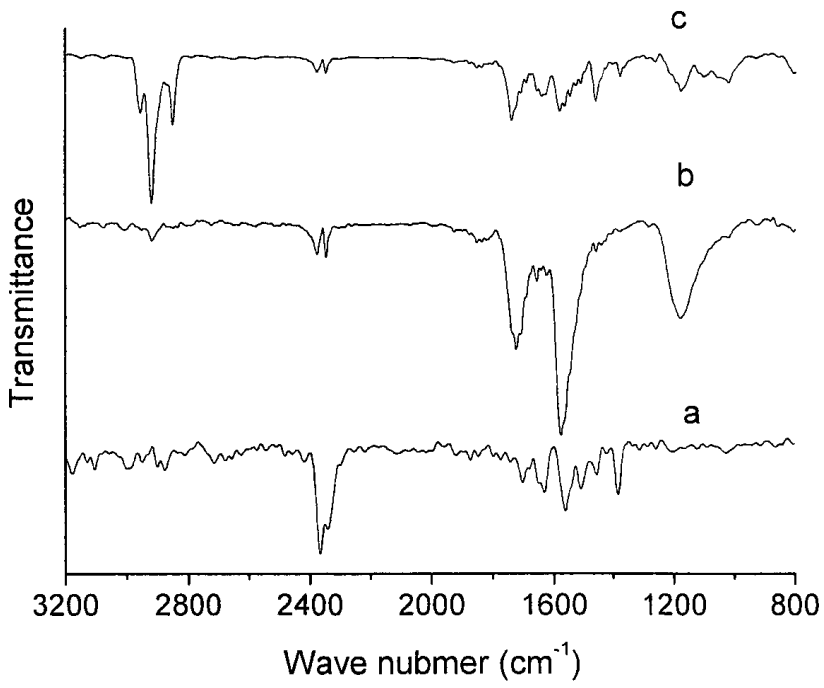

Fig. 3.2 FT-IR spectra for (a) purchased MWCNTs, (b) shortened MWCNTs, and (c) **1**-sMWCNT.

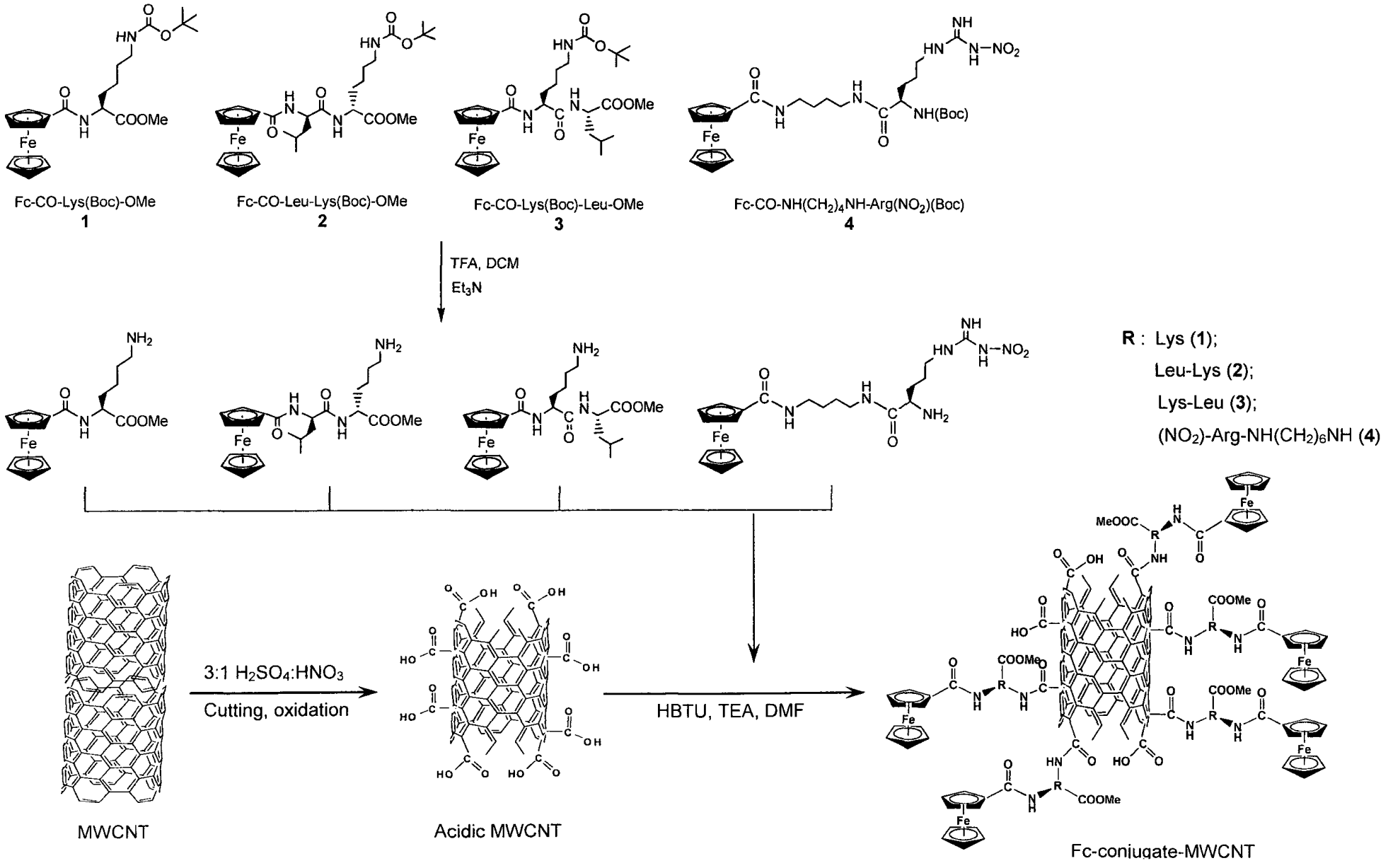

Scheme 3.2 MWCNT pretreatment and modification with Fc-conjugates

Table 3.2 Selective spectroscopic data for purchased and modified MWCNTs

	IR (KBr, cm^{-1})	Raman (cm^{-1})
Purchased MWCNTs	--	1579 (G-mode), 1342 (D-mode), I_D/I_G = 1.2
Shortened MWCNTs	1721 (C=O)	1578 (G-mode), 1355 (D-mode), I_D/I_G = 0.85
1-sMWCNT	1637 (C=O), 2887 (C-H)	1581 (G-mode), 1354 (D-mode), I_D/I_G = 1.0
2-sMWCNT	1657 (C=O), 2850 (C-H)	1580 (G-mode), 1354 (D-mode), I_D/I_G = 1.1
3-sMWCNT	1645 (C=O), 2950 (C-H)	1581 (G-mode), 1355 (D-mode), I_D/I_G = 1.1

The characterization of the MWCNT samples was also explored by Raman spectroscopy. For example, Fig. 3.3 shows the purchased MWCNT, shortened MWCNT and sMWCNT modified with compound **1**. The feature peak at around 1580 cm^{-1} represents the tangential mode (G-mode) and the peak at 1330–1360 cm^{-1} represents the disorder mode (D-mode).[128-130] The strength of the D-mode relative to the G-mode is a measure of the amount of disorder in the CNTs.[127] The commercial MWCNT shows a high I_D/I_G ratio (1.2) according to the high degree of defects in the nanotubes.[127] This ratio decreased slightly after acid-treatment (0.85). It might be due to the removal of those highly soluble nanotubes with small length and high degree of functionalization during the wash process. After modification with compound **1**, the I_D/I_G ratio increased slightly (1.0), suggesting an increment of disorder in the nanotubes which may be affected by the steric and electronic properties of the functional groups. Similar results were observed from the samples of sMWCNT modified with other Fc-conjugates and provided in Table 3.2. A distinct Raman difference was also observed in the radial breathing mode (250–500 cm^{-1}), depending not only on the

tube diameter and chirality but also on the functional group coverage and adsorption configurations.[115]

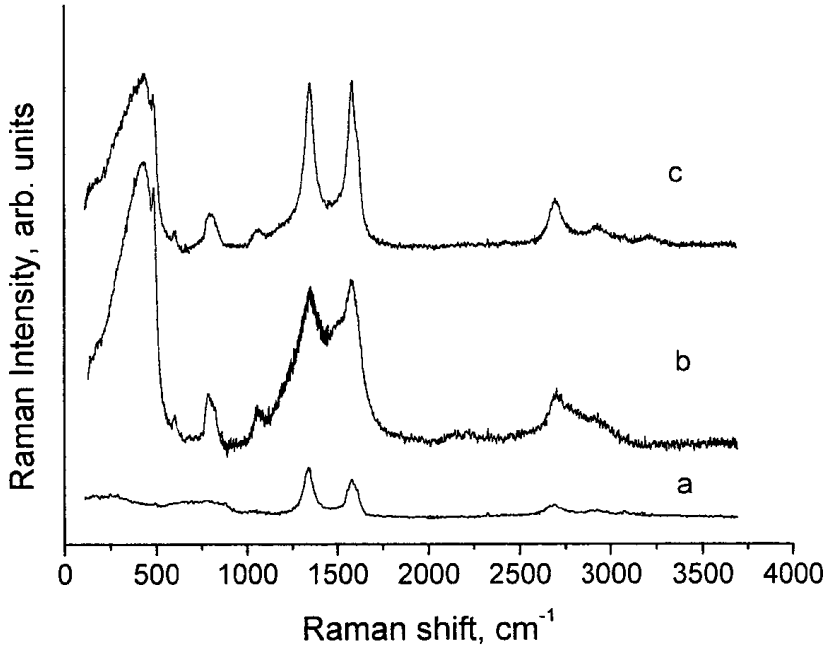

Fig. 3.3 Raman spectra for (a) purchased MWCNTs, (b) shortened MWCNTs, and (c) **1**-sMWCNT.

MWCNTs before and after acid treatment were observed by SEM as well. From Fig. 3.4 (a and b) one can see that the acid-treated tubes are much shorter than the original ones and exhibit aggregation probably due to hydrogen bonding related to the new generated carboxylic groups. Some of them also show shaggy edges and peels on the end and side walls (Fig. 3.4 c and d), which may be due to the defects introduced during the cutting process.

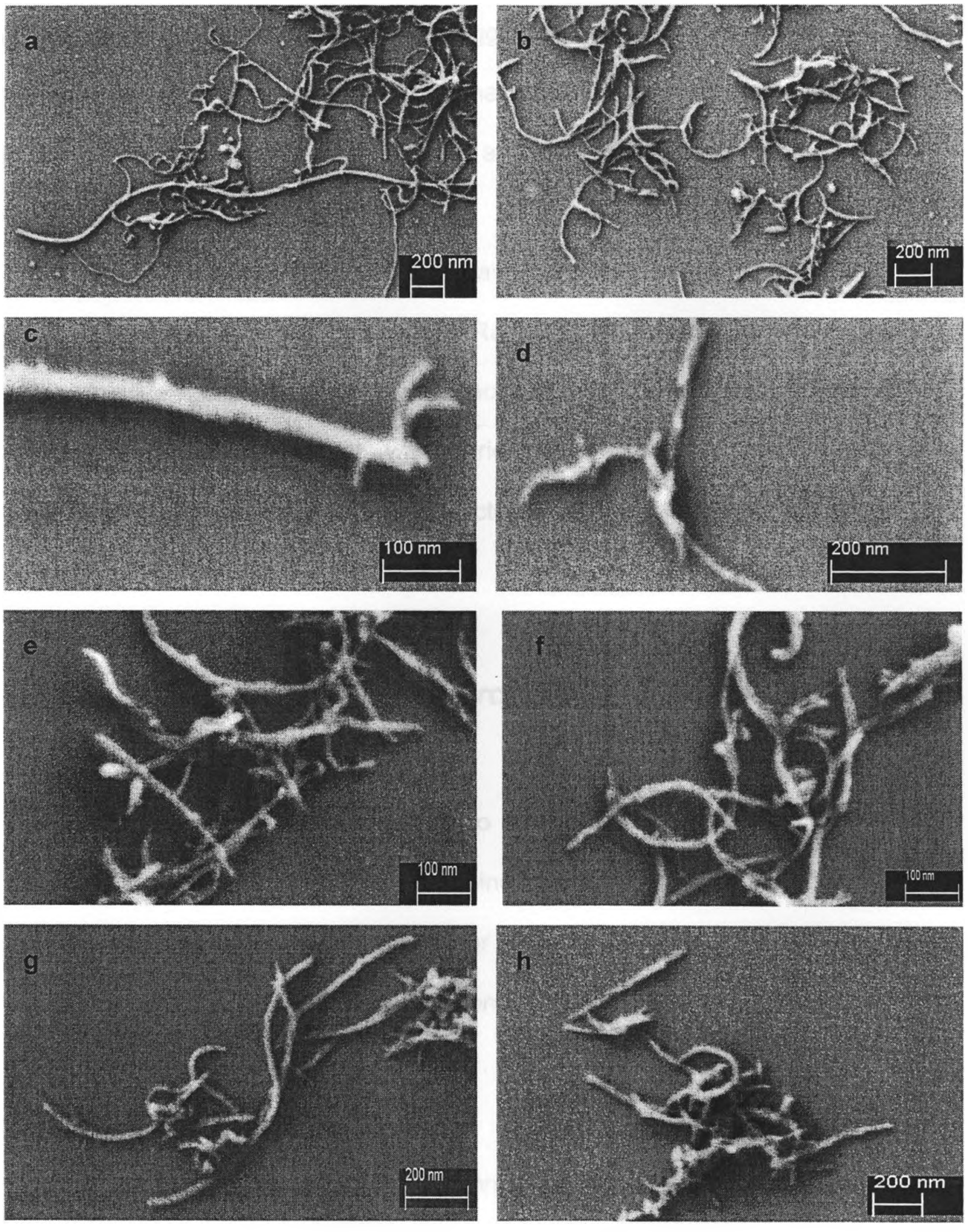

Fig. 3.4 SEM images of MWCNTs on silicon wafers: (a) purchased MWCNTs; (b, c, d) shortened MWCNTs; (e) **1**-sMWCNT; (f) **2**-sMWCNT; (g) **3**-sMWCNT; (h) **4**-sMWCNT.

SEM images of the Fc-conjugates modified MWCNTs show more shaggy edges on the tubes and significant aggregates of the tubes (Fig. 3.4 e-h). Hydrogen bonding may account for the main interaction between the tubes owing to the introduction of high extent of NH and CO groups from the functionalized reaction.

It seems that some of the tubes have something wrapping over the tubes, which make the tubes stick together. Residues from the modification reaction which involved many reagents may account for these wraps even though thorough wash for the products was carried out after the reaction. Defects and small molecules trapped in the defects on the tubes also destroyed the smoothness of the tubes.

3.3 Modification of ITO with Ferrocene-conjugates-sMWCNTs

3.3.1 ITO Surface

ITO films are of interest due to the combination of conductivity and transparency, which may enable a combined electrochemical and optical study in the future. They are coated on glass or more flexible materials like plastics as semiconductor electrodes for electrochemical utility. This kind of electrode can be made small, portable, and disposable, which is an advantage in the use of on-site detection.

The surface composition of commercial ITO films is complex, consisting of a mixture of oxides (In_2O_3), oxyhydroxide-like species (InOOH), and monomeric and oligomeric $In(OH)_3$-like species, in addition to carbonaceous

contaminants.[131] The forming of such species results from the hydrolysis of ITO surface upon exposure to even trace of water vapor.[132] Studies on the exposure of clean fresh ITO films to atmosphere showed that defect sites localized in the near-surface region are chemically reactive towards atmospheric water and hydrocarbons,[133] which could affect the electrochemical activity of the films (Fig. 3.5). In our studies ITO substrates were taken through a series cleaning steps including wash by detergent, MilliQ water, and ethanol, and dried in a steam of nitrogen prior to surface modification or device preparation.

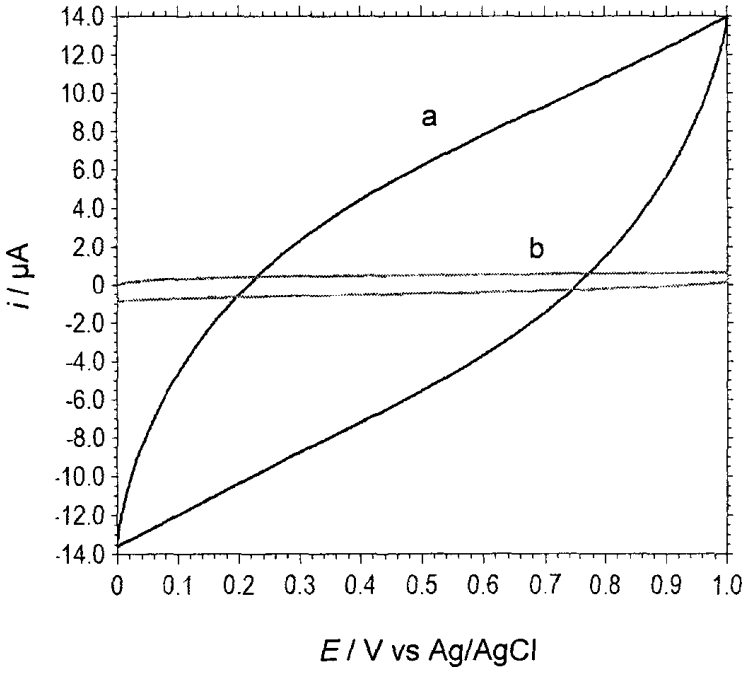

Fig. 3.5 CVs of ITO electrodes (a) before and (b) after surface cleaning. Measurements were carried out in aqueous solution of 2.0 M $NaClO_4$ at a scan rate of 100 mV s^{-1}.

As a semiconductor with complex composition on the surface, exchange current of an ITO electrode reaction is extremely low compared with that at a gold or glassy carbon electrode.[134] Due to the extraordinary small value of the

exchange current density, cyclic voltammogram of the $K_4[Fe(CN)_6]$ solution using ITO electrode shows a wide peak separation (trace b in Fig. 3.6), indicating a slow electron transfer between $[Fe(CN)_6]^{3-/4-}$ and ITO.

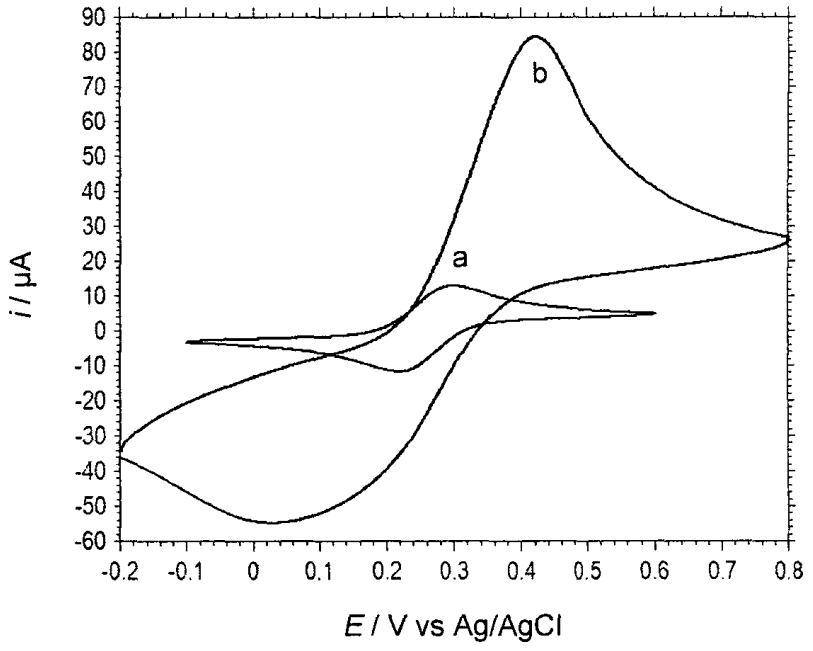

Fig. 3.6 CVs of aqueous solution of 1 mM $K_4[Fe(CN)_6]$ using (a) glassy carbon and (b) ITO substrate as working electrodes. Measurements were taken in aqueous solution of 2.0 M $NaClO_4$ as supporting electrolyte at a scan rate of 100 mV s^{-1}.

The solution of Fc-conjugates in MeCN exhibited a quasi-reversible one-electron oxidation when glassy carbon was used as working electrode in the CV measurements (Fig. 3.1 and Table 3.1). However, only a single irreversible reduction peak was observed for the solution of compound **1** when an ITO electrode was used (trace (b) in Fig. 3.7). Even after the deposition of compound **1** on the ITO surface, this modified electrode did not exhibit improved reversibility (trace (c) in Fig. 3.7), with the anodic peak disappearing after ten running cycles.

This may be due to the fact that only a fraction of the ITO surface is capable of supporting electron transfer to the absorbed molecules because conventional ITO surfaces have widely varying electronic conductivities, with "electrically active" and "electrically inactive" regions distributed uniformly on a submicron scale.[135, 136] Aggressive cleaning and pre-treatment can increase the electroactive area but this state lasts only a few minutes in atmosphere.[137]

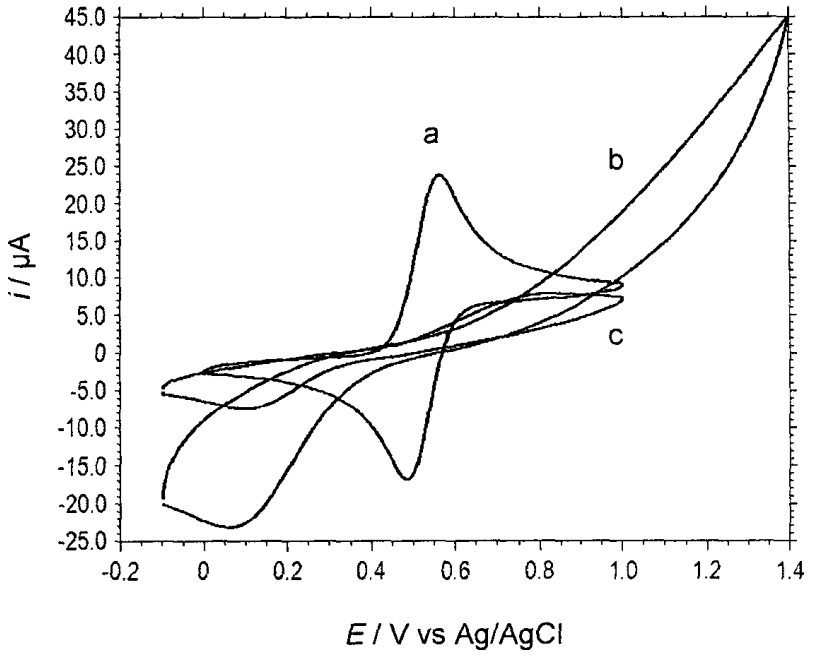

Fig. 3.7 CVs of 1 mM solution of compound **1** of MeCN using (a) glass carbon and (b) ITO substrate as working electrodes. (c) Compound **1** deposited on ITO surface as working electrode. Measurements were taken in solution of 0.1 M $LiClO_4$ as supporting electrolyte in MeCN at a scan rate of 100 mV s^{-1}.

3.3.2 Modification of ITO Surface with sMWCNTs

ITO electrodes that were modified with sMWCNTs (by deposition) showed great mechanical stability in both aqueous and organic solvents, indicating a

strong adhesion of sMWCNTs on the ITO surface. Cyclic voltammograms of $K_4[Fe(CN)_6]$ system using these modified ITO electrodes also showed a dramatic enhancement in electrochemical activity (Fig. 3.8). The anodic to cathodic current peak separation value (ΔE) for $[Fe(CN)_6]^{3-/4-}$ system was much smaller with sMWCNTs-modified-ITO electrodes (134 mV) than that with unmodified ones (463 mV) (Table 3.3), which indicated an increased electron transfer for $[Fe(CN)_6]^{3-/4-}$ pair placed in solution. A large increase in the current intensity was also observed with the modified ITO electrode system, which suggested a high

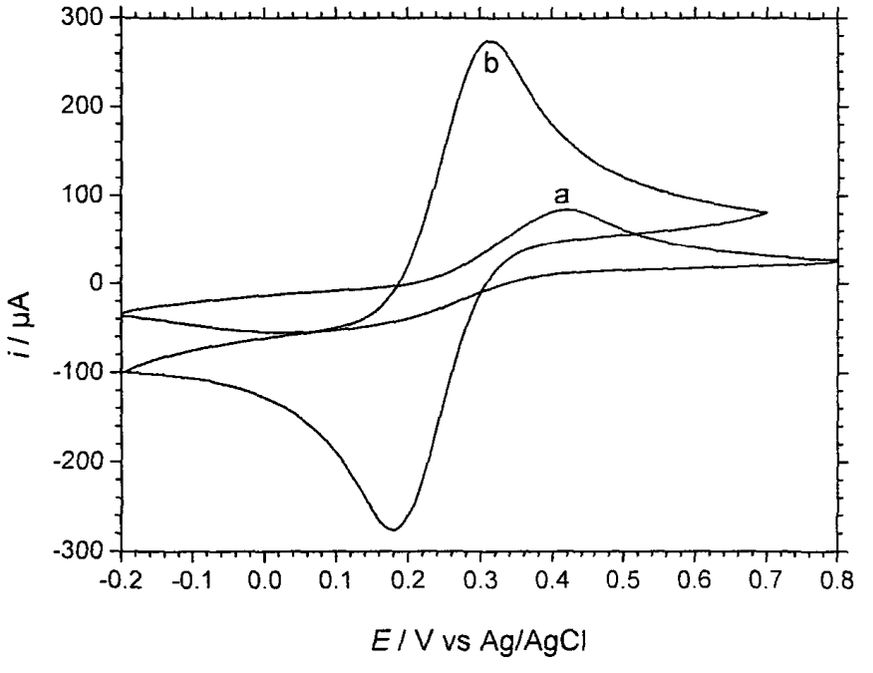

Fig. 3.8 CVs of aqueous solution of 1 mM $K_4[Fe(CN)_6]$ using (a) bare ITO electrode and (b) sMWCNT-ITO electrode. Measurements were taken in aqueous solution of 2.0 M $NaClO_4$ as supporting electrolyte at a scan rate of 100 mV s^{-1}.

coverage of $[Fe(CN)_6]^{3-/4-}$ on the electrode surface. The enhancement of adsorption of $[Fe(CN)_6]^{3-/4-}$ on the electrode surface contributed to the sMWCNTs with carboxylic acid functionality that favors hydrogen bonding attraction .

Table 3.3 Companion of CV parameters for $[Fe(CN)_6]^{3-/4-}$ system on ITO and sMWCNT on ITO

Electrode	$E_{1/2}$ / mV	ΔE / mV	i_{pa} / i_{pc}
ITO	224 (±2)	463 (±2)	0.91 (±0.02)
sMWCNT-ITO	246 (±0.5)	134 (±0.5)	1.01 (±0.01)

Experimental conditions were as described in **Fig. 3.8**.

3.3.3 Modification of ITO Surface with Ferrocene-Conjugates-sMWCNTs

Since the sMWCNTs modification gave the ITO electrode a better electrical activity to solution probes, it should work better for the probes on the electrode surface. Compared to the voltammogram of compound **1** (Fc-CO-Lys(Boc)-OMe) deposited on ITO surface (trace (b) in Fig. 3.9), we found that the conjugate **1**-sMWCNTs deposited on ITO (**1**-sMWCNT-ITO) showed a much better reversibility (trace (c) in Fig. 3.9) and exhibited a quasi-reversible one-electron oxidation with a formal potential (E^0 = 429 mV) value cathodically shifting with respect to the **1**-ITO sample (E^0 = 449 mV), indicating that this system is easier to oxidize (Table 3.4). Though both of the peak current ratios of these two systems were close to unity, the separation of the anodic and cathodic current peaks for **1**-sMWCNT-ITO (ΔE = 87 mV) was much smaller than that of **1**-ITO (ΔE = 661 mV). It is suggested that the electrodes with sMWCNTs were more

reversible than those without MWCNT, which again conforms to the well-known charge transfer-enhancing characteristic of CNTs.[138, 139]

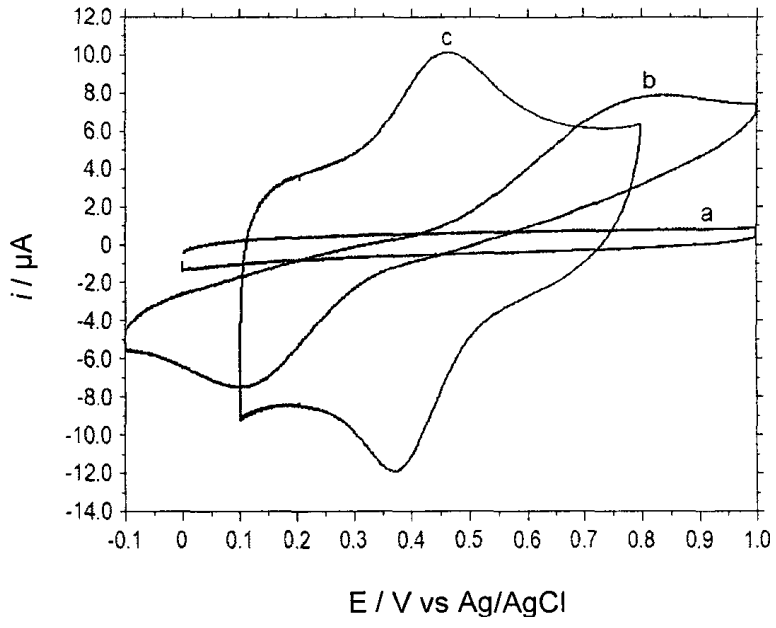

Fig. 3.9 CV responses of (a) sMWCNT deposited on ITO, (b) Fc-CO-Lys(Boc)-Ome deposited on ITO (**1**-ITO), and (c) **1**-sMWCNT deposited on ITO (**1**-sMWCNT-ITO) in aqueous solution of 2.0 M $NaClO_4$ as supporting electrolyte at a scan rate of 100 mV s^{-1}, respectively.

Table 3.4 CV parameters for Fc-conjugates-sMWCNT-ITO

	E^0 / mV	ΔE / mV	i_{pa} / i_{pc}
1-ITO	449 (±4)	661 (±12)	1.02 (±0.14)
1-sMWCNT-ITO	429 (±1)	87 (±2)	0.95 (±0.01)
2-sMWCNT-ITO	424 (±2)	131 (±1)	0.76 (±0.04)
3-sMWCNT-ITO	419 (±3)	99 (±7)	1.02 (±0.04)
4-sMWCNT-ITO	390 (±2)	98 (±3)	1.55 (±0.08)

Experimental conditions were as described in **Fig. 3.9** and **Fig. 3.10**.

The CVs for the ITO electrodes modified with the other Fc-modified-sMWCNT are shown in Fig. 3.10 and the parameters are summarized in Table 3.4. **3**-sMWCNT-ITO exhibited ΔE and i_{pa}/i_{pc} values similar to those of **1**-sMWCNT-ITO, indicating a good reversibility of the one-electron oxidation reaction. In contrast, **2**-sMWCNT-ITO has a ΔE = 131 mV and i_{pa}/i_{pc} = 0.76 indicated less reversibility. **1**-sMWCNT-ITO and **3**-sMWCNT-ITO showed similar CV responses owing to their similar structures—both possess lysine group which binds the Fc to a sMWCNT via amide bonds. In **2**-sMWCNT-ITO, the Fc is separated from a sMWCNT via both a lysine group and a leucine group; an arrangement which is likely to reduce the effect of the MWCNT on ferrocene. **4**-sMWCNT-ITO also indicated less reversibility with i_{pa}/i_{pc} value of 1.55. For compounds **1–4** we observe in the CVs that the ITO electrodes with Fc-conjugates modified-MWCNT exhibited much better reversibility than those without MWCNT. Further, it seemed that the proximity of MWCNT to the Fc group enhances reversibility.

On the other hand, when compare with the $E_{1/2}$ values (Table 3.1) of compound **1–4** in solution, the formal potential values (E^0) here show cathodically shifts, suggesting compounds on the electrode surface are easier to oxidize than those in solution.

While **1**-sMWCNT, **2**-sMWCNT, and **3**-sMWCNT were well dispersed in DMF, it is hard to find a dispersive solvent for **4**-sMWCNT. The conjugates were immediately precipitated from DMF, ethanol, methanol, or their mixture upon the stop of ultrasonication. SEM images reveal the tendency of aggregation for the samples of **4**-sMWCNT (Fig. 3.11). The big pieces were thought to be

aggregates of nanotubes formed in the dispersion solution because quick drying of the sample on a hotplate was carried out when the dispersion was dropped on the silicon wafer surface. The forming action of multiple H-bonds between the carboxylate and the positively charged guanidinium group may account for this aggregation. Since the weak electrochemical signals obtained from them, **4**-sMWCNT-ITO electrodes were not used in further studies including the detection of CWA mimics.

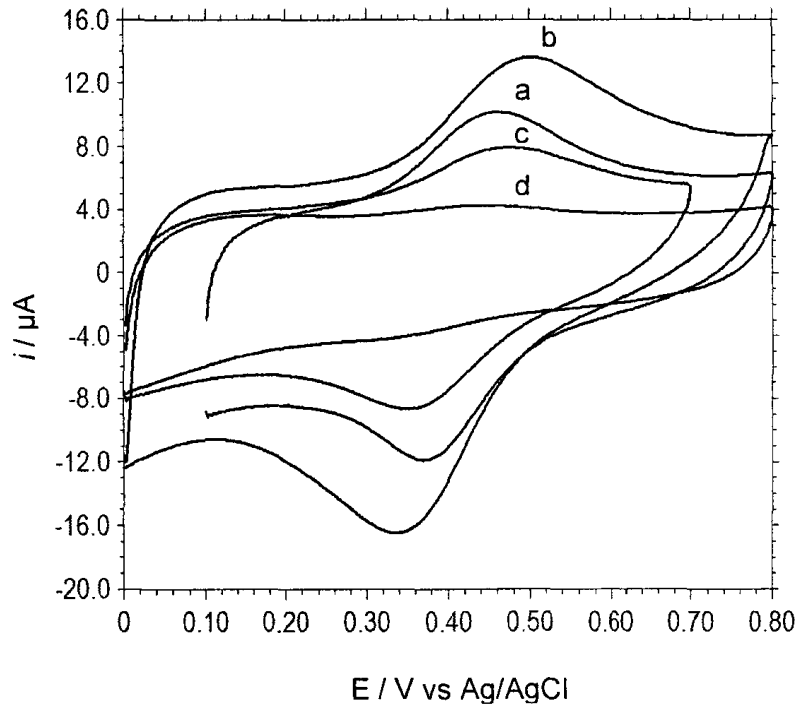

Fig. 3.10 CV responses of (a) **1**-sMWCNT-ITO, (b) **2**-sMWCNT-ITO, (c) **3**-sMWCNT-ITO, and **4**-sMWCNT-ITO in aqueous solution of 2.0 M $NaClO_4$ as supporting electrolyte at a scan rate of 100 mV s^{-1}, respectively.

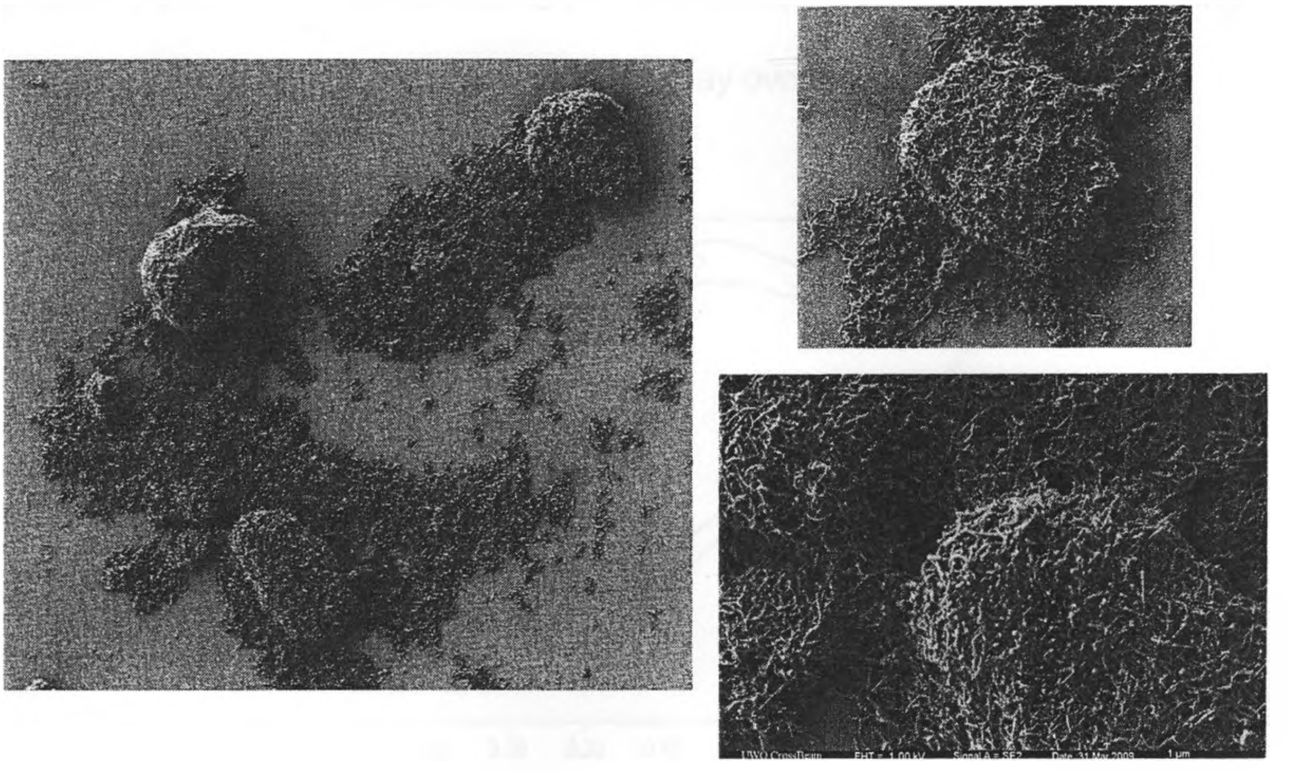

Fig. 3.11 SEM images of **4**-sMWCNT on silicon surface. A droplet of diluted dispersion solution of **4**-sMWCNT was put on the surface and dried immediately.

3.3.4 Stability of the Ferrocene-Conjugates-sMWCNT-ITO Surface

The dry surface of Fc-conjugates-sMWCNT-ITO electrodes was found to be stable when kept in a dry place at a low temperature (i.e. in a fridge at 4°C). Two samples of **1**-sMWCNT-ITO electrode were prepared. CV measurements were taken for one of them immediately after drying and the voltammogram was shown in Fig. 3.12 (trace (a)). The other one was kept in the fridge at 4°C for two months before the measurements were carried out. Its voltammogram (trace (b) in Fig. 3.12) looks very similar to the first one (trace (a)) and both of them are showing good reversibility with close parameter results shown in Table 3.5. It seems that the current intensity of the stored one is a little bit lower than the fresh

prepared one. This may be due to the insufficient dryness in the fridge. Using a desiccator to store the electrodes in fridge may overcome this problem.

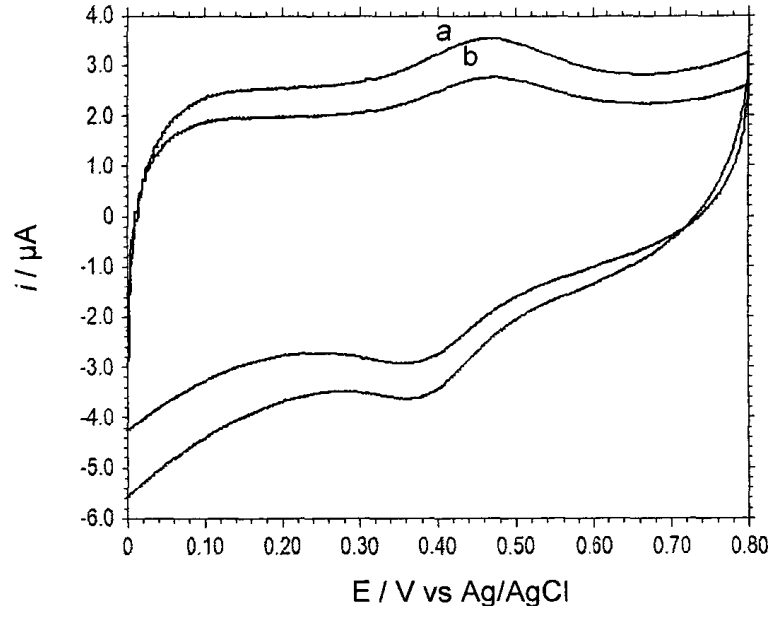

Fig. 3.12 CV responses of **1**-sMWCNT-ITO recorded (a) immediately after preparation and (b) two months after preparation. Measurements were taken in aqueous solution of 2.0 M $NaClO_4$ as supporting electrolyte at a scan rate of 100 mV s^{-1}.

Table 3.5 CV parameters for **1**-sMWCNT-ITO

a) freshly prepared; b) stored for two months at 4 °C

	E^0 / mV	ΔE / mV	i_{pa} / μA	i_{pc} / μA	i_{pa} / i_{pc}
a	424 (±1)	82 (±2)	0.88 (±0.01)	0.88 (±0.02)	1.00 (±0.03)
b	426 (±1)	87 (±2)	0.74 (±0.05)	0.75 (±0.01)	0.99 (±0.05)

Experimental conditions were as described in **Fig. 3.12**.

Fc-conjugates-sMWCNT-modified-ITO electrodes were also found to be very stable in aqueous electrochemical detecting systems. Fig. 3.13 (A) shows

the continuous CV responses of sample electrode, **1**-sMWCNT-ITO, versus Ag/AgCl in solution of 2.0 M $NaClO_4$. The intensity of the current responses decreased dramatically at the first 24 hours, but stabilized at the second day and lasted for at least one week. The measurement of current under various scan rates was carried out when the current responses were getting stable and the results were plotted in Fig. 3.13 (B). The linear relationship between current responses and the scan rates indicated that **1**-sMWCNT was successfully bound to the ITO surface. Fig. 3.13 (C) and (D) also indicated the stability of the modified ITO electrode surface whose current responses were still observed even after ten washing. As mentioned in section **3.3.2**, the carboxylic acid functionalities are thought to adsorb to oxide surfaces through weak electrostatic and H-bonding interactions and for some oxides coordination between the carboxylate and the metal ion defect sites.[133] Though some of the carboxyl groups on sMWCNTs were replaced by more hydrophobic Fc-CO-Lys-Ome groups in **1**-sMWCNT, our results show that **1**-sMWCNT retains a strong affinity to the ITO surface which has many oxides. Similar results were obtained from ITOs modified with **2**-sMWCNT and **3**-sMWCNT. They also showed mechanical and electrochemical stable in aqueous electrolyte solution.

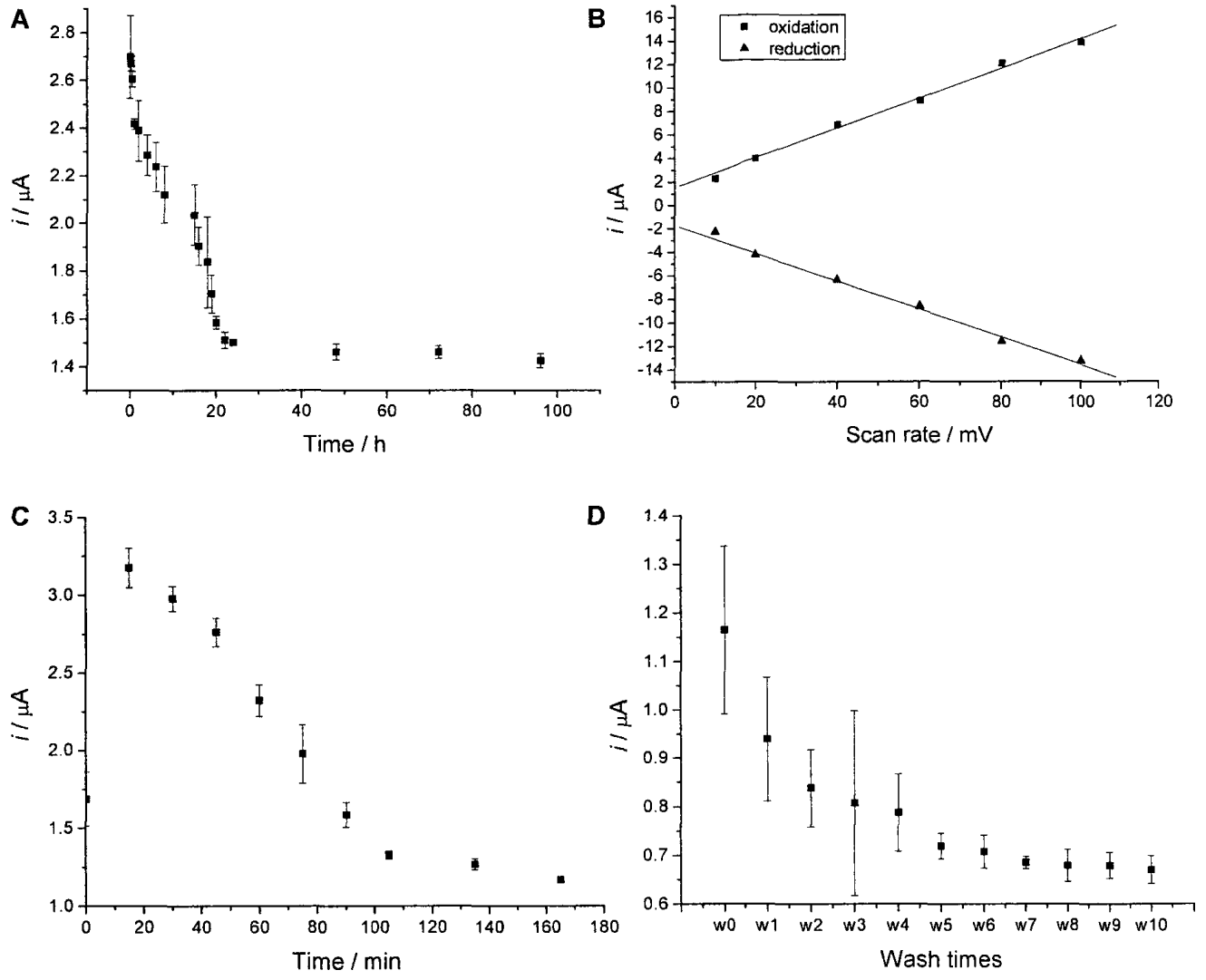

Fig. 3.13 The plots for the CV responses as a function of time (A, C), scan rate (B, after measurements of A), times of electrode surface wash (D, after measurement of C) for the **1**-MWCNT-ITO electrodes. Measurements were taken in aqueous solution of 2.0 M $NaClO_4$ (for A, B, C, D) at a scan rate of 100 mV s^{-1} (for A, C, D).

3.4 Detection of CWA Mimics

Several organophosphonates and one organosulfide were selected to simulate chemical warfare agents for detection experiments (Fig. 3.14). They were ethyl methylphosphonate (EMP), a hydrolysis product of VX, pinacolyl

methylphosphonate (PMP), hydrolysis product of Soman, diethyl cyanophosphonate (DECP), a mimic of hydrolysis product of Tabun, methylphosphonic (MPA), a final hydrolysis product of all nerve agents, and 2-chloroethyl ethyl sulfide (2-CLEES), a mimic of sulfur mustard.

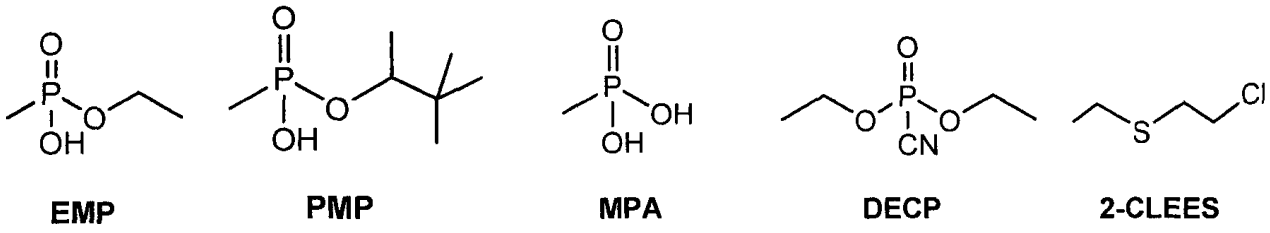

Fig. 3.14 Chemical drawings of the chemical warfare agent mimics: ethyl methylphosphonate (EMP), pinacolyl methylphosphonate (PMP), methylphosphonic acid (MPA), diethyl cyanophosphonate (DECP), and 2-chloroethyl ethyl sulfide (2-CLEES).

The Fc-conjugate-sMWCNT-ITO electrodes were used for the electrochemical detection of CWA mimics. A photograph of ITO electrodes and an SEM image of the electrode surface are shown in Fig. 3.15. Cyclic voltammetry (CV) and differential pulse voltammetry (DPV) were primarily used in these measurements.

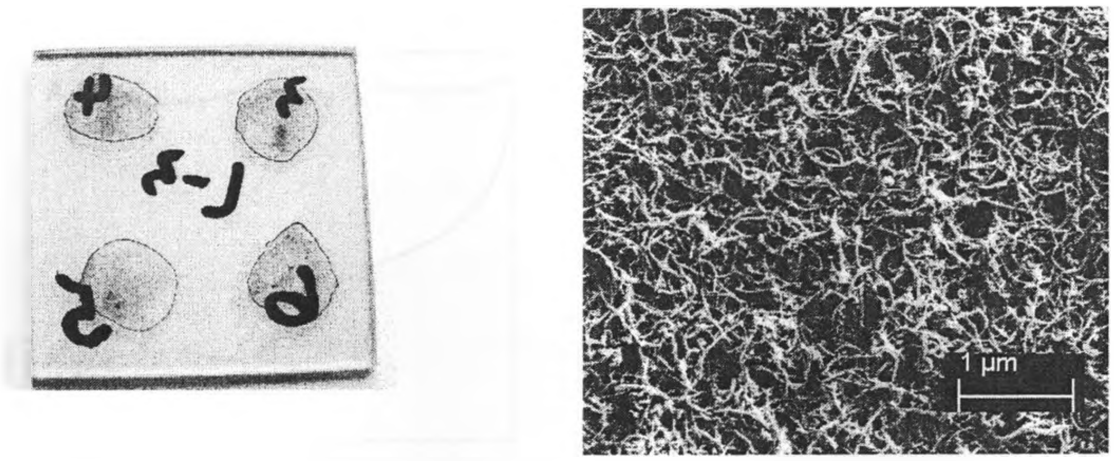

Fig. 3.15 Photograph of **1**-sMWCNT-ITO electrodes (left) and an SEM image of an electrode surface (right).

3.4.1 Detection of CWA Mimics using 1-sMWCNT-ITO Electrodes

As shown in Fig. 3.16 (A), the CV response of (Fc-CO-Lys-Ome) **1**-sMWCNT-ITO surface in blank electrolyte resembled a quasi-reversible process, where one electron was involved in the reaction (n = 1). The anodic and cathodic current responses in DPV show a sharp peak (Fig. 3.16 (B) and (C)) around 400 mV, indicating the oxidation and reduction processes of Fc group on the electrode surface in a cycle runs. Because the electrochemical response signals from DPV were stronger than those from CV, DPV technique has been basically used in the following detection of CWA mimics.

CV and DPV measurements were carried out on a series titration of CWA mimics in 2.0 M $NaClO_4$ supporting electrolyte solution using **1**-sMWCNT-ITO electrodes.

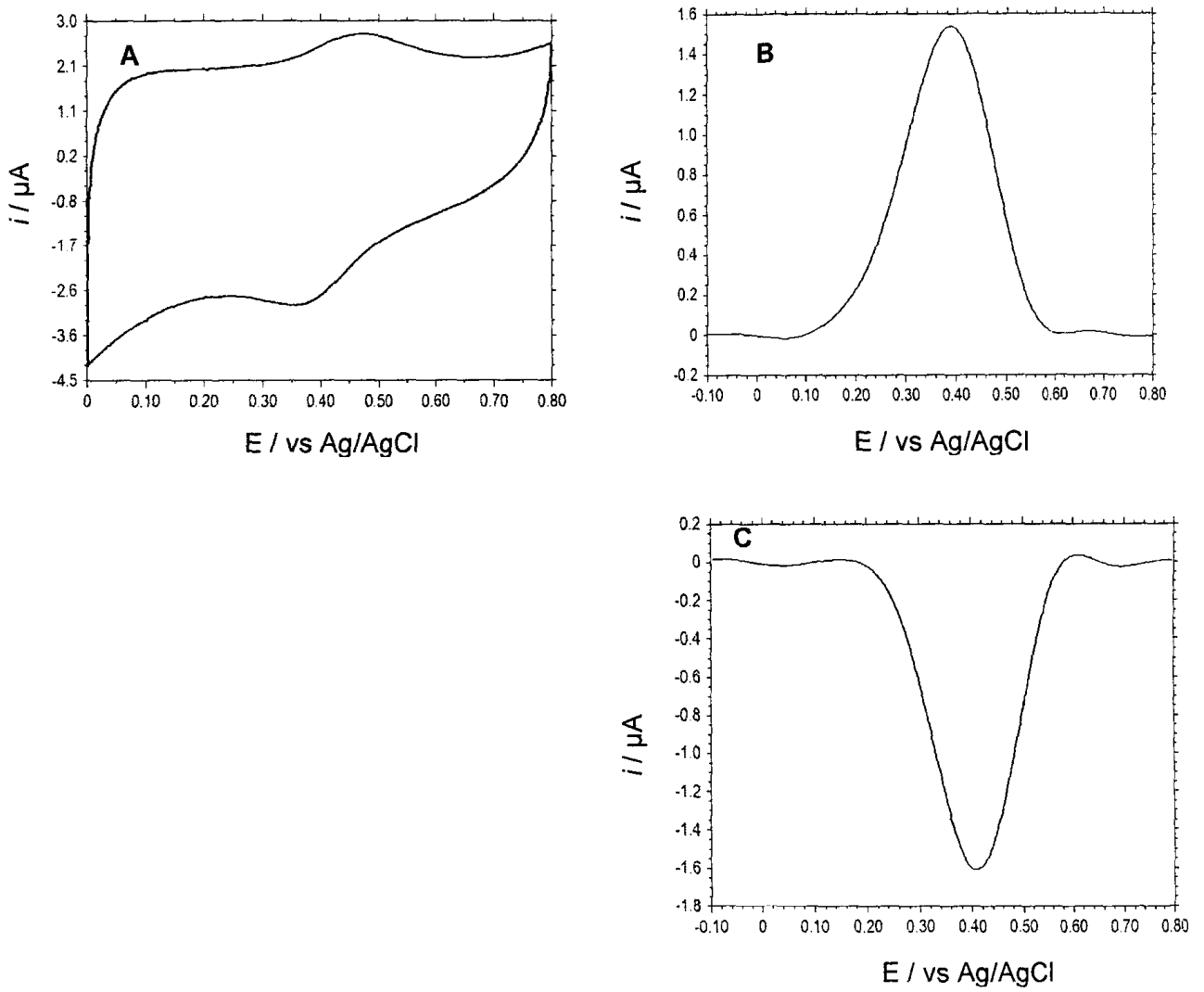

Fig. 3.16 CV responses (A) and DPV responses (B and C) of **1**-sMWCNT-ITO electrodes. Measurements were taken in aqueous solution of 2.0 M $NaClO_4$ as supporting electrolyte at a scan rate of 100 mV s^{-1}.

3.4.1.1 Detection of EMP

We have obtained the concentration-dependent and time-dependent DPV responses of the **1**-sMWCNT-ITO surface upon titration with EMP. Trace (a) in Fig. 3.17B shows the anodic current response of the **1**-sMWCNT-ITO surface in blank electrolyte solution. This anodic peak was getting broader and its intensity decreasing on the titration of EMP in the electrolyte solution in a series of

elevated concentration (from 1 pM to 10 μM, trace (b) to (e) in Fig. 3.17B). A second current response—a broad peak, started to appear at around the potential of 60 mV when the concentration of EMP reached 50 μM (trace (f) in Fig. 3.17B). This second peak was getting bigger and positively shifting to around 200 mV as the concentration of EMP continuously increased (from 50 μM to 500 μM, trace (f) to trace (h) in Fig. 3.17B).

Fig. 3.17D exhibited the change of first current responses as a function of EMP concentration. The current intensity decreased with increasing concentration of EMP. We believe that EMP mainly interacts with the CNTs on electrode surface via absorption and H-bonding interaction. The attraction of hydrophilic EMP molecules on the electrode surface potentially could prevent the Fc group for getting close to the surface, resulting in a decrease of the anodic current due to Fc oxidation. The larger amount of EMP molecules was on the surface, the more effect of block was observed.

However, the significant changes in the electrochemical properties of the sensing surface took place at the concentration of 50 μM of EMP as the second DPV response appeared at a lower potential (trace (f) in Fig. 3.17B). In order to understanding the nature of the interaction giving rise to this second signal, we used sMWCNT-ITO as working electrode to detect EMP. The resulted DPV voltammogram is shown in Fig. 3.18. Compared to the absence of EMP (trace (a) in Fig. 3.18), the current response of the electrode did not change in the presence of EMP at a low concentration of 10 μM (trace (b) in Fig. 3.18). As more EMP was added, a second signal appeared at a potential of about 100 mV, at which the second responses in **1**-sMWCNT-ITO systems appeared. It was

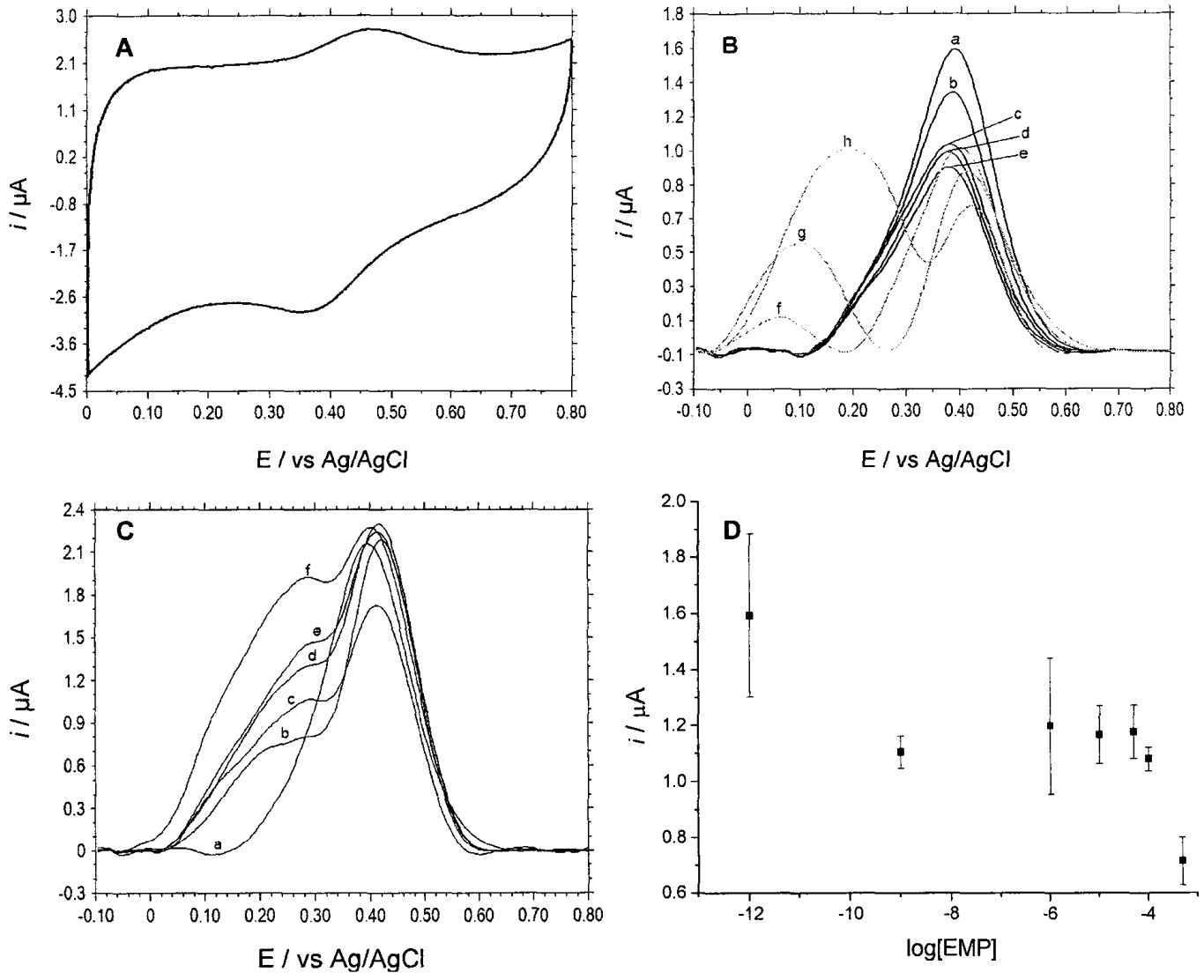

Fig. 3.17 (A) CV for **1**-sMWCNT-ITO surface in 2.0 M $NaClO_4$ solution as supporting electrolyte at a scan rate of 100 mV s^{-1}. (B) DPV for the interaction of EMP with **1**-sMWCNT-ITO surface. The DPV signal represents (a) in the absence of EMP in blank electrolyte solution, 2.0 M $NaClO_4$. DPV response as the concentration of EMP increased from 1 pM (b), 1 nM (c), 1 µM (d), 10 µM (e), 50 µM (f), 100 µM (g), to 500 µM (h). (C) The responses obtained after the addition of 1 mM EMP to the 2.0 M $NaClO_4$ solution. The measurements were taken at 0 min (b), 15 min (c), 30 min (d), 45 min (e), and 60 min (f) after the addition of EMP into the electrolyte solution. (D) The plot of DPV responses (first peak) as a function of the concentration of EMP.

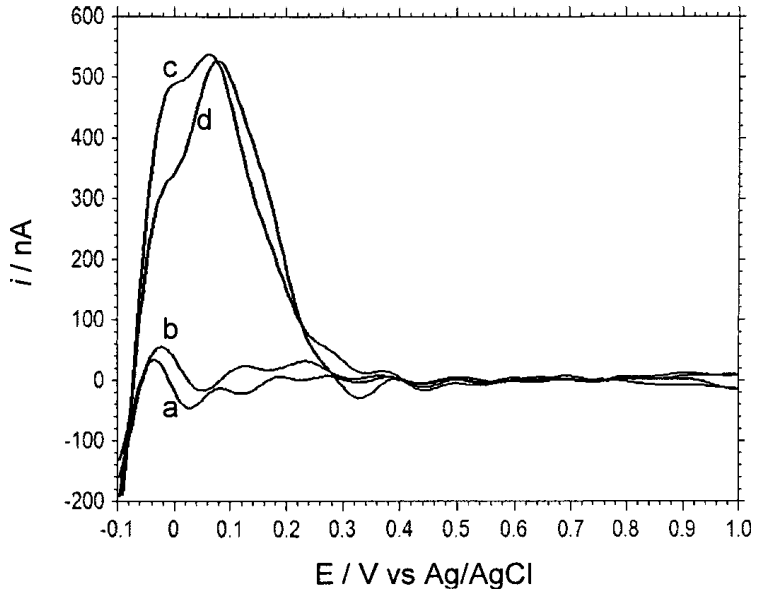

Fig. 3.19 DPVs for the interaction of EMP with sMWCNT-ITO surface. The DPV signal represents in the absence of EMP in blank electrolyte solution of 2.0 M $NaClO_4$ (a), in the presence of EMP in concentration of 10 μM (b), 50 μM (c), and 100 μM (d) in electrolyte solution of 2.0 M $NaClO_4$ at a scan rate of 100 mV s^{-1}.

demonstrated that the second responses at the lower potential were related to the interaction of EMP with CNTs, which may be an adsorption/desorption process. Maybe due to the interaction of functional groups (Fc-conjugates and carboxyls) on the CNT surface and CNTs themselves, this second current response appeared in **1**-sMWCNT-ITO systems positively shifted and increased as the concentration of EMP enhanced, which was not observed for sMWCNT-ITO systems. Since the significant change happened at the concentration of 50 μM, it is suggested that 50 μM can be the limited level for **1**-MWCNT-ITO sensors to detect EMP.

On the other hand, the electrochemical properties of **1**-MWCNT-ITO surface as a function of time in 1 mM EMP were also investigated by DPV

measurements. In Fig. 3.17C, we note that a shoulder peak emerges upon the addition of EMP, and that this feature becomes more pronounced with increasing elapsed time. It is known that phosphonate derivatives can undergo subsequent, slower hydrolysis to MPA.[28, 91] It is possible that the second current response in trace (b) of Fig. 3.17C, which shows an increasing current response as a function of time after the addition of EMP, may be due to the detection of the hydrolysis product, MPA, as well as EMP itself. In order to verify this assumption, we used MPA as the analyte to investigate the change of the electrochemical properties of **1**-sMWCNT-ITO surface.

3.4.1.2 Detection of MPA

DPV measurement results are shown in Fig. 3.19, from which we can see that the current response was getting asymmetrically broader with a shoulder peak at lower potential upon the addition of MPA solution (1 pM, trace (b) in Fig. 3.19B). The shoulder peak became stronger at the enhanced concentration of MPA (from 1 pM to 10 μM, trace (b) to (e) in Fig. 3.19B), and separated from the first peak at the concentration of 50 μM (trace (f) in Fig. 3.19B). The intensity of first peak was decreasing as the concentration of MPA increased (Fig. 3.19C). As discussed above, more mimic molecules were absorbed on the electrode surface to form a cover and fewer Fc groups could reach the surface to do an oxidation reaction. Hence the current intensity dropped as the concentration rose. While on the other hand, the intensity of this second peak was getting bigger as the concentration of MPA increased (trace (f) to (h) in Fig. 3.19B).

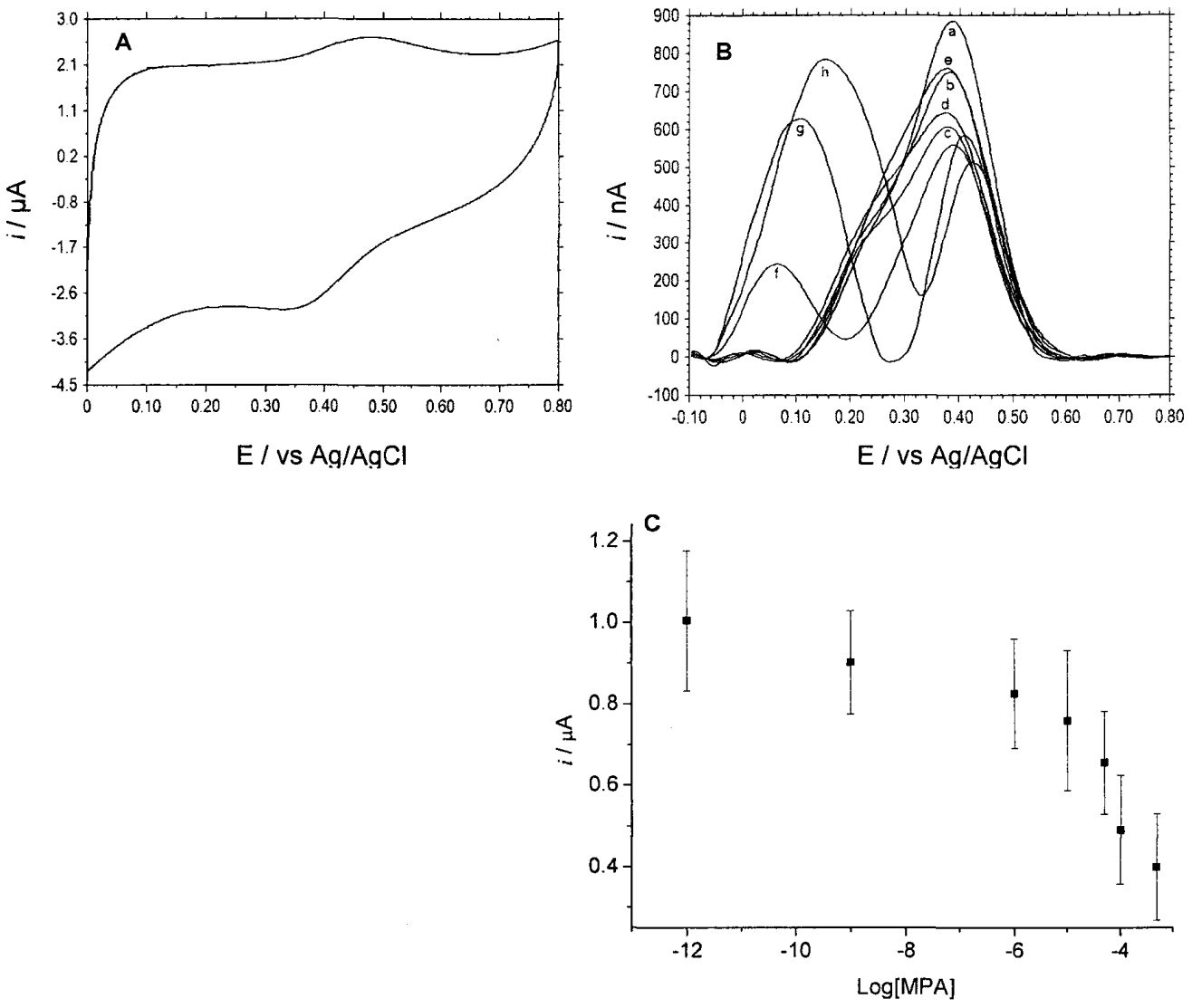

Fig. 3.19 (A) CV for **1**-sMWCNT-ITO surface in a solution of 2.0 M $NaClO_4$ as supporting electrolyte at a scan rate of 100 mV s^{-1}. (B) DPV for the interaction of MPA with **1**-s MWCNT-ITO surface. The DPV signal represents (a) in the absence of MPA in blank electrolyte solution of 2.0 M $NaClO_4$. DPV response as the concentration of MPA increased from 1 pM (b), 1 nM (c), 1 μM (d), 10 μM (e), 50 μM (f), 100 μM (g), to 500 μM (h). (C) The plot of DPV responses (first peak) as a function of concentration of MPA.

These results suggest that **1**-sMWCNT-ITO surface was sensitive to MPA with a detection limit down to 1 pM. From the detection results of EMP and MPA, we would say that the sensors with **1**-sMWCNT-ITO surface can be used to

detect both EMP and hydrolysis product MPA and are more sensitive to MPA (1 pM) than EMP (> 10 μM) by using electrochemical technique—DPV.

We believe that CWA mimics mainly interact with **1**-sMWCNT-ITO surface via absorption and H-bonding interaction, which further affects the electronic properties of the Fc-conjugate and CNTs. During the period of our measurement, MPA solution was supposed to have more H-bonding sites than EMP solution due to their different composition of molecules. Furthermore, EMP solution may have some MPA exist, but not much because of the slow rate of hydrolysis of EMP. That's may be the reason that the modified ITO sensors were more sensitive to MPA than EMP in the experimental period.

3.4.1.3 Detection of PMP

The detection of PMP had similar results as that of EMP. Voltammograms shown in Fig. 3.20B indicated the second anodic current response started to appear significantly at lower potential in the presence of PMP at concentration of 50 μM (trace (f) in Fig. 3.20B) as found in the detection of EMP. However, the current intensity of this second response did not increase much as the concentration of PMP increased. Compared with EMP, PMP has a pinacolyl group which is bigger and more rigid than the ethyl group in EMP. The hydrophobic pinacolyl group to some extent reduces the interaction of PMP molecule with CNTs, such as H-bonding interaction. The size and the steric effect also prevent the adsorption of PMP molecules to CNTs. Hence, even at high concentration the responses mainly reflecting interaction of PMP with CNTs

didn't have many changes. PMP can be surely detected at concentration of 50 μM using **1**-sMWCNT-ITO sensors.

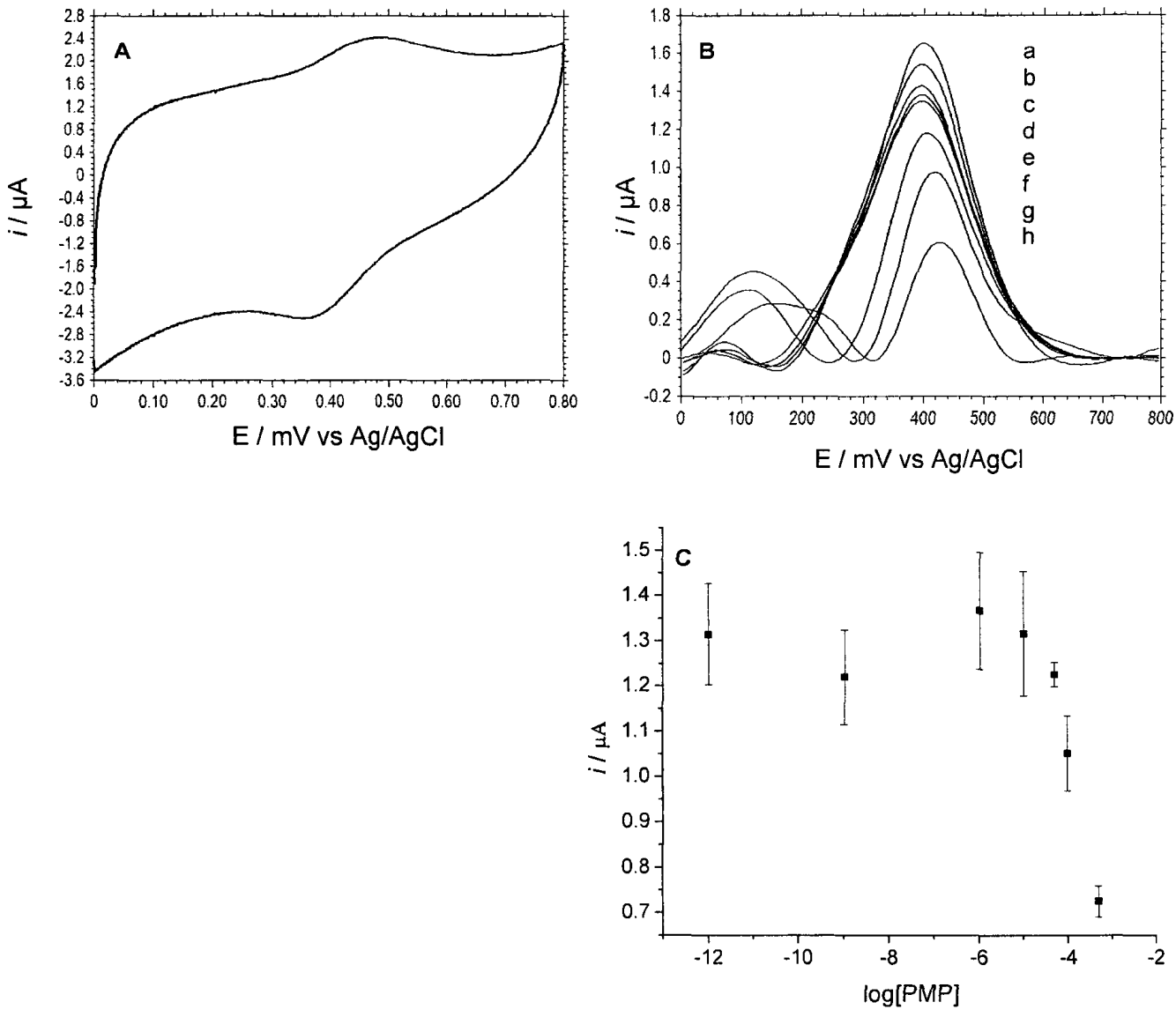

Fig. 3.20 (A) CV for **1**-sMWCNT-ITO surface in the solution 2.0 M $NaClO_4$ as supporting electrolyte at a scan rate of 100 mV s^{-1}. (B) DPV for the interaction of PMP with **1**-sMWCNT-ITO surface. The DPV signal represents (a) in the absence of PMP in blank electrolyte solution of 2.0 M $NaClO_4$. DPV response as the concentration of PMP increased from 1 pM (b), 1 nM (c), 1 μM (d), 10 μM (e), 50 μM (f), 100 μM (g), to 500 μM (h). (C) The plot of DPV responses (first peak) as a function of concentration of PMP.

3.4.1.4 Detection of DECP

The detection of DECP was also carried out using **1**-sMWCNT-ITO electrodes in 2.0 M $NaClO_4$ electrolyte solution. The anodic current peaks of the DPV responses were getting broader and shifting about -40 to -60 mV when DECP solution was added (Fig. 3.21B). Besides, the current intensity dropped dramatically upon the solution of DECP added (1pM, trace (b) in Fig. 3.21B), followed by a sharp rise when the concentration of DECP increased to 1 nM (trace (c) in Fig. 3.21B). Current intensity then decreased gradually as the concentration further increased (trace (d) to (g) in Fig. 3.20B, and Fig. 3.21C).

A second current response at lower potential appeared when there is a high concentration (500 μM) of DECP in the electrolyte solution (trace (g) in Fig. 3.21B). The significant DPV responses change of the sensing surface to the addition of DECP may be due to the CN group in DECP (Fig. 3.14), which is an electron donor that binds to ferrocenium when ferrocene group was oxidized; therefore the anodic current peaks shifted negatively. This suggests that the **1**-sMWCNT-ITO surface is sensitive to DECP that allow a successful detection at a concentration as low as 1 pM.

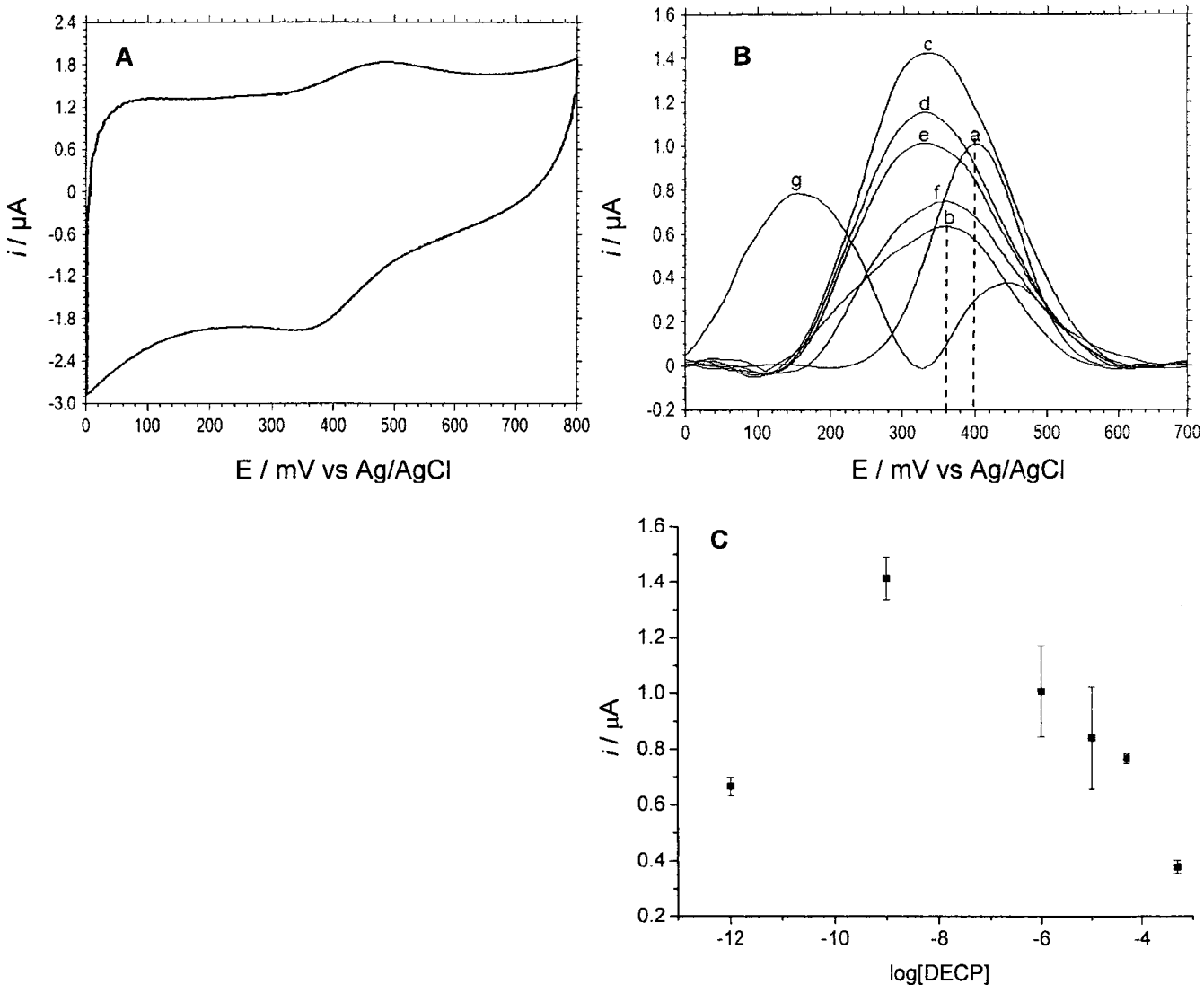

Fig. 3.21 (A) CV for **1**-MWCNT-ITO in 2 M $NaClO_4$ solution at a scan rate of 100 mV s^{-1}. (B) DPV for the interaction of DECP with **1**-MWCNT-ITO surface. The DPV signal represents (a) in the absence of DECP in blank electrolyte, 2 M $NaClO_4$. DPV response in the presence of DECP in concentration of 1 pM (b), 1 nM (c), 1 µM (d), 10 µM (e), 50 µM (f), and 500 µM (g). (C) The plot of DPV responses (first peak) as a function of concentration of DECP.

3.4.1.5 Detection of 2-CLEES

The stimulant for sulfur mustard, 2-CLEES, was detected using **1**-sMWCNT surface as well. The DPV voltammograms show reduced intensity of the anodic peak current of Fc group as the concentration of 2-CLEES enhanced

from 1pM to 500 μM (Fig. 3.22B and C), and a second peak appeared at lower potential when the concentration reached 500 μM (trace (h) in Fig. 3.22B). It

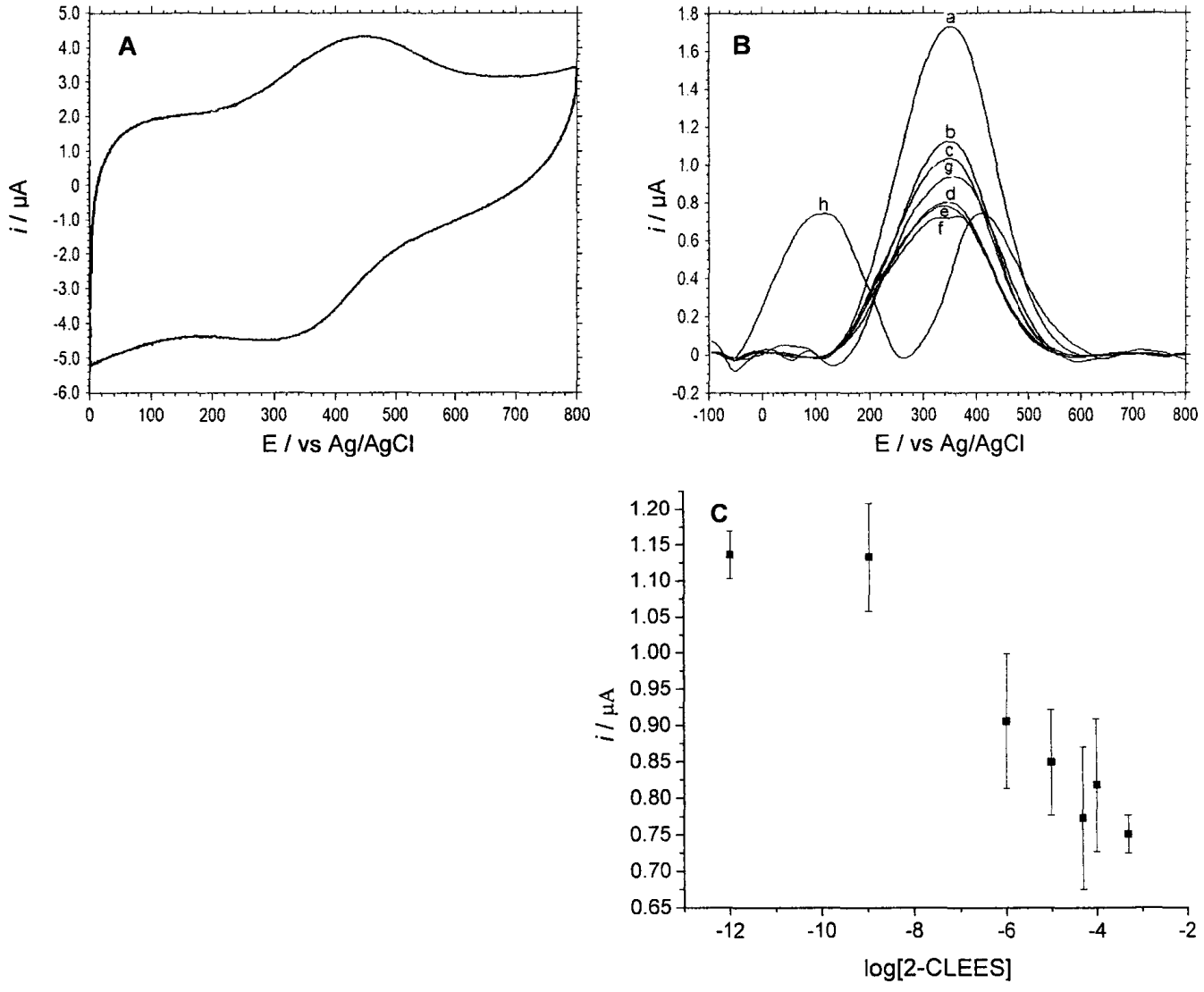

Fig. 3.22 (A) CV for **1**-sMWCNT-ITO in the solution of 2.0 M $NaClO_4$ as supporting electrolyte at a scan rate of 100 mV s^{-1}. (B) DPV for the interaction of 2-CLEES with **1**-MWCNT-ITO surface. The DPV signal represents (a) in the absence of 2-CLEES in blank electrolyte solution of 2.0 M $NaClO_4$. DPV response in the presence of 2-CLEES in the concentration of 1 pM (b), 1 nM (c), 1 μM (d), 10 μM (e), 50 μM (f), 100 μM (g), to 500 μM (h). (C) The plot of DPV responses (first peak) as a function of concentration of 2-CLEES.

seems that the **1**-sMWCNT surfaces are much less sensitive to 2-CLEES than to the mimics for nerve agents, in which the significant change in the DPV responses took place at high concentration of 500 μM. The low sensitivity is attributed to the weak interaction between the surface and 2-CLEES which is a poor hydrogen bond acceptor that makes it mainly physisorb to the sensing surface.

The difference in the molecular structures of the selected mimics caused the different interaction of them with the sensing surfaces, which were expressed on the change of DPV responses. It is suggested that the modified surface is very sensitive to MPA, the final hydrolysis product of nerve agents, and DECP, the mimic of Tabun which contains cyanide. The mimic of mustard gas, 2-CLEES, which has little interaction with the surface, only can be surely detected at fairly high concentration.

3.4.2 Recycling of 1-sMWCNT-ITO Surface

DPV measurements were carried out to determine the nature of the interactions between EMP and the **1**-MWCNT-ITO surface. Trace (a) in Fig. 3.23B represents the DPV signal of **1**-sMWCNT-ITO in the absence of EMP in blank electrolyte (2.0 M $NaClO_4$). The effect of the addition of EMP on the DPV signal is presented in trace (b) of Fig. 3.23B. The **1**-MWCNT-ITO surface was next washed with MilliQ water and placed in a blank electrolyte, resulting in the disappearance of the second current response (which had been noted in trace (b)) in the DPV signal (see trace (c) in Fig. 3.23B). The response upon the subsequent addition of EMP, presented in trace (d) of Fig. 3.23B, is virtually

identical to that in trace (b), Fig. 3.23B. The interaction of the **1**-MWCNT-ITO surface with CWA mimic EMP was observed to be reversible and is consistent with a physisorption/desorption process. It is also suggested that this sensing surface can be easily recycled by washing with water.

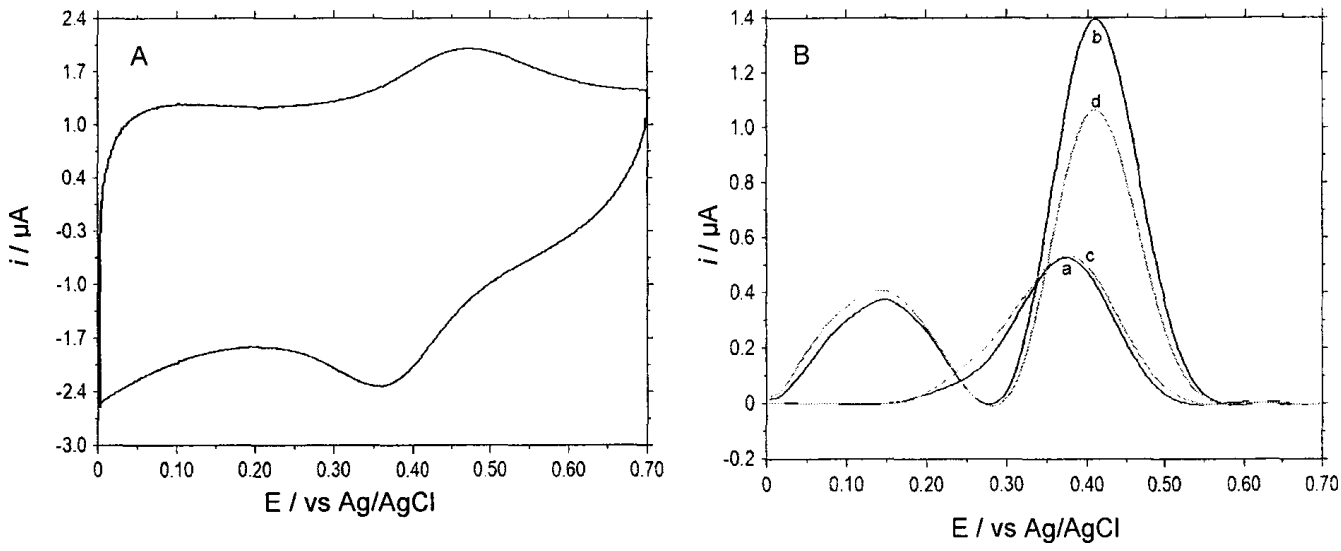

Fig. 3.23 (A) CV for **1**-MWCNT-ITO surface in solution of 2.0 M $NaClO_4$ as supporting electrolyte at a scan rate of 100 mV s^{-1}. (B) The DPV for the interaction of EMP with **1**-MWCNT-ITO surface. (a) in the absence of EMP in blank electrolyte solution (2.0 M $NaClO_4$), (b) in the presence of 1 mM EMP, (c) after the surface was washed with MilliQ water and in the absence of EMP in a blank electrolyte, and (d) after EMP was added.

3.4.3 2-sMWCNT-ITO and 3-sMWCNT-ITO Electrodes

2-sMWCNT-ITO and **3**-sMWCNT-ITO electrodes were used to detect CWA mimics as well and similar results as those of **1**-sMWCNT-ITOs were obtained. For example, the detection of MPA using **2**-sMWCNT-ITO and **3**-sMWCNT-ITO, respectively, exhibited significant changes in the anodic peak

current in the DPV voltammogram when MPA was added to the electrolyte solution (Fig. 3.24A & B). Upon the addition of a small amount of MPA (1 pM in electrolyte solution), a second response appeared as a shoulder peak of the first current response. This second response became stronger as the concentration of DECP increased. It is indicated that both **2**-sMWCNT-ITO and **3**-sMWCNT-ITO sensors can detect MPA to the limit of 1 pM according to the significant change in the anodic current responses in DPV.

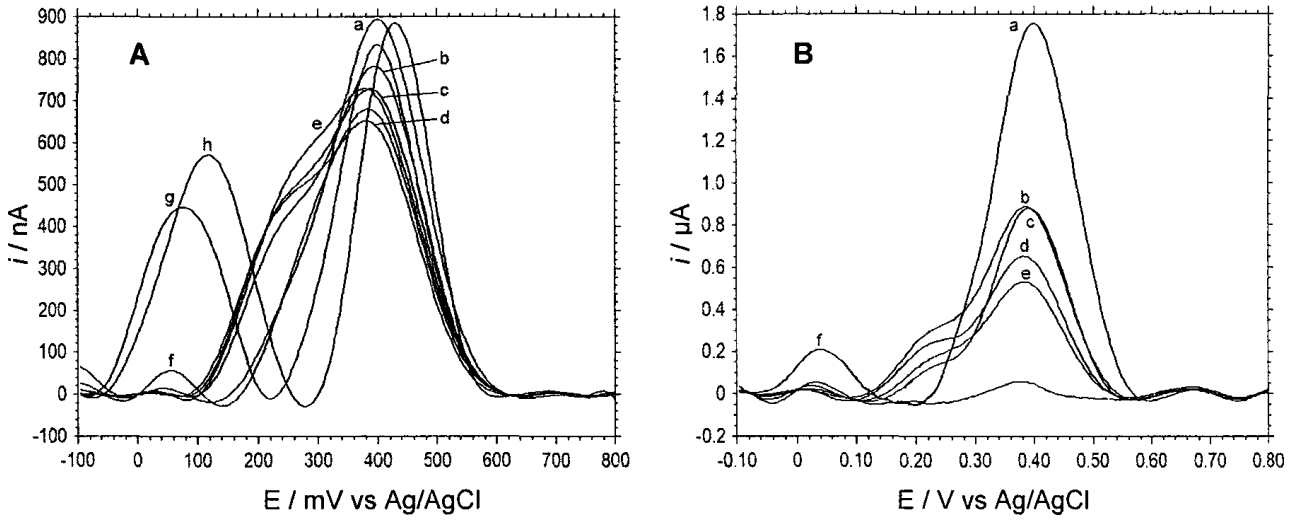

Fig. 3.24 DPV for the interaction of MPA with **2**-sMWCNT-ITO (A) and **3**-sMWCNT-ITO (B) surfaces. The DPV signal represents (a) in the absence of MPA in blank electrolyte solution of 2.0 M $NaClO_4$. DPV response as the concentration of MPA increased from 1 pM (b), 1 nM (c), 1 µM (d), 10 µM (e), 50 µM (f), 100 µM (g), to 500 µM (h).

However the reproducibility of the results was not as good as expected and their electrochemical signals were not as stable as for **1**-sMWCNT-ITO. For example, as shown in Fig. 3.24B, the first current response of **3**-sMWCNT-ITO, which is related to Fc group, drops quickly as the concentration of MPA increases.

When the concentration reached 50 μM, this response is almost lost completely. Similar results were observed for EMP and DECP with **2**-sMWCNT-ITO and **3**-sMWCNT-ITO sensors, respectively (Fig. 3.25), in which the first current response decreased fast even at low concentration of the analytes.

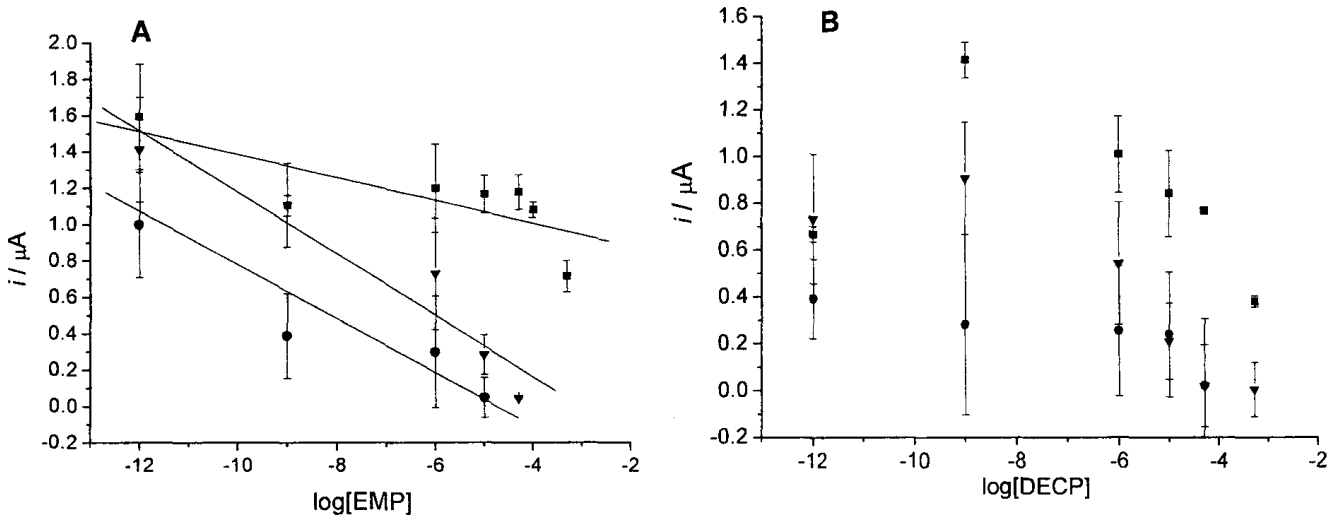

Fig. 3.25 The plot of DPV responses (first peak) as a function of concentration of EMP (A) and DECP (B) using **1**-sMWCNT-ITO (■), **2**-sMWCNT-ITO (▼), and **3**-sMWCNT-ITO (●), respectively.

In summary, sMWCNT-conjugates of compound **2** and **3** do not show better electrochemical performance than those with compound **1**. Instead the films had poorer properties. Neither was the selectivity of them to the CWA mimics since there are no specified groups in the molecules that have particular interaction with the CWA mimics. Hence no additional efforts have been devoted on improving their performance.

Chapter 4 CONCLUSION

In summary, the research presented in this thesis demonstrates that one kind of versatile electrochemical sensors for detection of CWA mimics in solution was developed. This kind of sensors which was based on Fc-conjugates modified MWCNTs as recognizing layer has shown high sensitivity and selectivity for hydrolysis of nerve agents and a mimic of Tabun.

Ferrocene-amino acid / peptide conjugates were synthesized according to the HBTU/HOBt protocol[126] for amide forming reactions. This method was also extended to be used in the chemical modification of acid-treated MWCNTs with Fc conjugates. This is the first report of MWCNTs successfully conjugated to Fc-amino acid / peptide conjugates covalently. This method is simple and easily handled, avoiding complicated fabrications.

Fc-conjugates-sMWCNTs were deposited on ITO surfaces as working electrodes. They have showed very good electrochemical reversibility and stability in aqueous solution. The electrochemical signal is stable and lasts for over one week in working condition. It is suggested that the electrochemical activity of the electrode surface can be reserved for months if kept in a dry place with low temperature (i.e. a desiccator in fridge), which is more economic and convenient than those enzyme-based biosensors. Furthermore, the reuse of the sensor is possible by washing the electrode surface with water to remove any of the CWA mimics and re-generate the surface.

The application of **1**-sMWCNT-ITOs for the electrochemical detection for mimics / hydrolysis products of nerve agents and sulfur mustard showed that the

electrical properties of the sMWCNTs and Fc group were significantly affected upon the adding of CWA mimics to the system. DPV offered large dynamic ranges for the detection of EMP, PMP, DECP, MPA, and 2-CLEES in water. Electrochemical measurements indicated spectacular changes on the electrostatic interaction between the Fc-conjugates-sMWCNT films and nerve agent related compounds at low concentration (Table 4.1). Compared to those chemosensors that may need time for chemical reaction during the detection, the electrochemical sensors discussed in this thesis had a quick response to the analytes.

In conclusion, a kind of novel and practical electrochemical sensors for the detection of CWA mimics was developed, which was readily fabricated and allowed trace-level detection of CWA mimics in aqueous solutions.

Table 4.1 Limit of detection for Fc-conjugates-sMWCNT-ITO sensors to CWA mimics

		EMP	**PMP**	**MPA**	**DECP**	**2-CLEES**
Limit of detection	**1**-sMWCNTs-ITO	50 μM	50 μM	1 pM	1 pM	500 μM
	2-sMWCNTs-ITO	50 μM	---	1 pM	1 pM	---
	3-sMWCNTs-ITO	50 μM	---	1 pM	1 pM	---
Significant change in DPV responses		Second anodic current peak appeared at lower potential			First anodic current peak shifted to lower potential	Second anodic current peak appeared at lower potential

Reference

1. Wikipedia. Available at URL: http://www.en.wikipedia.org/wiki/chemical_warfare. **2007**.

2. Romano, Jr. J. A.; Lukey, B. J.; and Salem, H. *Chemical Warfare Agents*, 2nd ed. CRC Press, **2008**.

3. Schecter, W. P. and Donald, E. F. *J. Am. Coll. Surg.* **2005**, 200, 128.

4. Wikipedia. Available at URL: http://en.wikipedia.org/wiki/Greek_fire. **2009**.

5. Dogaroiu, C. *Romanian J. Legal Med.* **2003**, 11, 132.

6. Prentiss, A. M. *Chemicals in War: A Treatise on Chemical Warfare.* McGrawHill, New York, NY, pp. 343.

7. Hanslian, R. *Chemical Warfare Bulletin.* **1936**, 22, 5.

8. Trumpener, U. *The J. of Modern History.* **1975**, 47, 460.

9. Mitretek. Available at URL: http://www.mitretek.org/ChemistryOfHMustard.htm. **2005**.

10. Kohn, S. *The Cost of the War to Russia.* Howard Fertig, New York, NY, **1973**.

11. MTS. Available at URL: http://www.mitretek.org/AShortHistoryOfTheDevelopmentOfNerveGases.htm. **2005**.

12. Harris, R. and Paxman, J. *A Higher Form of Killing: The Secret Story of Chemical and Biological Warfare.* New York, Hill and Wang, New York. **1982**, pp. 24, 117, 141.

13. Brophy, L. P.; Miles, W. D.; and Cochrane, R. C. *The Chemical Warfare Service: From Laboratory to Field.* Office of the Chief of Military History, Washington, DC, **1959**, 69.

14. Wikipedia. Available from URL: http://www.en.wikipedia.org/wiki/Nerve_agent. **2007**.

15. Smart, J. K. Available from URL: http://www.usuhs.mil/cbw/history.htm. **1997**.

16. Cooke, R. J. www.collegian.psu.edu/archives/2002/10/10-18-02news-06.asp. **1982**.

17. Mylroie, L. *Wall Street J.* July 26, **1994**, pp. A16. URL: http://www.fas.org/irp/wporld/iraq/956-tni.htm.

18. Biema, D. V. *Time*, April 3, **1995**, pp. 27.

19. Sun, Y.; Ong, K. Y. *Detection Technologies for Chemical Warfare Agents and Toxic Vapors*, CRC Press LLC, **2005**.

20. Sidell, F. R. Nerve agents, in *Medical Aspects of Chemical and Biological Warfare*, TMM Publications, Washington, **1997**, pp. 129.

21. Wiener, M. D and Hoffmann, R. S. *J. Intensive Care Med*, **2004**, 19, 22.

22. Harris, R. and Paxman, J. *A Higher Form of Killing: The Secret Story of Chemical and Biological Warfare*. New York, Hill and Wang, New York. **1982**, pp. 53.

23. Koelle, G. B. Anticholinesterase agents, in *The Phamacological Bais of Therapeutics, 4th edn* (eds. Goodman, L. S.; and Gilman, A.), Maemillan, New York, NY, **1970**, pp. 446.

24. Clark, V. M.; Hutchinson, D. W.; Kirby, A. I. and Warren, S. G. *Angew. Chem.* **1964**, 76, 704.

25. Fox, M. and Scott, D. *Mut. Res.* **1980**, 75, 131.

26. Byrne, M. P.; Broomfield, C. A. and Stites, W. E. *J. Protein Chem.* **1996**, 15, 131.

27. Rewick, R. T.; Shumacher, M. L. and Haynes, D. L. *Appl. Spectrosc.* **1986**, 40, 152.

28. Munro, N. B.; Talmage, S. S.; Griffin, G. D.; Waters, L. C.; Watson, A. P.; King, J. F.; Hauschild, V. *Environmental Health Perspectives*, **1999**, 107, 933.

29. Yang, Y. C.; Baker, J. A.; and Ward, J. R. *Chem. Rev.* **1992**, 92, 1729.

30. Hazardous Substance Data Base. Methyl phosphonic acid. Bethesda, MD: National Library of Medicine, **1997**. Bartlett, P. D. and Swain, C. G. *J. Am. Chem. Soc.* **1949**, 71, 1406.

31. Sanches, M. L.; Russell, C. R.; and Randolf, C. L. Chemical Weapon Convention (CWC) Signature Analysis. DNA-TR-92-73; ADB171788. Alexandria, VA: Defense Technical Information Centre, **1993**.

32. Franke, S. Textbook of Military Chemistry, Vol 1. USAMIIA-HT-039-82, AD B062913. Alexandria, VA: Defense Technical Information Centre, **1982**.

33. Monill, I. G.; Reed, L. W.; and Chinn, K. S. K. Toxic Chemicals in the Soil Enviroment Vol 2. TECOM project 2-CO-210-049 (DTIC: AD-A158215). Stillwater, OK: Oklahoma State University, **1985**.

34. Rosenblatt, D. H.; Small, M. J.; Kimmell, T. A.; Anderson, A. W. Agent Decontamination Chemistry: Technical Report. U.S. Army Test and Evaluation Command (TECOM) Technical Support, phase I. Prepared for the Environmental Quality Office, U. S. Army Test and Evaluation Command, by Argonne National Laboratory, Washington, DC, **1995**.

35. U.S. Army. Potential Military Chemical / Biological Agents and Compounds. FM 3-9, NAVFAC P-467, AFR 355-7. Fort McClellan, Al: Headquarters, Department of the Army, Navy and Air Force, **1990**.

36. Small, M. J. Tech. Rept. 8304; AD A149515. Fort Detrick, MD: US. Army Medical Bioengineering Research and Development Laboratory, **1984**.

37. Clark, D. N. Review of Reactions of Chemical Agents in Water, AD-A213 287. Alexandria, VA: Defense Technical Information Centre, **1989**.

38. Kingery, A. F. and Allen H. E. *Toxicol. Environ. Chem.* **1995**, 47, 155.

39. Epstein, J.; Callahan, J. J.; and Bauer, B. E. *Phosphorus*, **1974**, 4, 157.

40. Szafraniec, L. J.; Szafraniec, L. L.; Beaudry, W. T.; and Ward, J. R. On the Stoichiometry of Phosphonothiolate Ester hydrolysis. ADA-250773. Aberdeen Proving Ground, MD: US. Army Chemical Research Development and Engineering Centre, **1990**.

41. Kaaijk, J. and Frijlink, C. *Pestic. Sci.* **1977**, 8, 510.

42. Rewick, R. T.; Shumacher, M. L. and Haynes, D. L. *Appl. Spectrosc.* **1986**, 40, 152. (42)

43. Bartlett, P. D. and Swain, C. G. *J. Am. Chem. Soc.* **1949**, 71, 1406.

44. Fitch, J. P.; Raber, E.; Imbro, D. R. *Science* **2003**, 302, 1350.

45. Benschop, H. P.; Van der Schans, G. P.; Noort, D.; Fidder, A.; Mars-Groenendijk, R. H.; De Long, L. P. A. *J. Anal. Toxicol.* **1997**, 21, 249.

46. Phlhujis, M.; Langenberg, J. P.; Benschop, H. P. *Toxicol. Appl. Pharmacol.* **1997**, 146, 146.

47. Noort, D.; Hulst, A. G.; Platenburg, D. H. J. M.; Polhuijs, M.; Benschop, H. P. *Arch. Toxicol.* **1998**, 72, 671.

48. Hill, H. H. Jr. and Martin, S. *J. Pure Appl. Chem.* **2002**, 74, 2281.

49. Ballantine, D. J. Jr.; Martin, S. J.; Ricco, A. J.; Frye, G. C.; Zellers, E. T.; White, R. M.; Wohltjen, H. *Acoustic Wave Sensors: Theory, Design and Physic0-Chemical Applications*, Academic Press, San Diego **1996**.

50. Mulchandani, A.; Mulchandani, P.; Chen, W.; Wang, J.; Chen, L. *Anal. Chem.* **1999**, 71, 2246.

51. Mulchandani, P.; Chen, W.; Mulchandani, A. *Environ. Sci. Techno.* **2001**, 35, 2562.

52. Royo, S.; Martínez-Máñez, R.; Sancenón, F.; Costero, A. M.; Parra, M.; Gil, S. *Chem. Commun.* **2007**, 4839.

53. Arribas, A. S.; Vázquez, T.; Wang, J.; Mulchandani, A.; Chen, W. *Electrochem. Commun.* **2005**, 7, 1371.

54. Li, G.; Lin, Y. *Anal. Chem.* **2006**, 78, 835.

55. Frishman G.; Amirav, A. Field Anal. *Chem. Technol.* **2000**, 4, 170.

56. Steiner, W. E.; Clowers, B. H.; Matz, L. M.; Siems, W. F.; Hill, H. H. Jr. *Anal. Chem.* **2002**, 74, 4343.

57. Wang, J.; Pumera, M.; Collins, G. E.; Mulchandani, A. *Anal. Chem.* **2002**, 74, 6121.

58. Syage, J. A.; Nies, B. J.; Evans, M. D.; Hanold, K. A. *J. Am. Soc. Mass Spectrom.* **2001**, 12, 648.

59. Lopez-Avila, V. *Anal. Chem.* **1997**, 69, 289R.

60. Wolfbeis, O. S. *Anal. Chem.* **2004**, 76, 3269.

61. Wolfbeis, O. S. *Anal. Chem.* **2006**, 78, 3859.

62. Royo, S.; Martínez-Máñez, R.; Sancenón, F.; *et al. Chem. Commun.* **2007**, 4839.

63. Hambrook, J. L.; Howells, D. J.; and Utley, D. *Pestic. Sci.* **1971**, 2, 172.

64. Grate, J. W. *Chem. Rev.* **2000**, 100, 2627.

65. Wolff, U.; Dickert, F. L.; Fischerauer, G. K; *et al. IEEE Sens. J.* **2001**, 1, 4.

66. Grate, J. W.; Patrash, S. J.; and Aboaham, M. H. *Anal. Chem.* **1995**, 67, 2162.

67. Alizadeh, T.; Zeynali, S. *Sensors & Actuators B*, **2008**, 129, 412.

68. Ying, Z.; Jiang, Y.; Du, X.; *et al. Europ. Poly. J.* **2008**, 44, 1157.

69. Joo, B-S.; Huh, J-S.; and Lee, D-D. *Sensors & Actuators B*, **2007**, 121, 47.

70. Van Houten, K. A.; Heath, D. C.; and Pilato, R. S. *J. Am. Chem. Soc.* **1998**, 120, 12359.

71. Zhang, S-W. and Suager, T. M. *J. Am. Chem. Soc.* **2003**, 125, 340.

72. Dale, T. J. and Rebeek, J. Jr. *J. Am. Chem. Soc.* **2006**, 128, 4500.

73. Ilhan, F.; Tyson, D. S.; and Meador, M. A. *Chem. Mater.* **2004**, 16, 2978.

74. Bencic-Nagale, S.; Sternfeld, T.; and Walt, D. R. *J. Am. Chem. Soc.* **2006**, 128, 5041.

75. Costero, A. M.; Gil, S.; Parra, M.; *et al. Chem. Commun.* **2008**, 6002.

76. Wallace, K. J.; Morey, J.; Lynch, V. M.; *et al. New J. Chem.* **2005**, 29, 1469.

77. Wallace, K. J.; Fagbemi, R. I.; Folmer-Anderson, F. J.; *et al. Chem. Commun.* **2006**, 3886.

78. Hewage, H. S.; Wallace, K. J.; and Anslyn, E. V. *Chem. Commun.* **2007**, 3909.

79. Jenkins, A. L.; Uy, O. M.; and Murray, M. *Anal. Chem.* **1999**, 71, 373.

80. Southard, G. E.; Van Houten, K. A.; Ott, E. W. Jr.; *et al. Anal. Chim. Acta.* **2007**, 581, 202.

81. Koskela, H.; and Vanninen, P. *Anal. Chem.* **2008**, 80, 5556.

82. Rainina, E.; Simonian, A.; Efremenko, A.; *et al. Biosens. Bioelectron.* **1996**, 11, 991.

83. Dumas, D. P.; Wild, J. R.; and Raushel, F. M. *Biotech. Appl. Biochem.* **1989**, 11, 235.

84. Dumas, D. P.; Durst, H. D.; Lardis, W. G.; *et al. Arch. Biochem. Biophys.* **1990**, 277, 155.

85. Lai, K.; Stolowich, N. J.; and Wild, J. R. *Arch. Biochem. Biophys.* **1995**, 318, 59.

86. DeFrank, J. J.; and Chang, T-C. *J. Bacteriology*, **1991**, 173, 1938.

87. Simonian, A.; Flounders, A. W.; and Wild, J. R. *Electroanalysis*, **2004**, 16, 1896.

88. Papouskova, B.; Bednar, P.; Bartak, P.; *et al. J. Separation Sci.* **2006**, 29, 1531.

89. John, H.; Worek, F.; and Thiermann, H. *Anal. Bioanal. Chem.* **2008**, 391, 97.

90. Richardson, D. D.; and Caruso, J. A. *Anal. Bioanal. Chem.* **2007**, 388, 809.

91. Pumera, M. *J. Chroma. A*, **2006**, 1113, 5.

92. Martin, A. N.; Farquar, G. R.; Frank, M.; *et al. Anal. Chem.* **2007**, 79, 6368.

93. Richardson, D. D.; Sadi, B. B. M.; and Caniso, *J. A. J. Anal. Atomic Spec.* **2006**, 21, 396.

94. Shu, Y. R.; Su, A. K.; Liu, J. T.; *et al. Anal. Chem.* **2006**, 78, 4697.

95. Wang, S. X.; and Li, G. *IEEE Trans. On Magnetics*, **2008**, 44, 1687.

96. Yogeswaran, U.; and Chen, S. M. *Sensors*, **2008**, 8, 290.

97. Vichchulada, P.; Lipscomb, L. D.; Zhang, Q. H.; *et al. J. Nanosci. Nanotech.* **2009**, 9, 2189.

98. Dai, H. *Surf. Sci.* **2002**, 500, 218.

99. Strano, M. S.; Dyke, C. A.; Usrey, M. L.; *et al. Science*, **2003**, 301, 1519.

100. Reich, S.; and Thomsen, C. *Phys. Rev. B*, **2000**, 62, 4273.

101. Banks, C. E.; Davies, J. J.; Wildgoose, G. G.; *et al. Chem. Commun.* **2005**, 14.

102. Ahammad, A, J. S.; Lee, J-T.; and Rahman, Md. A. *Sensors*, **2009**, 9, 2289.

103. Merkoci, A.; Pumera, M.; Llopis, X.; *et al. Trends in Anal. Chem.* **2005**, 24, 826.

104. Gong, K.; Du, F.; Xia, Z.; *et al. Science*, **2009**, 323, 760.

105. Wildgoose, G. G.; Banks, C. E.; Leventis, H. C.; *et al. Microchim. Acta.* **2006**, 152, 187.

106. Niyogi, S.; Hamon, M. A.; Hu, H.; *et al. Acc. Chem. Res.* **2002**, 35, 1105.

107. Liu, J.; Rinzler, A. G.; Dai, H.; *et al. Science*, **1998**, 280, 1253.

108. Liao, Q.; Sun, J; and Gao, L. *Chem. Lett.* **2007**, 36, 1446.

109. Chen, J.; Hamon, M. A.; Hu, H.; *et al. Science*, **1998**, 282, 95.

110. Kong, J.; Franklin, N. R.; Zhou, C.; *et al. Science*, **2000**, 287, 622.

111. Collins, P. G.; Bradley, K.; Ishigami, M.; *et al. Science*, **2000**, 287, 1801.

112. Kumar, O.; Singh, Y.; Rao, V, K.; *et al. Defense Sci. J.* **2008**, 58, 617.

113. Novak, J. P.; Snow, E. S.; Houser, E. J.; Park, D.; Stepnowski, J. L.; McGill, R. A. *Appl. Phy. Lett.* **2003**, 83, 4026.

114. Wang, F.; Gu, H.; Swager, T. M. *J. Am. Chem. Soc.* **2008**, 130, 5392.

115. Khan, M. A. K.; Kerman, K.; Petryk, M.; Kraatz. H-B. *Anal. Chem.* **2008**, 80, 2574.

116. Joshi, K. A.; Prouza, M.; Kum, M.; Wang, J.; Tang, J.; Haddon, R.; Chen, W.; Mulchandani, A. *Anal. Chem.* **2006**, 78, 331.

117. Deo, R. P.; Wang, J.; Block, I.; *et al. Anal. Chim. Acta*, **2005**, 530, 185.

118. Lin, G. and Lin, Y. *Anal. Chem.* **2006**, 78, 835.

119. Joshi, K. A.; Tang, J.; Haddon, R.; Wang, J.; Chen, W.; Mulchandani, A. *Electroanalysis* **2005**, 17, 54.

120. Lin, Y.; Lu, F.; and Wang, J. *Electroanalysis*, **2004**, 16, 145.

121. Mulchandani, A.; Mulchandani, P.; and Chen, W. *Anal. Chem.* **1999**, 71, 2246.

122. Cattanach, K.; Kulkarni, R. D.; Kozlov, M.; Manohar, S. K. *Nanotechnology* **2006**, 17, 4123.

123. Privett, B. J.; Shin, J. H.; and Schoenfisch, M. H. *Anal. Chem.* **2008**, 80, 4499.

124. Khan, M. A. K.; Long, Y.; Schatte, G.; Kraatz. H-B. *Anal. Chem.* **2007**, 79, 2877-2884.

125. Gooding, J. J.; Wibowo, R.; Liu, J.; *et al. J. Am. Chem. Soc.* **2003**, *125*, 9006.

126. Satio, T.; Matsushige, K.; Tanaka, K. *Physica B*, **2002**, 323, 280.

127. Marcolongo, G.; Ruaro, G.; Gobbo, M.; Meneghetti, M. *Chem. Commun.* **2007**, 4925.

128. Zhang, Y.; Li, J.; Shen, Y.; Wang, M.; Li, J. J. *Phys. Chem. B* **2004**, 108, 15343.

129. Dyke, C. A.; Tour, J. M. *Chem.-Eur. J.* **2004**, 10, 812.

130. Cioffi, C.; Campidelli, S,; Brunetti, F. G.; Meneghetti, M.; Prato, M. *Chem. Commun.* **2006**, 2129.

131. Kim, J. S.; Cacialli, F.; and Friend, R. H. *Thin Solid Films*, **2003**, 445, 358.

132. Kim, J. S.; Friend, R. H.; and Cacialli, F. *Appl. Phys. Lett.* **1999**, 74, 3084.

133. Carter, C.; Brumbach, M.; Armstrong, N. R.; *et al. J. Phys. Chem. B*, **2006**, 110, 25191.

134. Nagai, J. *SPIE*, **3788**, 22.

135. Liau, Y. H.; Scherer, W. F.; and Rhodes, K. *J. Phys. Chem. B*, **2001**, 105, 3282.

136. Brumbach, M.; Veneman, P. A.; Marrikar, F. S.; *et al. Langmiur*, **2007**, 23, 11089.

137. Marrikar, F. S.; Brumbach, M.; Evans, D. H.; *et al. Langmiur*, **2007**, 23, 1530.

138. Granot, E.; Basnar B.; Cheglakov, Z; Katz, E,; Willner, I. *Electroanalysis*, **2006**, 18, 26.

139. Tan, C. K.; Loh, K. P.; John, T. T. L. *Analyst*, **2008**, 133, 448.

APPENDIX OF SPECTRA

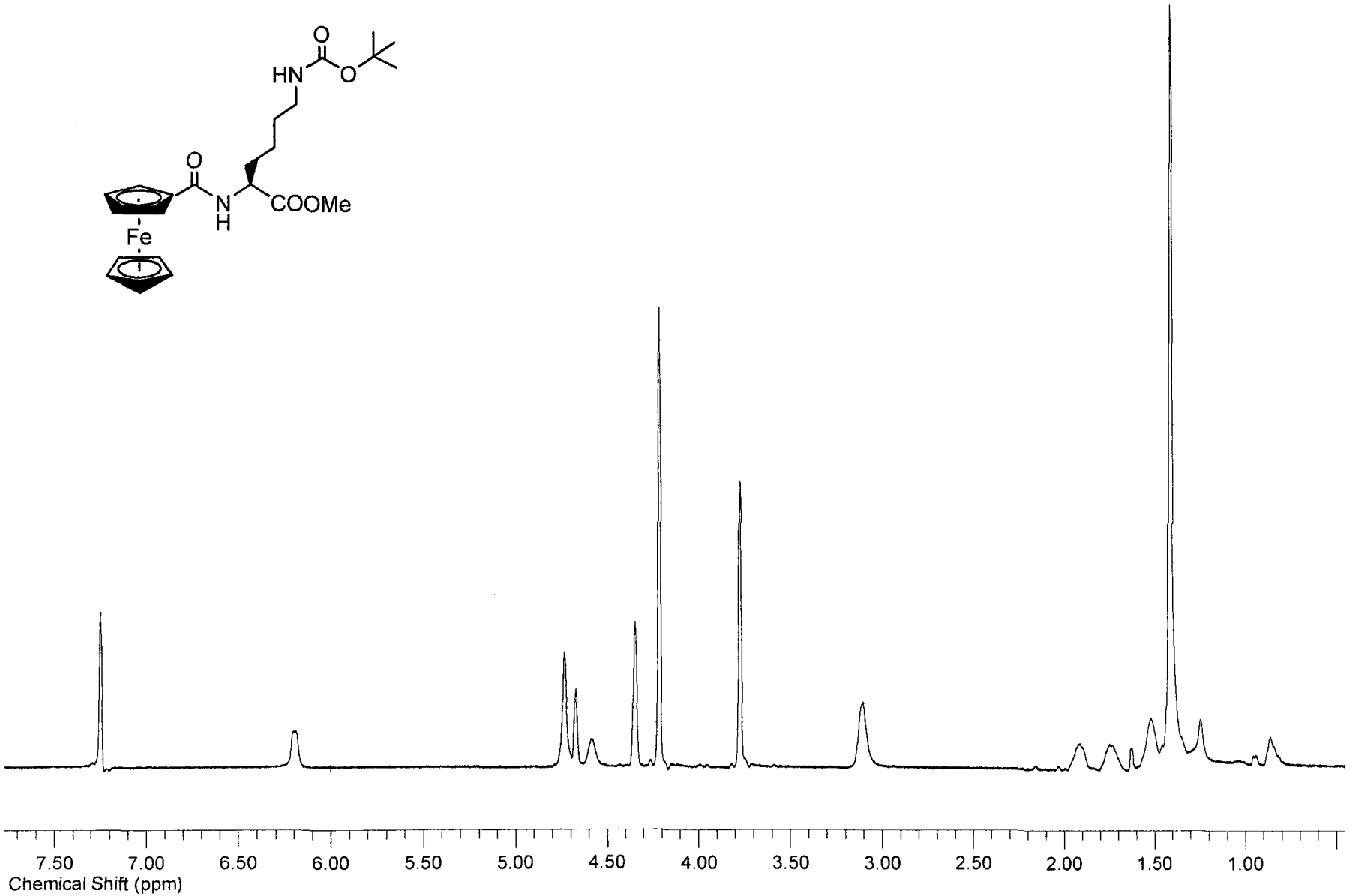

Compound **1**: Fc-CO-Lys(Boc)-OMe

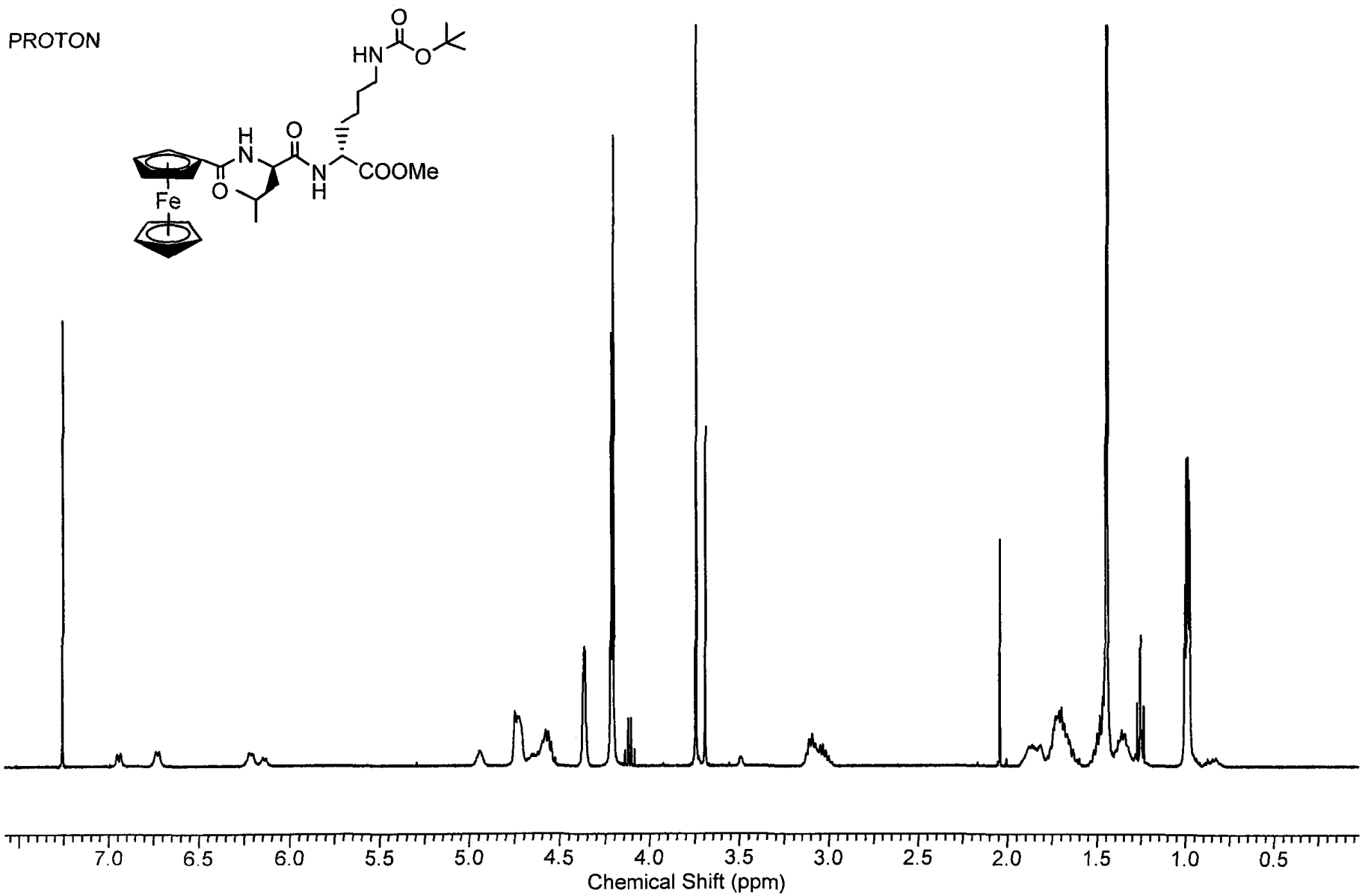

Compound **2**: Fc-CO-Leu-Lys(Boc)-OMe

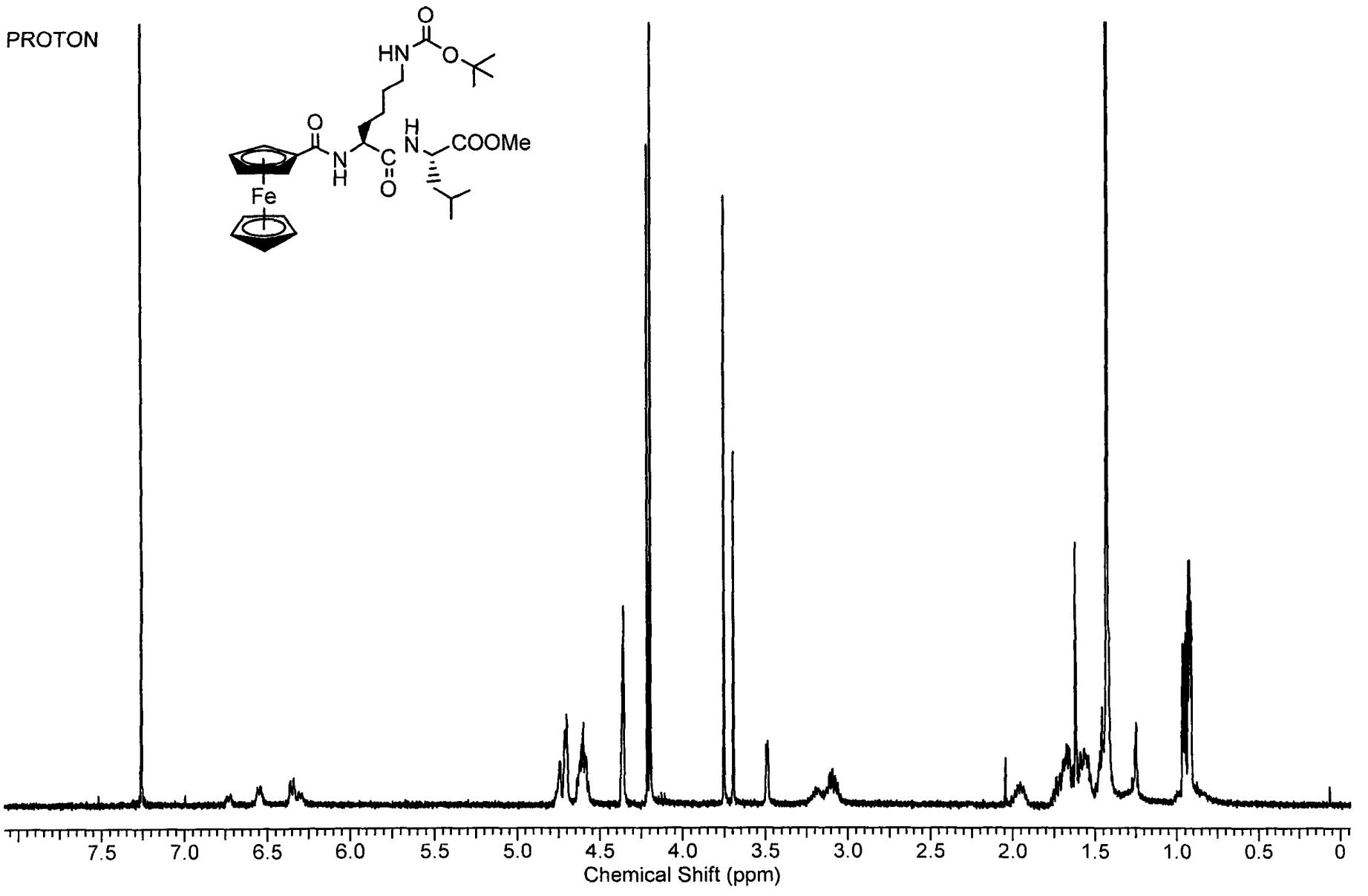

Compound **3**: Fc-CO-Lys(Boc)-Leu-OMe

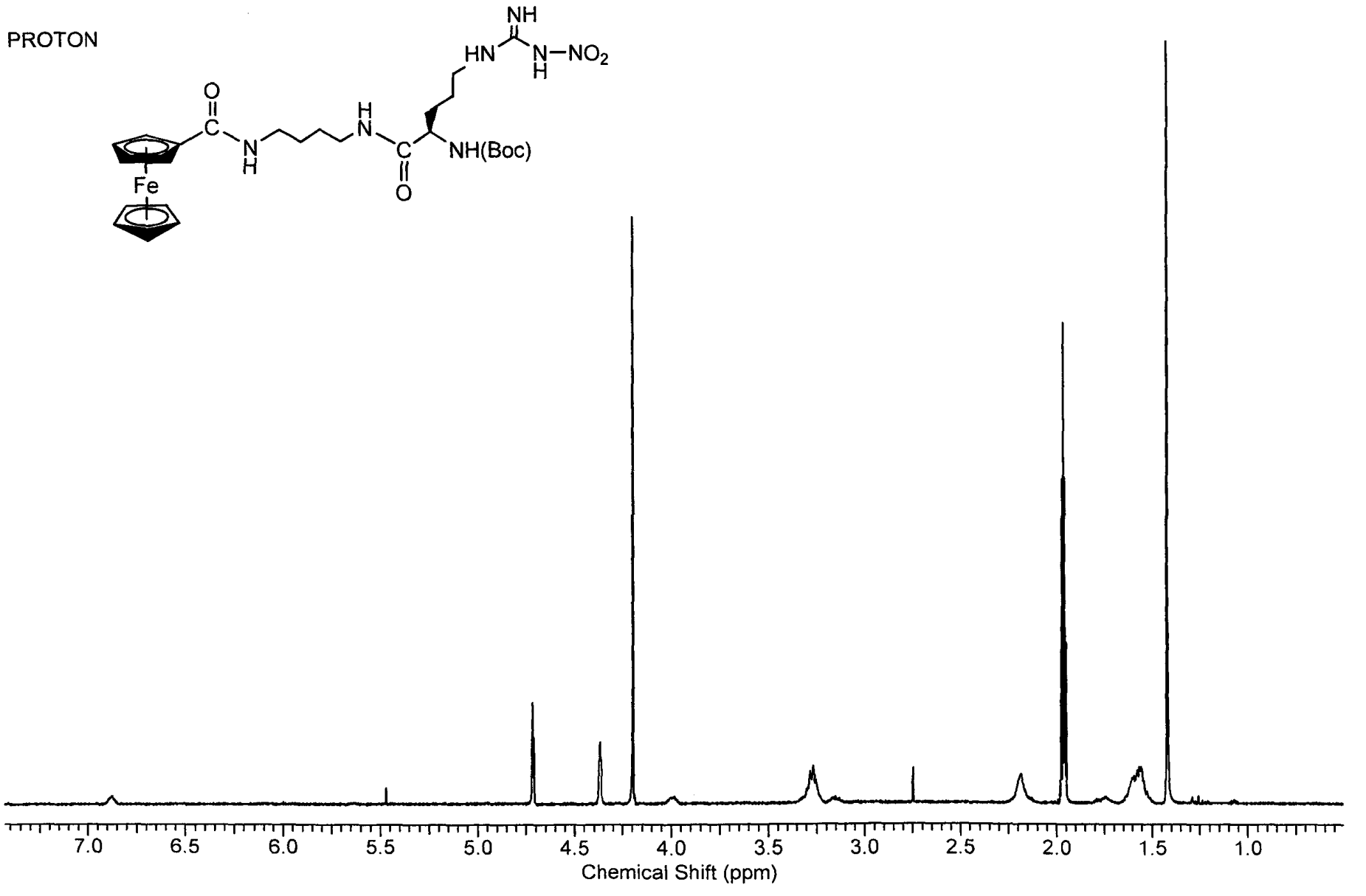

Compound **4**: (Boc)Arg(NO_2)-NH(CH_2)$_4$NH-CO-Fc